

The tectonic evolution of the Arctic since Pangea breakup: Integrating constraints from surface geology and geophysics with mantle structure



Grace E. Shephard*, R. Dietmar Müller, Maria Seton

School of Geosciences, University of Sydney, NSW 2006, Australia

ARTICLE INFO

Article history:

Received 25 February 2013

Accepted 22 May 2013

Available online 16 June 2013

Keywords:

Plate reconstructions

Arctic

Tectonics

Amerasia Basin

Panthalassa

South Anuyi Ocean

ABSTRACT

The tectonic evolution of the circum-Arctic, including the northern Pacific, Siberian and North American margins, since the Jurassic has been punctuated by the opening and closing of ocean basins, the accretion of autochthonous and allochthonous terranes and associated deformation. This complexity is expressed in the uncertainty of plate tectonic models of the region, with the time-dependent configurations and kinematic history remaining poorly understood. The age, location, geometry and convergence rates of the subduction zones associated with these ancient ocean basins have implications for mantle structure, which can be used as an additional constraint for refining and evaluating plate boundary models. Here we integrate surface geology and geophysics with mantle tomography models to generate a digital set of tectonic blocks and plates as well as topologically closed plate boundaries with time-dependent rotational histories for the circum-Arctic. We find that subducted slabs inferred from seismic velocity anomalies from global P and S wave tomography models can be linked to various episodes of Arctic subduction since the Jurassic, in particular to the destruction of the South Anuyi Ocean. We present a refined model for the opening of the Amerasia Basin incorporating seafloor spreading between at least 142.5 and 120 Ma, a “windshield” rotation for the Canada Basin, and opening orthogonal to the Lomonosov Ridge for the northern Makarov and Podvodnikov basins. We also present a refined pre-accretionary model for the Wrangellia Superterrane, imposing a subduction polarity reversal in the early Jurassic before accretion to North America at 140 Ma. Our model accounts for the late Palaeozoic to early Mesozoic opening and closure of the Cache Creek Ocean, reconstructed between the Wrangellia Superterrane and Yukon–Tanana Terrane. We suggest that a triple junction may also explain the Mid-Palaeozoic opening of the Slide Mountain, Oimyakon and South Anuyi oceans. Our digital tectonic model forms the basis for the development of future plate deformation and geodynamic models and provides a framework for analysing the formation and evolution of regional sedimentary basins and mountain belts.

© 2013 Elsevier B.V. All rights reserved.

Contents

1.	Introduction	149
2.	Discussion of regional tectonics	152
2.1.	The South Anuyi Ocean	152
2.2.	Timing of Amerasia Basin opening and rotation of the AACM	159
2.3.	Kolyma–Omolon Superterrane and subduction zone	161
2.4.	NE Asia–Pacific margin/Uda–Murgal arc	162
2.5.	North Pacific/northern North American subduction	163
2.5.1.	The Yukon–Tanana Terrane and the Slide Mountain Ocean	163
2.5.2.	Stikinia and Quesnellia and the Cache Creek Ocean	164
2.5.3.	Wrangellia Superterrane and the Cache Creek Ocean	165
2.5.4.	Summary	167
2.5.5.	Cretaceous deformation	167
3.	New plate model	167
4.	Mantle structure from seismic tomography	168

* Corresponding author at: Madsen Building F09, School of Geosciences, University of Sydney, NSW 2006, Australia. Tel.: +61 2 9351 8093 (office).
E-mail address: grace.shephard@sydney.edu.au (G.E. Shephard).

4.1. Circum-Arctic	168
4.2. North America	170
5. Conclusions	180
Acknowledgements	180
References	181

1. Introduction

One of the most elusive aspects of global plate reconstructions since the breakup of Pangea is the tectonic evolution of the circum-Arctic region, reflecting a paucity of regional datasets, both from within the oceanic basins and from adjacent onshore and offshore continental margins. While significant progress has been made over the last decade with amalgamating geological and geophysical data to generate Phanerozoic plate reconstructions of the Arctic (e.g. Nokleberg et al., 1998a, 2000; Lawver et al., 2002; Golonka, 2011 and references therein), many of these models are limited to reconstructing individual tectonic elements or selected plate boundaries without a consideration of plate

boundary geometries through time, the evolution of adjacent plate margins or the implied history of subduction as imaged by mantle tomography. The construction of more comprehensive models is complicated by a myriad of individual, and often conflicting, observations and inferences, usually from studies focused on a particular region of the circum-Arctic. Furthermore, many attempts at reconstructing the Arctic are limited to a single reconstruction time (i.e. a Myr) or are very broad in terms of reconstruction periods (tens of Myrs). The circum-Arctic has a very complex Phanerozoic history, marked by various periods of compression, extension and deformation, significant changes in geometry, location and dynamics of plate boundaries and multiple reactivation events.

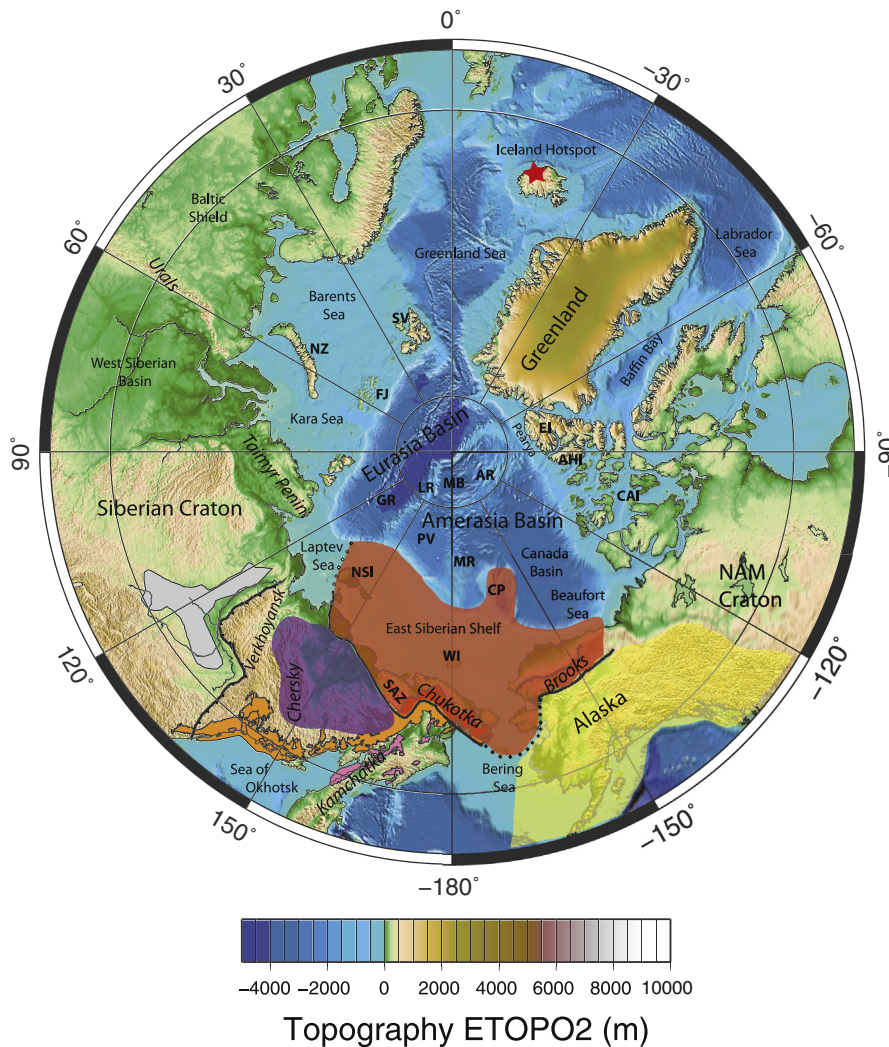


Fig. 1. Topography of the circum-Arctic (ETOPO2) with major topographic and structural features labelled. AHI Axel Heiberg Island, AR Alpha Ridge, CAI Canadian Arctic Islands, CP Chukchi Plateau, EI Ellesmere Island, GR Gakkel Ridge, FJ Franz Josef Land, MB Makarov Basin, MR Mendeleev Ridge, NSI New Siberian Islands, NZ Novaya Zemlya, PV Podvodnikov Basin, SAZ South Anuyi Suture, SV Svalbard, WI Wrangel Island. Shaded polygons are approximate regions: purple Kolyma–Omolon Superterrane, red Arctic Alaska–Chukotka Microplate (AACM), yellow Alaska and northern North America, orange Okhotsk–Chukotka Volcanic Belt, pink Koryak–Kamchatka Volcanic Belt and light grey Viluy LIP. Red star indicates approximate location of present-day Iceland Hotspot.

A present-day elevation map (Fig. 1) shows two major bathymetric features of the Arctic Ocean; the sub-triangular Amerasia Basin and the elongate Eurasia Basin. The evolution of the Eurasia Basin is relatively well constrained with seafloor spreading along the Gakkel Ridge since ~56 Ma (e.g. Vogt et al., 1979; Brozena et al., 2003). Restoration prior to spreading in the Eurasia Basin places the Lomonosov Ridge adjacent to the Barents Shelf. The Amerasia Basin incorporates the Canada, Makarov and Podvodnikov basins, the extended continental crust of the Chukchi Plateau and Borderland, and the Alpha–Mendeleev Ridge. The present-day Canada Basin constitutes a large portion of the Amerasia Basin and has a maximum depth of 4000 m. It is largely bound by the Canadian Arctic Islands to the east and by the Chukchi Borderland to the west. Seismic profiling suggests that the thickness of the oceanic crust within the Canada Basin is 4–8 km, with 6–11 km thick sedimentary cover (Grantz et al., 1990). The Arctic Ocean is surrounded in the western hemisphere by the Canadian Arctic Islands, Greenland and the North American craton and in the eastern hemisphere by the Barents Shelf and the Baltic Shield as well as the Siberian continental shelf and craton.

One of the main tectonic reconstruction challenges is the origin and timing of the opening of the Amerasia Basin. The central location of the Amerasia Basin within the Arctic province makes it a centrepiece in plate tectonic models; however its pre-rift configuration and kinematic development remains elusive. A robust tectonic model accounting for seemingly contrasting observations would yield insights into Arctic palaeo-geography and palaeo-climate, the driving forces of ocean basin closure and opening, and has major implications for resource exploration within the dozens of sedimentary basins of the circum-Arctic. However, nearly all aspects of the proposed models for the opening of the Amerasia Basin including timing, geometry, data sources and the associated interpretations are debated.

Here, we aim to approach these controversies of the pre- and post-opening Amerasia Basin plate configuration by assuming a larger-scale viewpoint; through an extensive review of published data and models we synthesise and reconcile the major tectonic events (Table 1) in a self-consistent and time-dependent rigid plate model, which can then be used to address more regional observations and inferences including extension and compression, and may form the

Table 1

Summary of major plate boundary event timings used in our plate model (directions relative to present-day) with inclusion of earlier events for reference. Main references used to define the explicit timing and reconstruction as integrated in our model are included, and where reasonably modified or refined by this paper this is noted, see manuscript for more details and references therein.

	Feature	Timing	Main references
South Anuyi Ocean and subduction	Rifting and seafloor spreading – formation of SAO	Devonian–Early Mississippian (?)	Zonenshain et al. (1990), Nokleberg et al. (2000) and Sokolov et al. (2002)
	Oloy Arc S–SW dipping	160–140.1 Ma	Nokleberg et al. (2000), Layer et al. (2001) and Shephard et al. (presented here)
	Koyukuk subduction S dipping (Kobuk Sea) and Nutesyn subduction N dipping	160–142.6 Ma	Plafker and Berg (1994), Nokleberg et al. (2000) and Shephard et al. (presented here)
	Koyukuk and Nutesyn subduction N dipping	142.5–120.1 Ma	Plafker and Berg (1994), Nokleberg et al. (2000) and Shephard et al. (presented here)
	Rifting of Amerasia Basin	195–142.6 Ma	Grantz et al. (2011b) and Shephard et al. (presented here)
	Seafloor spreading within Amerasia Basin – Makarov/Podvodnikov basins	142.5–120.1 Ma	Alvey et al. (2008), Døssing et al. (2013) and Shephard et al. (presented here)
Kolyma–Omolon Superterrane	Seafloor spreading within Amerasia Basin – Canada Basin	142.5–126.1 Ma	Alvey et al. (2008)
	Rifting and seafloor spreading – formation of Oimyakon Ocean Basin	Devonian–Early Mississippian (?)	Parfenov (1991), Parfenov et al. (1993) and Nokleberg et al. (2000)
	Back-arc subduction W-dipping/Kolyma–Omolon Superterrane amalgamation * <i>Alternative Model</i>	180–160.1 Ma	Parfenov (1991) and Oxman (2003)
Northern Pacific–NE Asia	Oimyakon E-dipping subduction under Uyandina–Yasachnaya arc	160–140.1 Ma	Nokleberg et al. (2000) and Layer et al. (2001)
	Koni–Taigonos arc and subduction	Triassic–Late Jurassic 160.1 Ma	Nokleberg et al. (2000) and Sokolov et al. (2002)
	Alazeya subduction zone of palaeo-Pacific N dipping * <i>Alternative Model</i>	Late Triassic to Early Jurassic 230 Ma–193 Ma	Nokleberg et al. (2000)
	Uda–Murgal arc N–NW dipping	160 Ma–108.1 Ma	Sokolov et al. (2002, 2009) and Nokleberg et al. (2000)
	Okhotsk–Chukotka arc and volcanic belt N–NW subduction	Cretaceous 108–67.1 Ma	Layer et al. (2001)
Northern Pacific–Alaska and northern NAM	Koryak–Kamchatka arc N–NW subduction	67–55.1 Ma	Parfenov et al. (1993) and Nokleberg et al. (2000)
	Aleutian–Bering arc and subduction	~55 Ma	Nokleberg et al. (2000)
	Arc magmatism and formation of Yukon–Tanana Terrane	Early Devonian (~385 Ma)	Nelson et al. (2006)
	Slab roll back, backarc rifting and seafloor spreading of Slide Mountain Ocean	Late Devonian to Carboniferous 360 (possibly 320) Ma	Plafker and Berg (1994), Nokleberg et al. (2000) and Nelson et al. (2006)
	Cessation of spreading Slide Mountain Ocean, polarity reversal, formation of main episode of Stikinia and Quesnellia arcs	260 Ma	Nokleberg et al. (2000) and Nelson et al. (2006)
	Relative rotation between Stikinia and Quesnellia	260–230 Ma	Nokleberg et al. (2000) and Mihalyuk et al. (1994)
	Opening of the Cache Creek Ocean	260–230 Ma	Nokleberg et al. (2000) and Shephard et al. (presented here)
	Subduction and closure of Slide Mountain and collision of Yukon–Tanana–Stikinia–Quesnellia terranes	230 Ma	Nokleberg et al. (2000), Nelson et al. (2006) and Seton et al. (2012)
	Accretion of Wrangellia Superterrane and closure of Cache Creek Ocean	140 Ma	Nokleberg et al. (2000), Trop et al. (2002) and Shephard et al. (presented here)
	Talkeetna–Bonanza arc	Late Triassic to Early Jurassic 230–185.1 Ma	Nokleberg et al. (2000) and Shephard et al. (presented here)
Gravina arc	Late Jurassic–Early Cretaceous 185–140 Ma	Nokleberg et al. (2000) and Shephard et al. (presented here)	

Table 2
Summary of acronyms used in reconstructed terrane and ocean features of our preferred model, as in Figs. 2–10.

Acronym	Name	Plate ID	Feature type	Comment
<i>Region 1 Northeast Siberia</i>				
AL	Alazeya arc and uplift	43205	Terrane (KOST)	See Table 1, accreted island-arc ^a
BE	Bering Shelf	16140	Terrane	Cretaceous–Palaeogene arc and back-arc units ^a over Paleozoic and Mesozoic fragments
BSW	Bering–Seward	43300	Terrane (AACM)	Part metamorphosed continental margin ^a
CH	Chukotka	43300	Terrane (AACM)	Passive continental margin ^a
CS	Chersky Range	43202	Terrane (KOST)	Overlapping Mid-Jurassic and Early Cretaceous arc and backarc terranes ^a
DL	De Long uplift	42100	Terrane (AACM)	Pre-Cambrian craton or Caledonian or Ellesmerian, “massif,” affinity to North Ellesmere Island, partly affected by HALIP ^b
EK	East Kamchatka	44100	Terrane	Island arc fragments ^a
EKO	East Kamchatka–Okhotsk	44103	Terrane	Island arc fragments ^a part overlapped by Okhotsk–Chukotka and Koryak–Kamchatka Volcanic Belts
EL	East Laptev	401	Terrane	Related to opening of Eurasia Basin
ES	East Siberia Shelf	42200	Terrane (AACM)	Mesozoic foreland basin (Late Mesozoic fold belts) beneath Cenozoic sediments? ^b
HO	Hope Basin	42300	Terrane	Transtensional basin ^b
KK	Koryak–Kamchatka	44102	Terrane	Island arc and oceanic fragments ^a part overlapped by Okhotsk–Chukotka and Koryak–Kamchatka Volcanic Belts
KN	Kotel'nyi	42101	Terrane	Passive margin Mid Ordovician–Upper Devonian ^b
KO	Kolyma Range	43200	Terrane (KOST)	Related to KOST collision, Overlapping Mid-Jurassic and Early Cretaceous arc and backarcs ^a
KOB	Kobuk Sea	(18100)	Ocean	See Table 1
KOST	Kolyma–Omolon Superterrane	43200	Plate	See Table 1
LA	Laptev Sea	42400	Terrane	Related to opening Eurasia Basin
MOK	Mongol–Okhotsk	380	Ocean	Prior to collision of Asia with Siberian Craton
NC	North Chukchi Basin	18203	Terrane	Mesozoic foreland basin (Late Mesozoic fold belts) beneath Cenozoic sediments?
NK	North Kamchatka	44101	Terrane	Island arc and oceanic fragments ^a part overlapped by Koryak–Kamchatka Volcanic Belt
NV	Novaya Block	42102	Terrane (AACM)	Transtensional basin ^b
OB	Outer Bering	16141	Terrane	Oceanic, Mid-Late Tertiary back-arc units and abyssal plains ^a
OK	Okhotsk	43400	Terrane	Siberian cratonal affinities ^a part overlapped by Okhotsk–Chukotka Volcanic Belt
OL	Oloy	43206	Terrane (KOST)	Accreted island-arc ^a
OM	Omolon	43201	Terrane (KOST)	Siberian cratonal affinities ^a
OMY	Oimyakon Ocean	401	Ocean	See Table 1
OV	Omulevka	43204	Terrane (KOST)	Passive continental margin ^a
PK	Prikolyma	43203	Terrane (KOST)	Passive continental margin ^a
SAO	South Anuyi Ocean	41200	Ocean and Plate	See Table 1
SAZ	South Anuyi Suture Zone	42201	Terrane (AACM)	Oceanic ^a highly deformed, separates KOST and AACM
SC	(Southern) North Chukchi Basin	18202	Terrane	Franklinian basement under Mesozoic foreland basin beneath Cenozoic sediments? ^b
SIB	Siberian Craton	401	Terrane	Fixed to Eurasia (301) for period of our model
VI	Vil'kitski Trough Basin	42103	Terrane (AACM)	“Pre-Cenozoic/Post Ellesmerian” multi-phase rift basin ^b
VG	Viligia	43400	Terrane	Passive continental margin ^a
VL	Vetlovskiy	44100	Terrane	Oceanic ^a
WI	Wrangel Island Terrane	42300	Terrane (AACM)	Neoproterozoic metamorphosed rocks, Mesozoic foreland basin (Late Mesozoic fold belts) beneath Cenozoic sediments? ^b
WV	Western Verkhoysansk	43101	Terrane	Related to KOST collision, see Table 1, underlain by Riphean to Mid Palaeozoic carbonate-clastics ^b
YA	Yarakvaam	43207	Terrane (KOST)	Accreted island-arc ^a
<i>Region 2 Arctic Ocean and Amerasia Basin</i>				
AACM	Arctic–Alaska Chukotka Microplate	18100	Plate	See Table 1, Siberian, Baltican and Laurasian affinities, Passive continental margin ^a
AM	Amerasia Basin	101/42100	Ocean	See Table 1
CK	Chukchi Plateau	113, 18200	Terrane (AACM)	Post Ellesmerian platform with Cenozoic extension (Northwind Basin) ^b
ESM	East Siberia Microplate	42150	Plate	Division of AACM, see Table 1
EU	Eurasia Basin	114, 301	Ocean	Oceanic, rifting from ~53 Ma
LO	Lomonosov Ridge	114	Terrane	Related to opening Eurasia Basin
NSM	North Slope Microplate	18150	Plate	Division of AACM, see Table 1
<i>Region 3 North America and Panthalassa</i>				
AN	Angayucham	18103	Terrane	Oceanic ^a
AU	Aleutian arc terrane	16130	Terrane	Accreted island-arc ^a , see Table 1
AX	Alexander Terrane	16111	Terrane	Part of Wrangellia Superterrane, Accreted island-arc ^a , “Insular” NAM terrane group ^c , assumed Baltican affinity
CA	Cassiar	16106	Terrane	Passive continental margin ^a “Inboard” NAM terrane group ^c
CC	Cache Creek Terrane	16113	Terrane	Oceanic ^a , “Intermontane” NAM terrane group ^c
CCR	Cache Creek Ocean	131	Ocean and Plate	Part of Panthalassa Ocean, see Table 1
CG	Chugach	16121	Terrane	Oceanic and part turbidite ^a
d NAM	deformation	101	Line feature	Western limit of Cordilleran deformation ^c
FAR	Farallon Plate	902	Plate	Part of Panthalassa Ocean
FW	Farewell–Dillinger–Mystic	18104	Terrane	Passive continental margin ^a
GO	Goodnews	18105	Terrane	Oceanic ^a
IZA	Izanagi Plate	926	Plate	Part of Panthalassa Ocean
KY	Koyukuk	18106	Terrane	See Table 1, accreted island-arc ^a
KT	Kootenay	16107	Terrane	“Inboard” NAM terrane group ^c
m	Metamorphic rocks	16124	Terrane	“Intermontane” NAM terrane group ^c
NAM	NAM Craton	160, 101	Terrane	“Inboard” NAM terrane group ^c
NS	North Slope	103	Terrane (AACM)	Passive continental margin ^a
NXF	Nixon Fork	18104	Terrane	Passive continental margin ^a
PE	Peninsula	16112	Terrane	Part of Wrangellia Superterrane, Accreted island-arc ^a , “Insular” NAM terrane group ^c

(continued on next page)

Table 2 (continued)

Acronym	Name	Plate ID	Feature type	Comment
QS	Quesnellia	16102	Terrane	Accreted island-arc ^a , related to Slide Mountain, see Table 1, “Intermontane” NAM terrane group ^c
RCO	Ruby–Coldfoot	18102	Terrane	Metamorphosed continental margin ^a
RU	Ruby	18102	Terrane	Metamorphosed passive continental margin ^a
SM	Slide Mountain Terrane	16103	Terrane	Oceanic ^a , “Intermontane” NAM terrane group ^c
ST	Stikinia	16101	Terrane	Accreted island-arc ^a , related to Slide Mountain, see Table 1, “Intermontane” NAM terrane group ^c
TG	Togiak	18108	Terrane	Accreted island-arc ^a
WR	Wrangellia	16110	Terrane	Part of Wrangellia Superterrane, Accreted island-arc ^a , “Insular” NAM terrane group ^c
YK	Yakutat	16123	Terrane	Turbidite ^a and oceanic plateau
YTT	Yukon–Tanana	16104	Terrane	Passive continental margin ^a , related to Slide Mountain, see Table 1, “Intermontane” NAM terrane group ^c
YTU	Yukon–Tanana Upland	16105	Terrane	“Inboard” NAM terrane group ^c

^a Nokleberg et al. (2000).

^b Drachev et al. (2010).

^c Colpron et al. (2007).

basis for developing models that account for the many phases of plate deformation. Complementary to our discussion of major rifting, seafloor spreading and subduction events and a refined plate kinematic model, we also present for the first time, an analysis of deep mantle structure inferred from the long history of circum-Arctic subduction. We review mantle structure including slabs imaged by seismic tomography models and link them temporally and spatially to the subduction zones of our plate model.

The tectonic history of the circum-Arctic cannot be reconstructed without a regional consideration of the adjacent continental margins of NE Asia and North America (NAM), of which both have experienced extensive subduction, compression, extension and island arc formation/evolution during the Mesozoic and Cenozoic. We summarise changes in plate motions based on the major subduction zones involved, and below group them into five main regions/events (Fig. 1) (Tables 1 and 2):

- (1) Collision of the Arctic Alaska–Chukotka Microplate (AACM) and Siberia and the destruction of an intervening ocean basin (South Anuyi Ocean).
- (2) Opening of the Amerasia Basin and rotation of the AACM.
- (3) Kolyma–Omolon Superterrane (KOST) collision with Siberia and the destruction of the intervening ocean basin (Oimyakon Ocean).
- (4) Subduction of Panthalassa under NE Asia and associated arc accretion.
- (5) Subduction of Panthalassa under Alaska and North America and associated arc accretion.

We refer to “Siberia” when describing the main continental portion of NE Asia comprising the Siberian Craton (which is attached to Eurasia during our reconstruction times) and also later when the Kolyma–Omolon Superterrane collides and accretes to this unit. We also use the term “Amerasia Basin” for the region between the Lomonosov Ridge and North American/Russian shelf and restrict the use of “Canada Basin” to the southern part of the Amerasia Basin between the Alpha–Mendeleev Ridge and North America. Unless otherwise specified, we refer to the relative locations between terranes or tectonic features with respect to present-day e.g. the eastward-dipping subduction zone of the Oimyakon Basin under the Kolyma–Omolon Superterrane, and the southern margin of the AACM prior to its counter-clockwise rotation. Subduction zones are herein referred to by the same name as their arc counterparts as previously discussed in the literature e.g. Oloy arc of Nokleberg et al. (2000) is now applied to the associated Oloy subduction zone.

2. Discussion of regional tectonics

2.1. The South Anuyi Ocean

Evidence for an ocean basin, known as the South Anuyi Ocean (SAO), located between Siberia and Laurentia in the Late Jurassic

before the rotation of the AACM is expressed along the South Anuyi Suture. This suture zone (SAZ, Figs. 1 and 2), stretching from near the New Siberian Islands through to the North Slope of Alaska, is up to 200 km wide and is delineated by ophiolites, turbidites, arc magmatism, granites and granodiorites and plutons (e.g. Rowley and Lottes, 1988; Zonenshain et al., 1990; Parfenov, 1991; Sokolov et al., 2002, 2003; Grantz et al., 2011a). Evidence for the suture zone is best preserved in the region north of the KOST (Fig. 2), however, the continuation of this suture zone offshore and to the west near the New Siberian Islands is contentious (Fig. 1) (e.g. Drachev et al., 1998; Lawver et al., 2002; Franke et al., 2008). Disparity in the continuation of the suture zone might largely be a function of ophiolite preservation, exposure due to younger deformation and sedimentary and glacial debris cover. It is largely agreed that the opening of the Amerasia Basin was contemporaneous with the destruction of the SAO along one or more subduction zones along both the southern margin of the AACM and the opposing northern margins of Siberia (Figs. 3–6). In alternative models, the SAO is sometimes described as being adjacent to, or included within the broader “Angayucham Ocean” and “Goodnews Ocean” or even the “palaeo-Pacific.” The relative locations of Laurentia and Siberia constrain the maximum limits of the SAO, and in our preferred model we refer to this entire region behind the convergent margin with the palaeo-Pacific as the SAO (Figs. 3–8, S1).

While noting great uncertainty in timing and plate boundary configuration, various authors (e.g. Zonenshain et al., 1990; Sokolov et al., 2002) suggest that the SAO existed between Siberia and Laurentia since opening in the Middle-Late Palaeozoic. Prior to this opening, several authors suggest a possible collision of Siberia (and Baltica) with Laurentia in the Silurian or Devonian, possibly during the Ellesmerian orogeny or the Scandian phase of the Caledonian orogeny (Trettin, 1991; Kos'ko et al., 1993; Lawver et al., 2002, 2011). The collision between Siberia and Laurentia, which saw the subduction of the Lapetus Ocean, is thought to have led to the transfer of Chukotka from the Siberian to Canadian margin, as well as the Pearya terrane to Ellesmere Island (Fig. 1) (Trettin, 1991; Kos'ko et al., 1993; Lawver et al., 2002, 2011). The accretion of components of the AACM to Laurentia was followed by a clockwise rotation of Siberia away from Laurentia towards Baltica and Kazakhstan. The subsequent rifting and seafloor spreading is inferred to have formed the SAO, or part thereof, and it may have connected to the ocean basins of Taimyr and the Polar Urals (Sokolov et al., 2002). Lawver et al. (2002) suggested that a mantle plume caused this rifting event, with the Oimyakon Basin (successful rift), and the Viluy Large Igneous Province and basin (failed rift) (Fig. 1) representing two arms of a plume-generated triple-junction. Kuzmin et al. (2010) support the notion that the Viluy Large Igneous Province was linked to a hotspot that may have existed before 400 Ma and suggest that during the Early Silurian to Late Devonian (435–360 Ma) a ~30° clockwise rotation of Siberia was not accompanied by significant changes in palaeo-latitude or longitude.

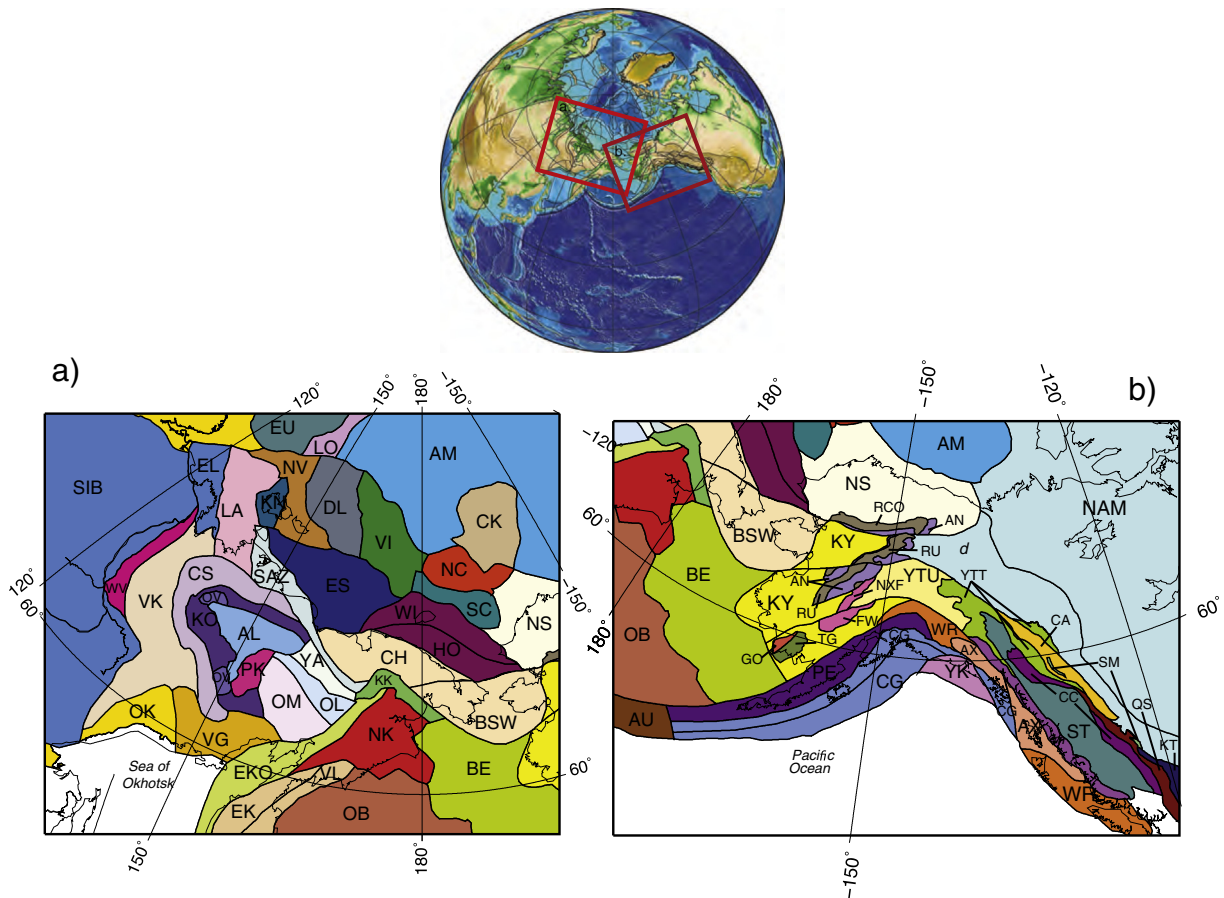


Fig. 2. Simplified set of major tectonic features and provinces of the circum-Arctic at present-day used in our reconstructions. Polygons filled according to Plate ID (Table 2). (a) Siberian terranes including parts of the Arctic Alaska–Chukotka Microplate, the Kolyma–Omolon Superterrane. AL Alazeya Arc and uplift, AM Amerasia Basin, BE Bering Shelf, BSW Bering–Seward, CH Chukotka, CK Chukchi Plateau, CS Chersky Range, DL De Long uplift, EK East Kamchatka, EKO East Kamchatka–Okhotsk, EL East Laptev (Siberia), EU Eurasia Basin, ES East Siberia Shelf, HO Hope Basin, KK Koryak–Kamchatka, KN Kotel’nyi, KO Kolyma Range, LA Laptev Sea, LO Lomonosov Ridge, NC North Chukchi Basin, NK North Kamchatka, NS North Slope (Arctic Alaska), NV Novaya Block, OB Outer Bering, OK Okhotsk, OL Oloy, OM Omolon, OV Omulevka, PK Prikolyma, SAZ South Anuyi (Suture) Zone, SC Southern North Chukchi Basin, SIB Siberian Craton, VI Viil’kitski Trough Basin, VG Viligia, VL Vetlovskiy, WI Wrangel Island, WV Western Verkhoyansk, YA Yarakvaam. (b) Alaska and North America. AM Amerasia Basin, AN Angayucham Terranes, AU Aleutian Arc, AX Alexander Terrane (Wrangellia Superterrane), BE Bering Shelf, BSW Bearing–Seward, CA Cassiar Terrane, CC Cache Creek, CG Chugach, *d* NAM west of eastern limit of Cordilleran deformation, GO Goodnews, FW Farewell–Dillinger–Mystic, KY Koyukuk, KT Kootenay, *m* metamorphic rocks, NAM North America (miogeocline), NS North Slope (Alaska), NXF Nixon–Fork, OB Outer Bering, PE Peninsula (Wrangellia Superterrane), QS Quesnellia, RCO Ruby–Coldfoot, RU Ruby, SM Slide Mountain, ST Stikinia, TG Togiak, WR Wrangellia (Wrangellia Superterrane), YK Yakutat, YTT Yukon–Tanana, YTU Yukon–Tanana Upland (North America Basinal).

This Latest Devonian to at least Early Mississippian rifting within the SAO was followed by sporadic or very slow seafloor spreading since the Pennsylvanian (Nokleberg et al., 2000) and may also account for the rifting of Alaskan terranes e.g. the Nixon Fork, Dillinger, Mystic and Kilbuck–Idono terranes (Fig. 2), which are thought to be of a NE Asian origin (e.g. Nokleberg et al., 2000; Blodgett et al., 2002 and references therein). This rifting may also account for the opening of the Oimyakon Ocean Basin (Figs. 4 and 5), which separated the terranes of the Kolyma–Omolon Superterrane from Siberia (Zonenshain et al., 1990; Nokleberg et al., 2000; Lawver et al., 2002). Furthermore, this event was broadly contemporaneous with arc magmatism beginning around 385 Ma and maybe an early phase of extension and rifting further east along the NAM margin including Yukon–Tanana Terrane and opening of the Slide Mountain Ocean (Figs. 2 and 9) (Nelson et al., 2006). A continental margin arc termed the Koni–Taigonos (or Kedon) arc and an associated subduction zone is described to have operated outboard of these rifting events, reaching from the Siberian and northern Laurentian margins at this time (Fig. 4) (Nokleberg et al., 2000; Sokolov et al., 2002). However, Nokleberg et al. (1998a) show long-lived, but likely slow or intermittent, seafloor spreading occurring within the SAO from the Devonian until at least ~163 Ma. Therefore, there is debate about

whether the SAO compares to an embayment of the palaeo-Pacific (e.g. Nokleberg et al., 2000) (Fig. 10) or was located behind a convergent margin running from Siberia to NAM (e.g. Parfenov, 1997) (Figs. 4 and 5). Sokolov et al. (2002) suggest that during at least the Late Jurassic–Early Cretaceous, or possibly since the late Palaeozoic, the SAO was separated from the Pacific by a convergent margin. They suggest a link along the Koni–Taigonos and Uda–Murgal arcs and subduction zones through the southern part of Chukotka and onto Alaska (see Section 2.4). Furthermore, Mihalyuk et al. (1994) propose that the Alexander terrane (of the Wrangellia Superterrane) forms part of this collisional setting, lying between the Kolyma–Omolon Superterrane and the Yukon–Tanana Terrane (see Section 2.5) in at least the “Pre-Triassic.”

Furthermore, Colpron and Nelson (2009) provide an extensive discussion of Palaeozoic affinities for terranes along the NAM Cordillera and suggest an alternative model for the Laurentian margin, which challenges some aspects of the above summary for the opening of the SAO. They propose that the Siberian, Baltican and Caledonian affinities of several outboard terranes including the basement of the Quesnellia arc, Farewell, Arctic Alaska and Alexander terranes (partial basement of the future Wrangellia Superterrane) (Fig. 2) can be explained through “Scotia-style” subduction and the creation of a “Northwest

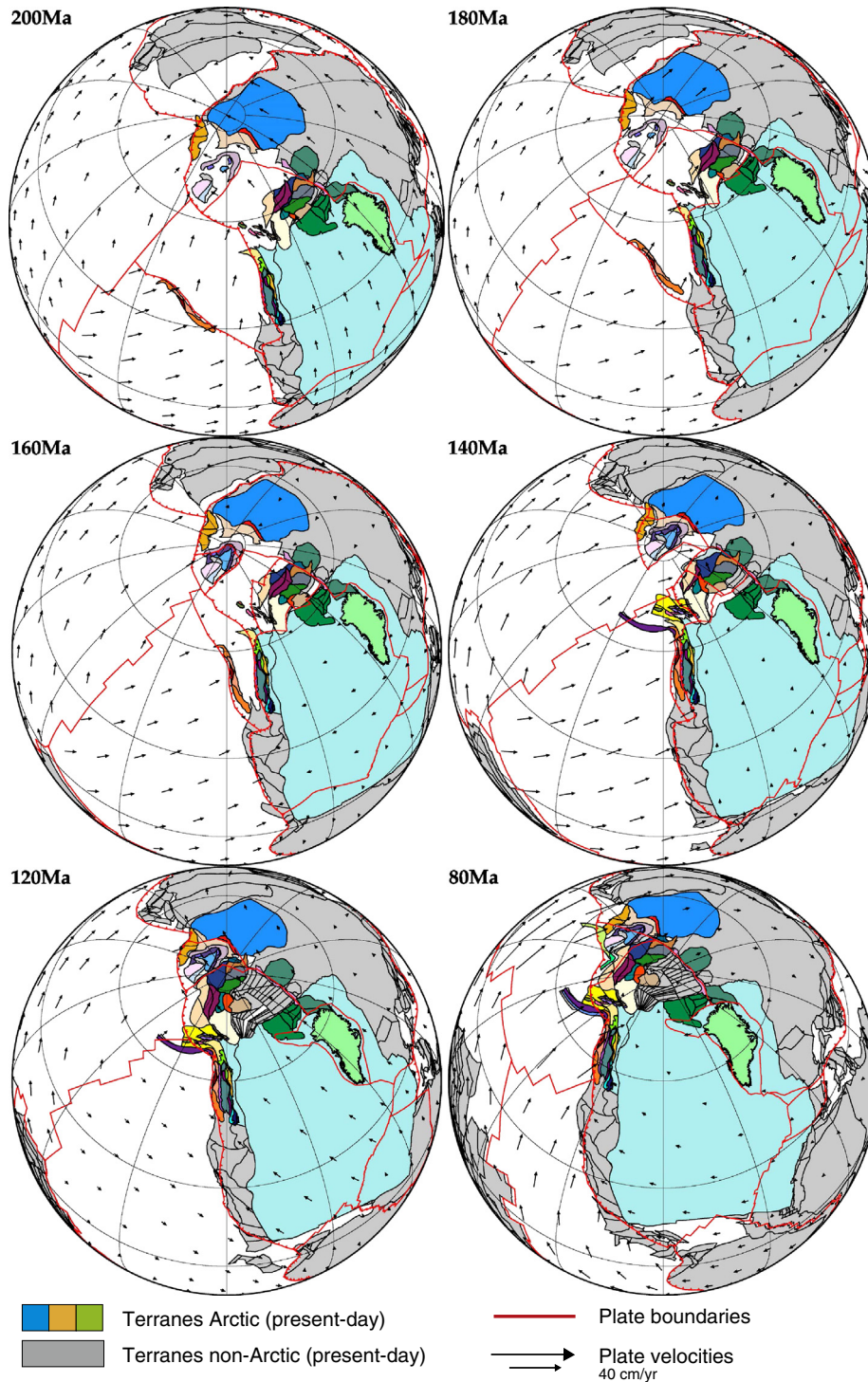


Fig. 3. Orthographic maps of our preferred plate model for the circum-Arctic for selected timesteps between 200 Ma and 80 Ma. Reconstructed present-day terranes and tectonic features (as in Fig. 2) coloured for circum-Arctic regions and grey for rest of world, plate boundaries in red. Other timesteps can be found in Fig. S1. Velocities in black, see inset for scale.

Passage.” The sinistral transpressive zone along western Laurentia (Canadian side) during the Devonian is described to account for the southward-movement of these terranes. The westward rollback of this subduction zone towards Panthalassa is suggested to be the cause of Devonian rifting of the Yukon–Tanana Terrane and opening of the Slide Mountain Ocean and by implication, we also suggest, the opening of the SAO. While a complete discussion of Palaeozoic tectonics predates the time range upon which we focus, their suggested cause of rifting does

not preclude the contemporaneous opening of the Oimyakon Ocean Basin and motion of the terranes of the Kolyma–Omolon Superterrane (see Section 2.5, Fig. 9). Regardless of the cause i.e. rotational rifting of Siberia away from Laurentia versus Scotia-style subduction rollback, the majority of the SAO is suggested to have opened by the end of the Carboniferous.

According to Nokleberg et al. (2000) and references therein, prior to the opening of the Amerasia Basin, the following subduction

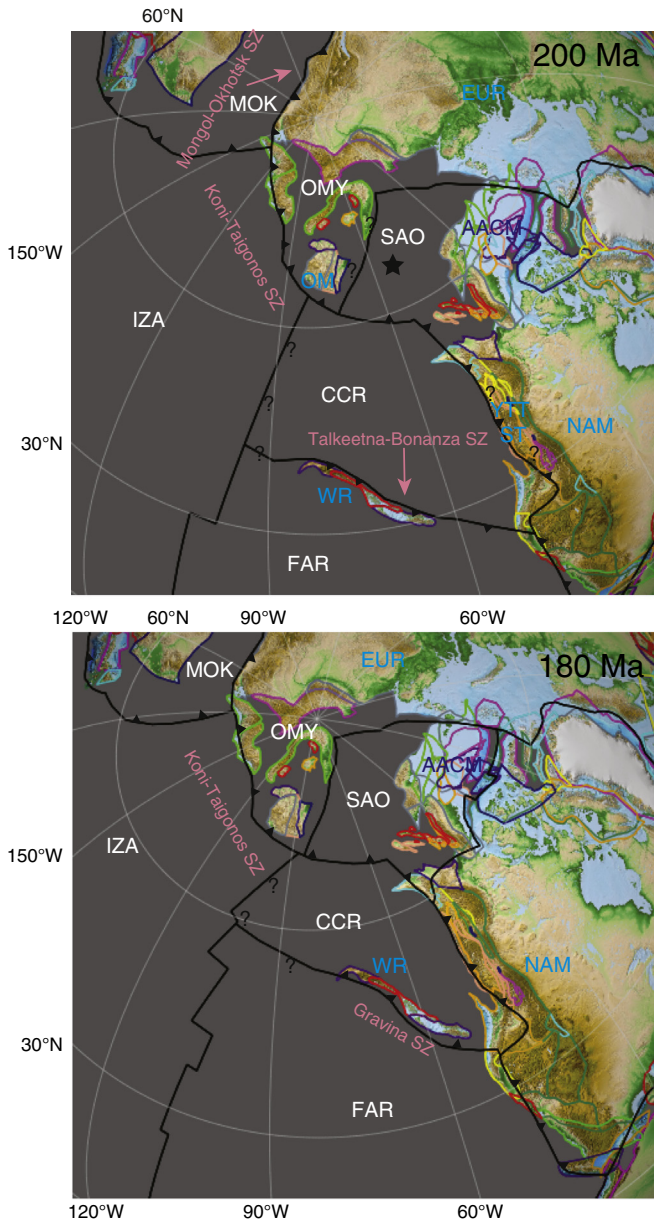


Fig. 4. Regional map of our preferred circum-Arctic model at 200 Ma and 180 Ma as viewed in GPlates (orthographic map projection) overlain with labels. Topography raster (ETOPO2) cookie cut to time-dependent reconstructed terranes (Fig. 2). Oceanic plates/basins labelled in white; CCR Cache Creek Ocean, FAR Farallon, IZA Izanagi, MOK Mongol–Okhotsk, OMY Oimyakon, SAO South Anuyi Ocean. Selected terranes labelled in blue as in Fig. 2. Subduction and associated arcs labelled in pink. Note that the accreted NAM and Alaskan terranes (Yukon–Tanana Terrane and Wrangellia Superterrane) are in present-day relative positions and do not incorporate any Cenozoic strike-slip or deformation (see in text). At 200–180 Ma the SAO is located behind a subduction zone, Koni–Taigonos, running continuously from near the MOK to along the western Laurentian margin. Star denotes that alternative ‘embayment’ model exists (Fig. 10). Wrangellia Superterrane migrating north–northeast towards the Laurentian margin. At 200 Ma subduction polarity along the Talkeetna–Bonanza arc is to the south–southwest, with the Cache Creek Ocean being subducted under the Farallon Plate. Subduction along western Laurentia is not necessary to subduct the Cache Creek from 200–185 Ma but is included for consistency and to link with the Koni–Taigonos arc. At 185 Ma subduction polarity along the Wrangellia Superterrane switches to dipping to the north–northeast along the Gravina arc inferring trench advance and Farallon subduction under the Cache Creek Ocean. Intersection between Talkeetna–Bonanza and Gravina arcs and the IZA–FAR–CCR mid-ocean ridge simplified with a transform boundary, however, configuration is likely more complicated. Rifting has commenced in the Amerasia Basin at 195 Ma, and at this time the SAO and AACM are located on a single plate.

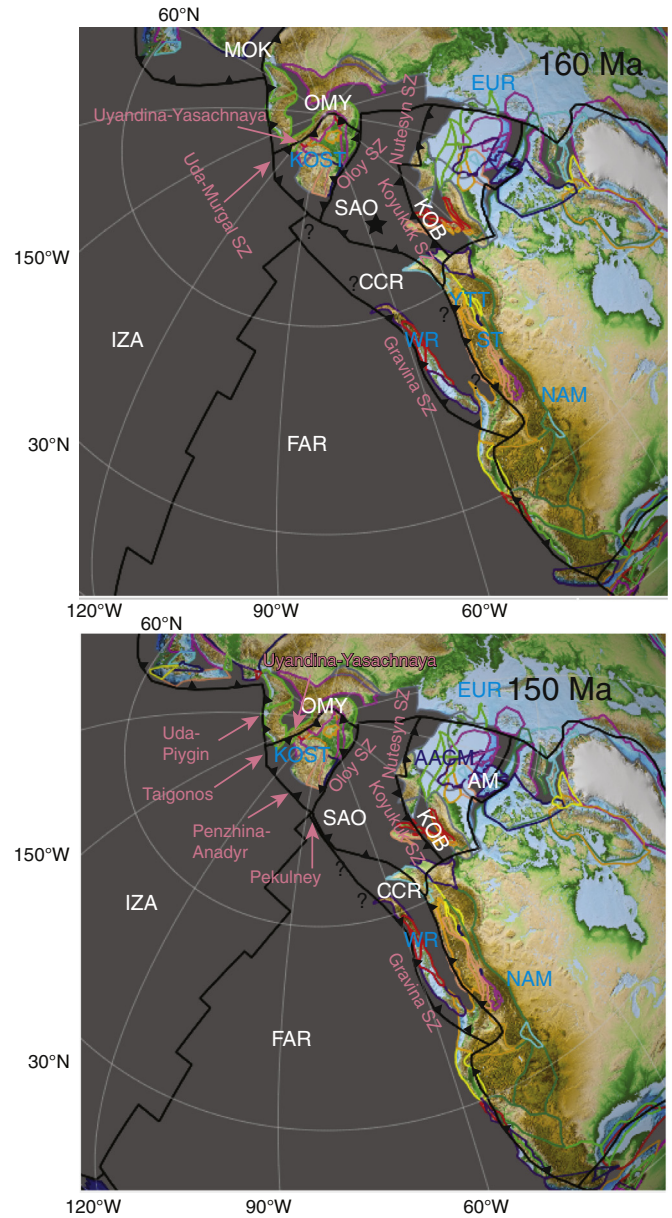


Fig. 5. Regional orthographic map of our preferred circum-Arctic model at 160 Ma and 150 Ma as viewed in GPlates. Labels as in Fig. 4. Star denotes that alternative ‘embayment’ model that exists (Fig. 10). At 160–150 Ma east-dipping subduction (relative to present-day) of the Oimyakon Ocean under the Kolyma–Omolon Superterrane (KOST) has commenced, the Kobuk Sea (KOB) is being subducted beneath the Koyukuk subduction zone, SAO is being subducted under the northern KOST margin along the Oloy subduction zone. The boundary between the SAO and AACM plates are now delineated and rifting is continuing in the Amerasia Basin. Outboard Uda–Murgal subduction margin is running from Siberia to Laurentia (further arc segment naming shown at 160 Ma). Wrangellia Superterrane is further approaching the Laurentian margin.

history is implied along the northern Siberian and Kolyma–Omolon Superterrane margin: from ~230 Ma an Alazeya island arc and subduction zone subducted part of the “ancestral Pacific Ocean” and “moved toward” the Omulevka terrane (of the later Kolyma–Omolon Superterrane), inferring trench advance (Figs. 4 and 10). The Alazeya arc is described to have existed from at least the Late Triassic, or possibly as early as the mid or late Palaeozoic, to the Early Jurassic when it was accreted to the Kolyma–Omolon Superterrane. How and if the Alazeya arc linked to, or was a segment of, the Koni–Taigonos arc is ambiguous during these periods. Parfenov (1991) suggests that the Alazeya subduction zone subducted the palaeo-Pacific from the Carboniferous to the Late Jurassic. Nokleberg et al. (2000) suggest a

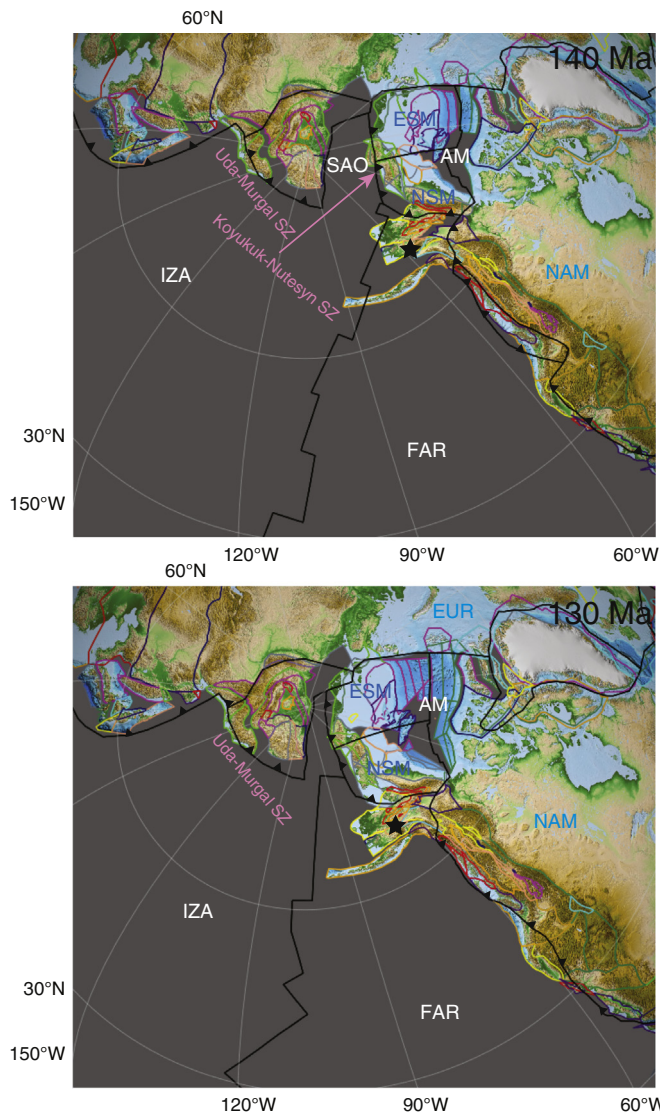


Fig. 6. Regional orthographic map of our preferred circum-Arctic model at 140 Ma and 130 Ma as viewed in GPlates. Labels as in Fig. 4. Star denotes that Arctic terranes are located in their relative present-day position and may be located further south along the NAM (behind the subduction zone) at this time. Seafloor spreading has commenced in the Amerasia Basin at 142.5 Ma with the AACM now being divided into the two microplates; North Slope (NSM) and Eastern Siberian (ESM). IZA–FAR–CCR ridge now propagated into the SAO, and SAO is being subducted along the Koyukuk–Nutesyn subduction zone. Wrangellia Superterrane recently accreted to the Laurentian margin with subduction jumping outboard.

correlation of the Alazeya arc and the mid-late Palaeozoic rocks of the Carboniferous Skolai arc of the Wrangellia Superterrane, which also matches the described Caledonian affinity for the Alexander terrane (Colpron and Nelson, 2009). The authors also suggest that the SAO as opposed to the “ancestral Pacific Ocean” or the Angayucham Ocean is behind the Alazeya arc and is not being subducted during the Late Jurassic (Figs. 3 and 4, S1). This is in contrast to other models, which suggest partial subduction of the SAO since at least the Late Palaeozoic or Middle Triassic to Middle Jurassic through a combination of the Alazeya and Oloy subduction systems (alternative spelling, Oloi, Oloy–Svyotov Nos or Oloi–Alazeya; Zonenshain et al., 1990; Sokolov et al., 2002, 2009) (Fig. 5). However, there appears to be ambiguity with reference to the Alazeya and Oloy arcs and whether they are a linked and contemporaneous system of arcs or sequential in time. For example Zonenshain et al. (1990) attribute Middle Triassic to Middle Jurassic-aged arc material within the Kolyma–Omolon Superterrane to the subduction near the “Oloi–Alazeya” arc, however,

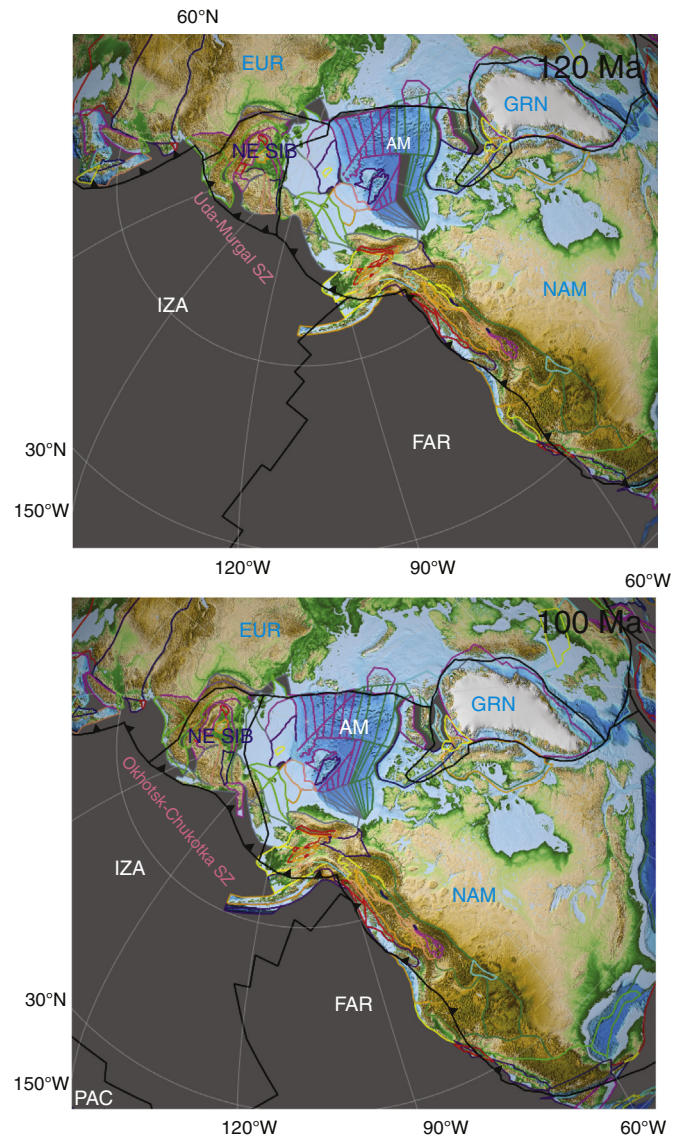


Fig. 7. Regional orthographic map of our preferred circum-Arctic model at 120 Ma and 100 Ma as viewed in GPlates. Labels as in Fig. 4. The Amerasia Basin has completed opening and subduction has now resumed running from the Siberian to western Laurentian margin, including the Uda–Murgai and later Okhotsk–Chukotka subduction zones.

also describe an “Oloi” arc of Upper Jurassic–Lower Cretaceous age (also shown in Sengör and Natal’in, 1996). Various authors refer to either a linked onstrike system i.e. Alazeya–Oloy arc as early as the Carboniferous (e.g. Sokolov et al., 2002, 2009) or separate system i.e. Alazeya arc and a later Oloy arc (e.g. Parfenov et al., 1993; Parfenov, 1997; Nokleberg et al., 2000) (Fig. 10). For simplicity and the evidence of separate arc histories, discussed below, we have chosen to separate these arcs temporally in our reconstructions (Figs. 4–6, 10).

From around the Bathonian (~193 Ma) the Alazeya arc and subduction zone is described to have undergone a polarity reversal and migrated towards the Kolyma–Omolon Superterrane (Nokleberg et al., 2000). How the Alazeya arc links to the Koni–Taigonos arc to the west and the Laurentian subduction zone to the east during this period of rollback and polarity reversal is also ambiguous. From around the Oxfordian (~163 Ma) the Oimyakon Ocean Basin was subducted along an eastward-dipping Uyandina–Yasachnaya subduction zone (Fig. 5) (see Section 2.3) (Nokleberg et al., 2000). It is possible that the described Alazeya polarity reversal represents either the inception of the Uyandina–Yasachnaya subduction zone or possibly the subduction of a back-arc within the Kolyma–Omolon Superterrane

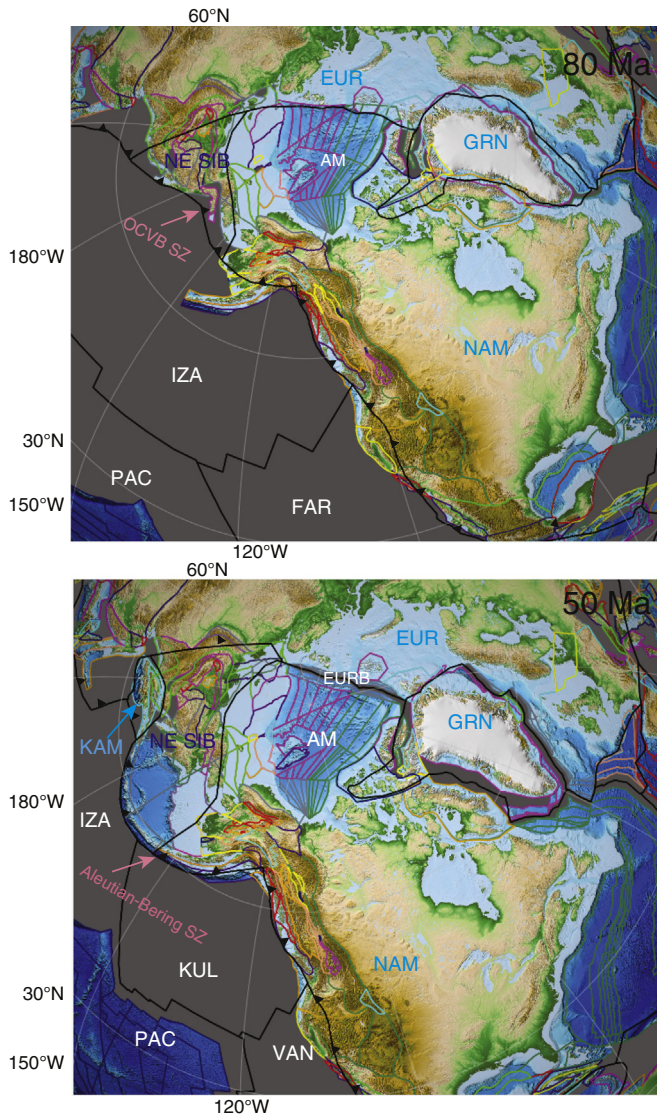


Fig. 8. Regional orthographic map of our preferred circum-Arctic model at 80 Ma and 50 Ma as viewed in GPlates. Labels as in Fig. 4. Progressive southward stepping of subduction along northern Panthalassa including the Okhotsk–Chukotka (OCVB) subduction, Koryak–Kamchatka and Aleutian–Bering subduction. Counter-clockwise rotation of Kamchatka microplate (KAM) and opening of Eurasia Basin (EURB) has commenced. The Izanagi Plate breaks into Kula Plate (KUL) and the Farallon Plate into the Vancouver (VAN) plate at 79 Ma and 53 Ma, respectively.

which is thought to have occurred from ~180 to 160 Ma (Parfenov, 1991; Oxman, 2003) (Section 2.3, Fig. 10). Also around this Mid to Late Jurassic time, part of the SAO was subducted under the northern margin of the Kolyma–Omolon Superterrane into a south–southwest dipping subduction zone associated with the Oloy arc (Fig. 5) (Parfenov et al., 1993; Nokleberg et al., 2000).

Furthermore, during the closure of the SAO, subduction zones associated with the Koyukuk and Nutesyn arcs (also referred to as Kulpolney or Togiak–Koyukuk) (Figs. 3, 5 and 6, S1) were located along the opposing margin of the AACM (e.g. Nokleberg et al., 2000; Sokolov et al., 2002, 2009). According to Nokleberg et al. (2000) the Nutesyn and Koyukuk arc existed from the Late Jurassic to mid-Cretaceous and associated subduction led to the accretion of the oceanic Velmay (within Bering–Seward terrane), Goodnews and Angayucham terranes and related island-arc terranes of Nutesyn, Koyukuk, Nyac (within Koyukuk terrane) and Togiak (Fig. 2, Table 2). Stratigraphic data suggest that, during the Late Proterozoic,

much of proto-Alaska and adjacent terranes including the Chukotka–Wrangell regions represented an Atlantic-type passive continental margin that faced the Palaeo-Pacific (Nokleberg et al., 2000). The Nutesyn arc is described as a continental margin arc with subduction dipping under the AACM (Parfenov, 1997). However, the adjacent Koyukuk subduction zone dipped initially towards the SAO (intraoceanic) leading to the subduction of the “Kobuk Sea” (Plafker and Berg, 1994) until its accretion around 160–145 Ma. Subduction polarity then flipped along the Koyukuk arc and subduction zone to match the Nutesyn arc system (Figs. 5 and 6). In this reversal model (Plafker and Berg, 1994; Nokleberg et al., 2000), the Koyukuk arc and subduction zone subducted part of the Kobuk Sea from perhaps as early as the Mid-Jurassic. Shortening of 200–500 km along the southern region of AACM has been suggested during the collision of the Koyukuk arc (Plafker and Berg, 1994). In contrast, Parfenov (1997) suggests that the Koyukuk arc was formed in the Early and Middle Jurassic during the continued seafloor-spreading within the SAO and accreted in the Late Jurassic. In either case, a subduction zone along the southern margin of the AACM is inferred to have consumed the majority of the SAO, culminating in the collision of the AACM and Siberia, as opposed to dominant subduction occurring along the south of the SAO (Oloy subduction). The counter-clockwise rotation of the AACM away from NAM and associated subduction of the SAO infers significant SAO slab-roll back along the Koyukuk–Nutesyn arc system (Figs. 6 and 7). Both subduction zones (Oloy and Koyukuk–Nutesyn) on opposing margins of the SAO may have been coeval for a period of several million years leading to rapid consumption of the ocean crust (Sokolov et al., 2002) (Fig. 5).

The existence of subduction along either, or both of, the northern Kolyma–Omolon Superterrane (Oloy arc) and southern AACM margins (Koyukuk and Nutesyn arcs) before the Late Jurassic is an important consideration for our plate model. During rifting or seafloor spreading of the SAO, albeit slowly or intermittently, the creation of new ocean crust must have been accommodated by either relative motion between NAM and Siberia and/or subduction along the SAO margins. Earlier Palaeozoic rifting between NAM and Siberia including the clockwise rotation of Siberia, collision with Kazakhstan and the closure of the “Palaeoasian Ocean” (Golonka, 2011) may have accommodated the hypothesised rifting and seafloor spreading within the SAO. However, significant relative divergent motion during the Jurassic is not accommodated by our rotations of Siberia (fixed to Eurasia) and NAM. Lack of rotational divergence could be a limitation of our plate model, however, it could also explain long-lived SAO subduction, or imply that seafloor spreading within the SAO was insignificant or absent during post-Devonian times. In our model, there is a period of relative convergence between NAM and Siberia from at least 200–190 Ma, which may have contributed to subduction in the SAO region during this time, however we choose not to incorporate such early subduction in our preferred model. The relative locations of NAM and Siberia in our model suggest that the maximum size of the South Anuyi Ocean during the Jurassic was less than 2000 km (as measured between the KOST and the south-western margin of the AACM).

Didenko et al. (2002) show subduction of the SAO along the Oloy arc during the Triassic–Early Jurassic (~200 Ma) and interestingly, suggest a northward-migrating island arc system (Kanchalan and Pekulney segments) close to 30–40°N at this time. However, following the interpretation of Nokleberg et al. (2000), the earliest subduction that existed along the southern AACM margin (represented by the Nutesyn–Koyukuk arc) was Late Jurassic and along the northern Kolyma–Omolon Superterrane margin (represented by the Oloy and Svyatov arcs) was during the Late Jurassic, after the reversal of the Alazeya arc. This timing is largely supported by Layer et al. (2001) who dated subduction along the northern Kolyma–Omolon Superterrane margin at 130–123 Ma. However, while Nokleberg et al. (2000) do not explicitly describe an arc or subduction zone setting within the SAO,

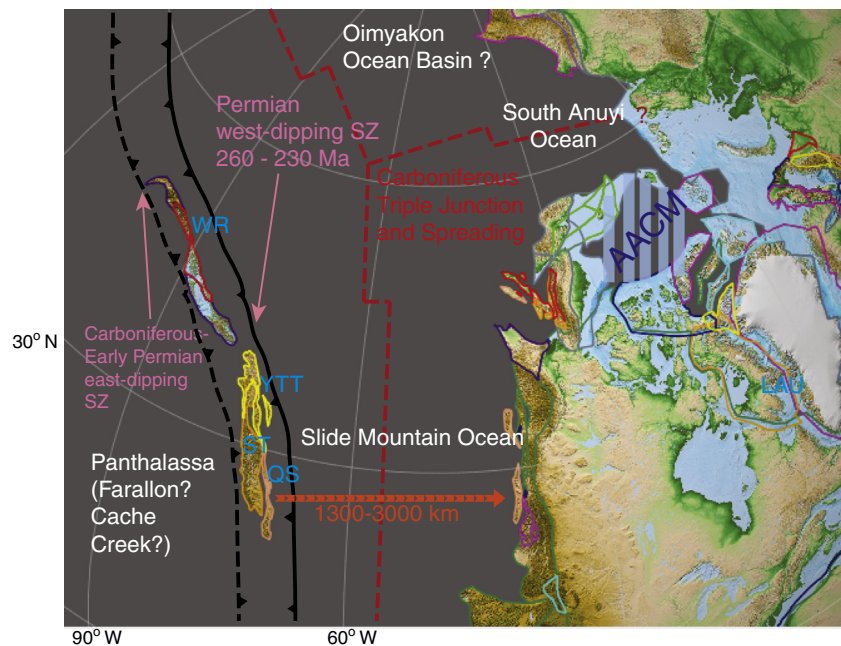


Fig. 9. Simplified regional orthographic map of the Slide Mountain Ocean and western Laurasia (base reconstruction shown ~260 Ma, longitudes and latitudes approximate) as viewed in GPlates overlain with our speculative earlier tectonic evolution of the region; Carboniferous mid-ocean ridge and triple junction, dashed red line, accounting for the opening of the Slide Mountain and likely the Oimyakon and South Anuyi oceans as well. Continuation of the mid-ocean ridge in the South Anuyi Ocean may have connected through towards Baltica, and/or transitioned to a passive plate boundary or transform. Additional subduction zones may have existed along the continental margins but are not shown. Locations of the terranes of the future Kolyma–Omolon Superterrane are not shown. Carboniferous to Permian subduction zone, dashed black line, dipping to the east as the Slide Mountain Ocean opened, inferring slab roll-back. The continuation of subduction north to the Siberian margin and south along southern Laurentia is unclear. Maximum width of Slide Mountain Ocean estimated to be 1300–3000 km. A subduction zone polarity reversal and jump is delineated by the solid black line (adapted from Nelson et al., 2006), with west-dipping subduction of the Slide Mountain Ocean and slab roll-back. We suggest that the Cache Creek Ocean opened during this period of closure, possibly in a back-arc setting (not shown here). Terranes labelled in blue as in Fig. 2; the terranes of the Yukon–Tanana (YTT), Stikinia (ST), Quesnellia (QS) terranes and Wrangellia Superterrane (WR) are located in their relative present-day configuration, respectively (not accounting for later Cenozoic deformation).

they do describe the accretion of the Koteln'nyi terrane to the Taimyr Peninsula during ~230–200 Ma and the “continued” migration of the passive-continental-margin Nixon–Fork and Dillinger–Mystic terranes towards the NAM margin during at least 208–193 Ma, suggesting that in fact subduction did exist in these areas, and by implication, this would have been contemporaneous with seafloor spreading. Furthermore Sokolov et al. (2002) also suggest that a widespread record of Late Palaeozoic and Early Mesozoic island–arc complexes, attributed to Alazeya–Oloy island–arc magmatism, supports subduction during this time. In contrast, Plafker and Berg (1994) show the Ruby, Nixon–Fork and Dillinger–Mystic terranes to be largely accreted to the NAM margin by the Late Devonian before the opening of the Slide Mountain Ocean. We chose to exclude a Mesozoic spreading ridge within the SAO for our preferred model, apart from during the opening of the Amerasia Basin and rotation of AACM when the Farallon–Izanagi–Cache Creek ridge propagates into the region.

In addition to the difficulty in constraining the onset and duration of subduction (and possible seafloor spreading) within the SAO, there are a multitude of published timings from the Kolyma–Omolon Superterrane and AACM regions referring to the final stages of SAO basin closure. Timings include syncollisional granitic plutons completed by 125–117 Ma and undeformed overlapping volcanic complexes of 106–78 Ma (U–Pb and $^{40}/^{39}\text{Ar}$ methods; Katkov et al., 2010), collision before 124–117 Ma ($^{40}/^{39}\text{Ar}$ dating; Toro et al., 2003), subduction granitoids dated 130–123 Ma ($^{40}/^{39}\text{Ar}$ dating; Layer et al., 2001), seismic unconformities dating the onset of the main orogenic phase in the Chukchi Peninsula to be 130–125 Ma (seismic stratigraphic unconformity; Drachev et al., 2010) and the presence of Bajocian to Kimmeridgian chert and shale complexes from an inferred southern SAO location (Sokolov et al., 2002). Hence, due to the poor constraints and mixed observations for the timing of subduction of the SAO, our closure timing is directly

associated with the rotation of the AACM and opening of the Amerasia Basin (142.5–120 Ma). We base our rotations for the AACM, including commencement of seafloor spreading (142.5 Ma) and rate, as presented in Alvey et al. (2008) with further modifications (see Section 2.2). This assumes that the main period of opening of the Amerasia Basin and rotation of the AACM is contemporaneous to the main subduction phase of the SAO, which we argue is reasonable considering the complementary convergent and divergent kinematics.

In our preferred tectonic model (Figs. 3–8, S1) (Table 1), we chose a simple reconstruction with a connection between the Koni–Taigonos/Uda–Murgal arc running along the northern Panthalassan margin where it links with eastward-dipping subduction under the NAM margin (e.g. Parfenov, 1997; Sokolov et al., 2002). The SAO is therefore located behind this convergent margin with Panthalassa and there is no subduction of the SAO until the inception of both the Oloy arc towards the south of the SAO and the Koyukuk and Nutesyn arcs along the north at 160 Ma (e.g. Parfenov et al., 1993; Nokleberg et al., 2000). We model an early phase of subduction along the northern SAO accounting for the subduction of the Kobuk Sea between 160 and 142.6 Ma along the Koyukuk arc and subduction zone (e.g. Plafker and Berg, 1994; Nokleberg et al., 2000). At 142.5 Ma the Koyukuk subduction zone switches polarity to match the Nutesyn arc and subduction zone, and continues from 142.5 Ma to 120.1 Ma. This is accompanied by seafloor spreading within the Amerasia Basin and associated rotation of the AACM between 142.5 and 126/120.1 Ma (see Section 2.2) whereby we propagate the Farallon–Izanagi–Cache Creek ridge into the SAO and relocate subduction north of the previous circum-Pacific subduction. For simplicity we do not incorporate any additional back-arc subduction within the Kolyma–Omolon Superterrane or a reversal of the Alazeya arc in this model.

As an alternative reconstruction we have generated a second “embayment” style model (Fig. 10) (Table 1) in which we suggest that

trench advance of the Alazeya arc occurred from 230 Ma until around 190 Ma when the described “polarity reversal” was instead subduction of a back-arc between the terranes of the Kolyma–Omolon

Superterrane (prior to amalgamation) between 180 and 165 Ma (e.g. Nokleberg et al., 2000; see Section 2.3). This earlier phase of subduction within the SAO facilitates amending the Farallon–Izanagi–Cache Creek ridge to extend into the SAO, inferring continuous seafloor spreading during the Jurassic. While subject to significant uncertainty, this alternative reconstruction matches the above interpretations, which incorporate an earlier phase of SAO subduction and/or model Early Jurassic seafloor spreading (e.g. Nokleberg et al., 1998a; 2000). Essentially the two models differ from the start of our reconstructions (200 Ma) until 142.5 Ma where the Farallon–Izanagi–Cache Creek ridge propagates into the SAO and subduction is represented by the Oloy and Koyukuk–Nutesyn arcs.

2.2. Timing of Amerasia Basin opening and rotation of the AACM

Numerous tectonic models have been proposed for the evolution of the Amerasia Basin (see Lawver and Scotese (1990) for a model summary). Amongst the most widely accepted are rotational or “windshield wiper” models. These models propose that the Arctic Alaska–Chukotka microplate (Fig. 1) underwent counter-clockwise rotation away from the Canadian margin due to rifting and seafloor spreading during Late Jurassic to Cretaceous (e.g. Grantz et al., 1990; Embry, 1990). First proposed by Carey (1958), this motion invokes a rotation pole of opening in the Mackenzie Delta and rotational angles of up to 66° (Halgedahl and Jarrard, 1987) have been suggested. This rotation generally implies that the Alpha–Mendeleev Ridge was emplaced afterwards and that the southern side of Lomonosov Ridge represents a shear margin. Supporting evidence is based on palaeomagnetic data from a single location (Halgedahl and Jarrard, 1987), the restoration of truncated facies (Embry, 1990), magnetic and gravity fabric evidence for a N–S trending extinct spreading ridge in the Canada Basin (Laxon and McAdoo, 1994), the interpretation of a rifted continental margin along Alaska (Grantz et al., 1990) and a shear-margin interpreted along the Lomonosov Ridge (Cochran et al., 2006). Furthermore, many authors discuss the collision of this rotating microplate with the Siberian margin and the synchronous, or possibly earlier, closure of the SAO.

More recent variations on this “windshield” rotation model include a more complicated or multi-phase rotational history (e.g. Grantz et al., 1998, 2011b). Grantz et al. (2011b) suggests a two-stage rotational history for the AACM and Amerasia Basin; the first phase from 195 to 160 Ma leading to stretching and “oceanic–continental transition” crust, and a seafloor spreading phase between 131 and 127 Ma. According to this model, these two episodes of rotation are separated by the rotation of the Chukchi Microcontinent between 145 and 140 Ma, and are followed by the emplacement of the Alpha–Mendeleev Ridge between 127 and 89–75 Ma. It is unclear, however, what this model infers for the Amerasia Basin between 160 and 145 Ma. A plate model by Golonka (2011) reconstructs a rotation of Arctic Alaska between 155 and 115 Ma. Whereas, Lawver et al. (2002) propose that rifting was initiated along a zone of crustal weakness in the north of the basin and propagated to the south–southeast. The authors suggest a rotation from ~135 to 120 Ma but state that closure between Chukotka and Siberia may have continued until the Cenozoic.

Alternatively, transform/strike-slip models which suggest a shear margin along Canadian Arctic Islands as Alaska rifted off the Lomonosov or Alpha ridge (e.g. Ostenso, 1974; Kerr, 1981) or a shear margin along Lomonosov and Alaska as Siberia rifted from Canada (e.g. Vogt et al., 1982; Lane, 1997) have also been proposed, as well as, combination models including extension of attenuated continental crust, transitional

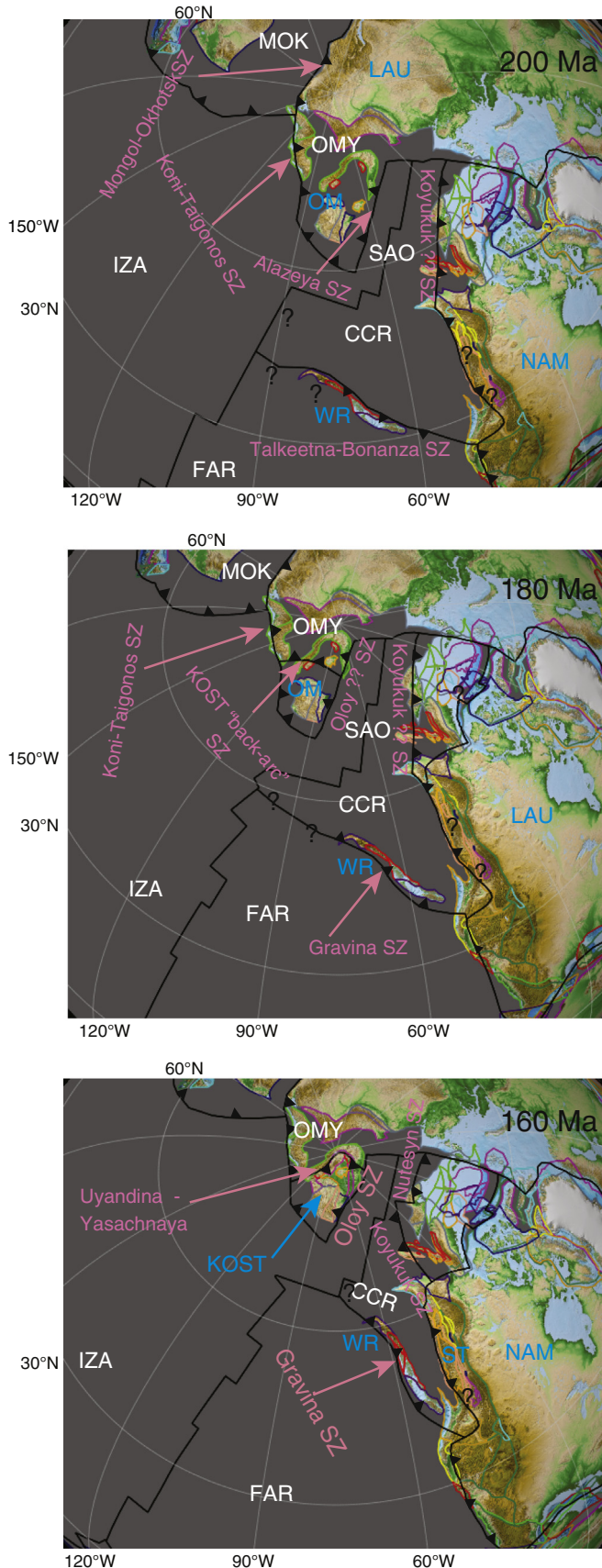


Fig. 10. Regional orthographic map of our alternative ‘embayment’ style model at 200, 180 and 160 Ma as viewed in GPlates (same as our preferred model after 142.5 Ma). Labels as in Figs. 4–6. This model incorporates the Alazeya arc, seafloor spreading and continuous subduction in the SAO (now comprising parts of the Izanagi and Cache Creek plates) for the Early Jurassic and closure of a “back-arc” between 180 and 160 Ma accounting for amalgamation of the Kolyma–Omolon Superterrane.

crust, or non-traditional oceanic seafloor spreading. Variations include rifting of the Makarov Basin (and Alpha–Mendeleev Ridge) parallel to the Lomonosov Ridge and double rotation models (e.g. Miller et al., 2008; Kuzmichev, 2009). Several recent publications (Miller et al., 2006, 2008; Harris et al., 2012) based on detrital zircon geochronology from Siberian sandstones add an additional complexity to the traditional rotation models. Based on provenance studies of Triassic sandstones, Miller et al. (2006) suggested that Chukotka originated closer to Taimyr and Verkhoyansk rather than the Canadian Arctic, presenting a reconstruction with relative motion between the Arctic Alaska and the Chukotka parts of the AACM (cf. our preferred plate model). In addition, based on syn-orogenic Jurassic–Cretaceous foreland basin sandstones in the New Siberian Islands, South Anuyi Suture and Chukotka regions, Miller et al. (2008) suggest that it is “impossible to break the [AACM] plate in the centre and rotate only the Chukotka part.” Furthermore, they suggest that the Siberian source for these sandstone deposits infers that the SAO must have been closed by the Tithonian (~145 Ma), and therefore before the opening of the Amerasia Basin. Subsequent orthogonal rifting of the Makarov Basin and transform motion along the South Anuyi Suture is invoked to explain why these seemingly proximal foreland basin sandstones are now separated ~1400 km along-strike.

Not only do the above tectonic models imply different opening mechanisms but they also differ in (1) the timing, location and rate of rifting and/or seafloor spreading in the Amerasia Basin, (2) the timing of rotation/displacement of the AACM, or components thereof, and (3) the location and timing of collision and SAO subduction, if at all. As previously noted by several authors, using a MacKenzie-Delta pole of opening for Arctic Alaska and treating the AACM as a single coherent block leads to significant overlap of the more westerly components of the AACM and the Lomonosov Ridge. The idea for (1) a multi-part rotational and/or extensional history of the Amerasia Basin, that is not accounted for with a single rotation (e.g. orthogonal to rotational rifting of Grantz et al., 1998) and (2) that the AACM can be broken into separate components has gained support by recent studies (e.g. Miller et al., 2006). A consideration of such complex deformation geometries and kinematics may therefore address observations that some parts of the AACM are of Siberian affinity during at least the Triassic (e.g. Miller et al., 2006, 2008) while also accommodating other observations that show complementary histories across Arctic Alaska and Chukotka, for example Neoproterozoic plutons (Moore et al., 1994) and Early Palaeozoic carbonate successions (e.g. Dumoulin et al., 2002). See also a discussion about a hypothesised separate “Arctida” or Lower Palaeozoic–Devonian AACM continent (e.g. Zonenshain et al., 1990; Sengör and Natal’in, 1996; Cocks and Torsvik, 2011). We note that some models which support an extensional/orthogonal rifting origin or a separate seafloor spreading history for the Makarov and Podvodnikov basins and the Alpha–Mendeleev Ridge, including a piece of trapped Jurassic oceanic crust (e.g. Miller et al., 2006; McAdoo et al., 2008; Alvey et al., 2008; Miller and Verzhbitsky, 2009), do not preclude a subduction zone existing in the more southern and eastern regions (with the exception of Miller et al. (2008) who suggest that the South Anuyi Suture may represent a transform fault). Furthermore, testing a subduction-based model for the opening of the Amerasia Basin and associated closure of the SAO is an obvious target when looking at mantle structure.

The apparently nonlinear pattern of the magnetic field within the Makarov and Podvodnikov basins, combined with the uncertainty in age and continental versus oceanic origins of the Alpha and Mendeleev ridges and the underlying crust, presents a particular challenge to constraining Amerasia Basin opening kinematics (e.g. Taylor et al., 1981; Lebedeva-Ivanova et al., 2006; Miller et al., 2006; Sokolov et al., 2009; Dove et al., 2010; Saltus et al., 2011). However, a recently published aerogeophysical survey by Døssing et al. (2013) found linear magnetic anomalies located between, and oriented orthogonal to, the Lomonosov Ridge (Fig. 1). The authors suggest that seafloor spreading anomalies within this region can be constrained to the Barremian or

lower Valanginian–Barremian (~138–126 Ma), which they note is broadly contemporaneous to major rift phases of the Amerasia Basin (e.g. Embry, 1991) and the onset of High Arctic Large Igneous Province (HALIP) intrusive volcanic activity in Franz Josef Land, Svalbard and Canadian Arctic Islands (Fig. 1) (e.g. Maher, 2001; Tegner et al., 2011). Furthermore, based on seismic refraction data, Funck et al. (2011) suggested that both the Alpha and Mendeleev ridges are resultant from plume interaction and sea-floor spreading parallel to the Canadian margin during the 130–80 Ma tholeiitic HALIP phase (Tegner et al., 2011). This timing is also broadly supported by Maher (2001) who suggest a 120–78 Ma emplacement for the Alpha Ridge. We also note that the elongate shape of the Alpha–Mendeleev Ridge and its approximate location on a small-circle of a rotation pole in the MacKenzie Delta might suggest partial LIP emplacement during spreading, as also noted for other mid-ocean ridge related LIPs including the Rio-Grande Rise and Walvis Ridge (Coffin and Eldholm, 1994). While speculation at this stage, we suggest this points to a complex contemporaneous plume-driven LIP emplacement and seafloor-spreading configuration with possible overprinting by later magmatism to account for the spectrum of ages proposed for HALIP activity.

Based on these considerations we suggest a basin-wide, multi-stage and three plate model for the opening of the Amerasia Basin, confining the “windshield-wiper” rotational history to the Canada Basin and applying an orthogonal rifting history for the Makarov–Podvodnikov basins from the Lomonosov Ridge (Table 1). We adopt the published rotations by Alvey et al. (2008) for the Canada Basin, which models a rotation of Arctic Alaska between 145 and 126 Ma, with seafloor spreading initiating at 142.5 Ma. We have chosen this reconstruction as it incorporates relatively recent geophysical data including gravity and magnetics. We find that if this singular rotational history is applied to the whole of the AACM, during 145–139 Ma, which coincides with the fastest period of rotation, 500–1000 km of rifting/seafloor is predicted in the northernmost regions of the Amerasia Basin (along the Lomonosov Ridge). This infers a full spreading rate 8–16 cm/yr, which compared to the predicted 100–500 km (4–8 cm/yr) of rifting and seafloor spreading in the Canada Basin, is extremely fast and we argue, unreasonable.

Furthermore, spreading anomalies interpreted by Døssing et al. (2013) point to a more reasonable 2.8–7.7 cm/yr full spreading rate near the Alpha Ridge. We therefore suggest that the traditional counter-clockwise rotational history of the Amerasia Basin is at least viable for the Canada Basin, however a more orthogonal rifting geometry for the northern regions is more likely. Incorporating a full spreading rate of 2.8 cm/yr between 142.5 and 131.6 Ma and 7.7 cm/yr from 131.5 to 126 Ma in the northern part of the Amerasia Basin and assuming at least 250 km of pre-existing stretched continental crust on each flank of the Amerasia Basin, we are able to account for over 1200 km of opening in these regions between 142.5 and 126 Ma. Assuming the above timing and rates of seafloor spreading are correct, the remaining ~350 km of inferred oceanic crust could be accounted for by an additional 5 Myr of seafloor spreading (at the rate of 7.7 cm/yr) i.e. spreading until 120.1 Ma, which is not unreasonable. Assuming a stretching factor of 2 (~250 km reconstructed continental crust), similar to that proposed for the Chukchi Plateau (Grantz et al., 1998), we reconstruct continental rifting from 195 Ma (Grantz et al., 2011b) until 142.6 Ma along the flanks of the Amerasia Basin, noting rifting may have initiated later. Alternative scenarios for opening of the Amerasia Basin may include an earlier or later onset of rifting and seafloor spreading, a faster rate of opening, that a greater portion of the present-day Amerasia Basin is underlain by extended continental crust, therefore reducing the area required for oceanic lithosphere, or an offset in timing of rifting and seafloor spreading between the northern and southern parts of the basin.

In summary, our new tectonic model for the opening of the Amerasia Basin implies a three-plate system whereby the AACM must be further

divided into two regions; which we refer to as the North Slope Microplate and East Siberia Microplate (Fig. 6). We do not retain the “Chukotka” naming of the AACM in either of these two new microplates due to uncertainty in the location of the plate boundary in the region. Based on affinities between the De Long and Pearya terranes (Figs. 1 and 2) and evidence for Caledonian or Ellesmerian deformation of Kotel’nyi (New Siberian Islands) and Wrangel Island (Fig. 1) (Drachev et al., 2010), combined with the spreading rates in Døssing et al. (2013) and suggestion of rifting as early as 195 Ma (Grantz et al., 2011b) we apply rotations to the East Siberian Microplate with rifting from 195 to 142.6 Ma and seafloor spreading between 142.5 and 120.1 Ma. Our location and delineation of the spreading ridge between at least 138–126 Ma in the northern basins is constrained by magnetic anomalies from Døssing et al. (2013). Similarly, following the rotations of Alvey et al. (2008) and rifting of Grantz et al. (2011b) we apply rifting of the North Slope Microplate 195–142.6 Ma and seafloor spreading 145.5–126.0 Ma (only the East Siberian Microplate requires the additional seafloor spreading until 120.1 Ma). A break in the AACM is therefore implied in the region of Wrangel Island and it is possible that the emplacement of the Alpha–Mendeleev Ridge is also related to this rotational–orthogonal transitional area due to inherent lithospheric weakness from relative motion. The along-strike separation of the Koyukuk arc from the Nutesyn arc during 142.5–120.1 Ma may correspond to a difference in spreading regimes within the Amerasia Basin (see Section 2.1). The delineation of this boundary between the East Siberian Microplate and North Slope Microplate could be further refined, particularly through the development of a deforming plate model. Significant shear is implied from 126 to 120.1 Ma between the two microplates due to the continued seafloor spreading in the northern basins relative to the Canada Basin. We note that the pre-collisional AACM margin has not been restored and post-opening extension or compressional effects have not been removed thus leading to significant overlap in the pre-rotated configuration. We endeavour to investigate this further with a deformation model and in particular, quantify the magnitude and timing of extension of the Siberian margin (Pease, 2011). Some authors suggest extension of 30–40% along the East Siberian Sea and Laptev Sea regions, up to 40% in the Barents/Kara Sea area (Franke et al., 2001; Pease, 2011), or even up to 100% (Miller et al., 2006; Miller and Verzhbitsky, 2009), therefore reiterating that the present-day size of the AACM is significantly larger than the original terrane.

2.3. Kolyma–Omolon Superterrane and subduction zone

The Verkhoyansk Fold Belt, located along the eastern margin of the Siberian platform, is over 2000 km long and 500 km wide (Fig. 1). Folding of the Verkhoyansk thrust front was initiated as early as the Late Jurassic and represents the collision of Siberia and the Kolyma–Omolon Superterrane (e.g. Zonenshain et al., 1990; Parfenov, 1991; Parfenov et al., 1993; Nokleberg et al., 2000) (Fig. 1). Collision of the Kolyma–Omolon Superterrane and Siberia is dated from the Late Jurassic to Neocomian (143–138 Ma; Lauer et al., 2001) and deformation is thought to have ended by the end of the Late Cretaceous with a reactivation during the Middle to Late Pleistocene (Parfenov et al., 1995). Deformation is described to have begun in the west and progressed to the east, and estimates of horizontal shortening of various Verkhoyansk segments are between ~20 and 50% (Parfenov et al., 1995) or 150–200 km (Parfenov et al., 1993). Parfenov et al. (1993) and Nokleberg et al. (2000) provide more in-depth descriptions of the terranes and features of northeastern Siberia.

The Kolyma–Omolon Superterrane is a collage of oceanic, continental and turbidite terranes, island arcs and cratonic fragments separated by imbricate thrust sheets (Fig. 2, Table 2) that amalgamated in the Mid Jurassic through various episodes of subduction, collision and extension (Parfenov et al., 1993, 1995; Nokleberg et al., 2000) (Figs. 4 and 5). Several constituent terranes e.g. the Omolon,

Prikolyma and Omulevka terranes (Fig. 2), are thought to have originally rifted from the Siberian Craton in the Late Devonian and Carboniferous (Parfenov, 1991; Parfenov et al., 1993; Nokleberg et al., 2000). Before this rifting event, the eastern Siberian margin is described to be largely a passive margin since the Late Pre-Cambrian (Zonenshain et al., 1990; Parfenov et al., 1995). The rifted oceanic, or thinned continental basin, sometimes referred to as the Oimyakon Ocean Basin (Nokleberg et al., 2000; Oxman, 2003; or Kular–Nera Ocean, Sengör and Natal’in, 1996), was then later subducted with the collision of the Kolyma–Omolon Superterrane and Siberia in the Oxfordian–Early Tithonian (Fig. 5) (Parfenov, 1991; Nokleberg et al., 2000). The deep-sea fan complex of the Kular–Nera terrane is interpreted to represent parts of this subducted basin (Nokleberg et al., 2000). By contrast, Didenko et al. (2002) suggest that the “Sugoi” basin separated Kolyma–Omolon Superterrane and Siberia and was closed by shortening and strike-slip faulting rather than a discrete subduction episode.

There have been numerous publications discussing the Palaeozoic and Mesozoic histories of the terranes of the Kolyma–Omolon Superterrane, before its amalgamation, mostly focusing on the Omulevka and Omolon terranes (e.g. see compilations by Nokleberg et al., 1998a, 2000; Stone et al., 2003), and are often based on a broad spread of palaeomagnetic poles and inferred rotations. Models which broadly support a Siberian affinity for the terranes of the later Kolyma–Omolon Superterrane, suggest that the largest latitudinal difference between these terranes and Siberia is likely to have been before the late Triassic and did not exceed a few thousand kilometres (Parfenov, 1991). From at least the Ordovician to Early Jurassic, Sengör and Natal’in (1996) reconstruct the terranes of the Kolyma–Omolon Superterrane to be continuously connected to each other through a “Verkhoyansk passive continental margin” which separated the Oimyakon Ocean from Panthalassa. Nokleberg et al. (2000) suggest that before the Middle Jurassic, the terranes comprising the Kolyma–Omolon Superterrane may have been displaced up to 20°S from present-day latitudes, after which the terranes have retained a similar latitude to present-day. Didenko et al. (2002) prefer a model by which the Omolon massif travelled from ~60°N in the western hemisphere to ~76°N in the eastern hemisphere via the polar region between the Middle Jurassic to Early Cretaceous, while rotating 30–40° counter-clockwise relative to Siberia. However, despite this relative motion they support a reconstruction of a continuous chain of terranes along the Oloy arc since 200 Ma that does not include a significant distance between them and Siberia e.g. the Omolon terrane was between 60 and 70°N. Stone et al. (2003) suggest that at least the Omulevka and Omolon terranes moved northward while rotating clockwise between the Permian to Late Jurassic time, minimising an offset of up to 40° latitude from the Siberian craton (also suggested by Zonenshain et al., 1990). With the uncertainty in palaeolatitudes and displacements from Siberia for the terranes of the Kolyma–Omolon Superterrane at least since the Early Jurassic, we have chosen to follow the reconstructions as shown in Nokleberg et al. (2000), concentrating on their latitudinal reconstructions and relative positions between the terranes (Figs. 4 and 5) (as also applied by Lawver et al., 2002).

The amalgamation of the Kolyma–Omolon Superterrane itself, before its collision with Siberia, may have involved an additional subduction zone. For example Oxman (2003) and Parfenov (1991) suggest a Triassic or Early–Mid Jurassic southwestward-dipping subduction zone (under Omulevka) leading to the collision of the Alazeya arc and the Omulevka terrane, and subsequently the other eastward terranes (e.g. Omolon and Prikolyma terranes) and destruction of the intermediate back-arc basin. It is unclear where this back-arc setting is derived from, whether it is related to the subduction of the palaeo-Pacific, or is a back-arc of the Uyandina–Yasachnaya arc (Zyryanka Basin, as interpreted by Nokleberg et al., 2000) or if it is related to the earlier Devonian rifting events. The horse-shoe

shape of the Kolyma range (Fig. 2) has also been attributed to Alazeya arc convergence or the subduction of an inlet of the SAO (Nokleberg et al., 2000). The SAO inlet closure was suggested to mark the end of a first phase of Kolyma–Omolon Superterrane collision, followed by lateral motion of the Superterrane to the northwest forming left-lateral strike-slip faults along the Chersky Range (Prokopiev and Oxman, 2009). The Yarakvaam terrane is also described to have possibly provided the link between the Oloy and Alazeya arcs (Parfenov et al., 1993; Nokleberg et al., 1994), however the geometry and timing of this, as well as a possible connection to the Koni–Taigonos and Uda–Murgal arcs is ambiguous. Furthermore, many reconstructions show the terranes of the Kolyma–Omolon Superterrane (pre-amalgamation and collision with Siberia) from west to east (Siberia to Pacific direction, depending on the model employed) to be Omulevka–Prikolyma–Omolon with the Yarakvaam terrane and Alazeya and Oloy arcs along the northern edge with the SAO (Figs. 4, 5 and 10, Table 2) (e.g. Nokleberg et al., 2000; Sokolov et al., 2002).

In our preferred model we have incorporated the Uyandina–Yasachnaya subduction zone to be active from 160 to 140 Ma (e.g. Layer et al., 2001), after which it is prescribed as a collisional, but non-subducting setting (Figs. 3–8, S1). We reconstruct the Uyandina–Yasachnaya subduction zone to be located adjacent to and dipping under the Kolyma–Omolon Superterrane (eastward, present-day reference) (Fig. 5). This follows reconstructions (e.g. Parfenov, 1991; Parfenov et al., 1993; Sengör and Natal'in, 1996; Nokleberg et al., 2000; Oxman, 2003) with NE dipping subduction during the Late Jurassic between the Siberian Craton and the Kolyma–Omolon Superterrane, subducting the intervening Oimyakon Ocean Basin. This subduction accounts for the Uyandina–Yasachnaya arc volcanics and thrust faulting. Additionally, this subduction history is also supported by Layer et al. (2001) who suggests an evolving east-dipping subduction ~160–140 Ma (possibly as early as 180 Ma) followed by collision from 143–138 Ma. This history matches major westerly-facing thrusts within the Verkhoyansk and Kolyma orogenic systems with some eastward vergence in the eastern areas of the fold belt (see Parfenov et al., 1995 for a more in-depth discussion of the frontal thrusts within the Verkhoyansk fold belt). However, how this subduction zone links to the Uda–Murgal arc and the Oloy arc is unclear. In our alternative “embayment” model (Fig. 10) we incorporate the additional subduction of a “back-arc” to account for the amalgamation of the Kolyma–Omolon Superterrane (note the relative motion between the terranes comprising the Superterrane, Figs. 3–5) from 180 to 165 Ma followed by the subsequent subduction of the Oimyakon Basin (160–140 Ma) and the collision of the Kolyma–Omolon Superterrane and Siberia (Figs. 3–5, S1). Due to the uncertainty and additional complexity we have refrained from incorporating this additional subduction zone in our preferred model.

The post-Kolyma–Omolon Superterrane accretion history for NE Asia is largely influenced by SAO subduction and collision of the AACM towards the north and the succession of subduction, island arc and terrane accretion and volcanism of the western Koryak–Kamchatka region towards the east and south-east (Figs. 6–8). Based on dikes and pluton trends in the Kolyma–Omolon Superterrane, the area underwent east–west extension during the Late Cretaceous between 135 and 124 Ma, ending in 120 Ma possibly due to strike-slip movement of the accreted Kolyma–Omolon Superterrane relative to Siberia (Layer et al., 2001) or from the closure of a small gulf of the SAO (Prokopiev and Oxman, 2009). This period also coincides with documented extension in the Alaskan interior (130–90 Ma; Miller and Hudson, 1991). A later phase of extension, between 110 and 93 Ma, was suggested to be due to collision along the South Anuyi Suture (although, this collision is much later than we reconstruct) or from subduction and collision along the Okhotsk–Chukotka Volcanic Belt (Layer et al., 2001). Alternatively, a phase of extension between 120 and 105 Ma is thought to represent the rifting of the Amerasia Basin (Miller et al.,

2009), however, this post-dates the main AACM rotation and collision event in our model.

In addition, we find that far-field effects related to the continued breakup of Pangea including the opening of the Atlantic predict significant plate convergence and crustal shortening in NE Asia. This is of particular consequence when assigning a plate hierarchy and relative motion of a particular terrane in the Siberian region to either NAM or Eurasia (see supplementary rotation file).

2.4. NE Asia–Pacific margin/Uda–Murgal arc

The continental margin between Siberia and the Pacific has experienced successive episodes of subduction and associated island arcs since at least the start of the Mesozoic, including Andean continental-style subduction as well as ensimatic and ensialic-style arcs (which include a component of back-arc extension) and suprasubduction. Origins for the associated ophiolites and accreted terranes include both autochthonous and allochthonous sources (Table 2). The “Uda–Murgal Arc” is described as the Late Jurassic to Early Cretaceous convergent margin between Siberia and the Pacific (e.g. Sokolov et al., 2002, 2009; cf. since the Late Triassic in Parfenov, 1997). This arc is sometimes described as following on from the Late Paleozoic–Early Mesozoic “Koni–Taigonos” arc (Sokolov et al., 2009), “Kedon” arc (Nokleberg et al., 2000) or “Koni–Murgal” arc (Zonenshain et al., 1990). The names, spelling, definition and timings of associated arcs vary according to author. Nokleberg et al. (2000) separate this arc system into the Late Jurassic to mid-Cretaceous “Uda” arc and the northeastern Late Triassic to mid-Cretaceous “Kony–Murdal” arc. Here we choose to follow the nomenclature by Sokolov et al. with an older Koni–Taigonos and a post-Late Jurassic Uda–Murgal arc (Figs. 4–7). The southern part of this subduction zone is described to be a continuation of the Mongol–Okhotsk subduction zone (Fig. 4), the latter of which saw the subduction and sinistral transpression of the Mongol–Okhotsk Ocean until the mid-Cretaceous (e.g. Zonenshain et al., 1990; Nokleberg et al., 2000). Successive episodes of island arc accretion, arc segments and subduction zone jumps through to the mid-Cretaceous along the margin with the palaeo-Pacific have also been identified e.g. Uda–Piyagin, Taigonos, Penzhina–Anadyr, Ust-Belaya and Pekulney segments (Fig. 5) (e.g. Sokolov et al., 2009) (see Nokleberg et al., 2000, for a detailed discussion). Sokolov et al. (2009) claim that only a northern segment (Pekulney and part of the southern Uda–Piyagin segment) of the Uda–Murgal volcanic arc contains evidence for an ensimatic island-arc and back-arc setting with the margin further south being an Andean-style continental margin setting. They suggest that this back-arc was linked to the SAO. Nokleberg et al. (2000) suggest an offshore extension of the eastern parts of Uda–Murgal arc during the Late Triassic. These reconstructions are in contrast to Golonka (2011), who suggests a parallel set of subduction zones with trench jumps and various episodes of terrane accretion along the Siberian–Panthalassa margin until at least approximately 80 Ma. As previously mentioned, the continuation of the Koni–Taigonos and Uda–Murgal arcs through the NAM subduction system during the Mesozoic is ambiguous. Several authors e.g. Parfenov (1997) suggest a link to the Stikinia arc (and Yukon–Tanana Terrane) via the Alazeya arc during the Jurassic and later through the Wrangellia Superterrane arcs (Figs. 4–6).

The 3000 km long Okhotsk–Chukotka volcanic belt or arc, which overlies the older accreted terranes of the Kolyma–Omolon Superterrane and parts of the AACM (Figs. 1, 7 and 8), is suggested to mark the eastern Albian–Late Cretaceous (108–68 Ma; Layer et al., 2001; 88.5–65 Ma Stone et al., 2009 or Hauterivian–Barremian, Vishnevskaya and Filatova, 2012) boundary between Siberia and the Pacific (e.g. Zonenshain et al., 1990; Parfenov et al., 1993; Nokleberg et al., 2000; Sokolov et al., 2009). Nokleberg et al. (2000) describe the Okhotsk–Chukotka volcanic belt as well as an adjacent Olyutorka arc to be of Late Cretaceous–early Tertiary age. Similarly, the 800 km long Kamchatka–Koryak belt (Fig. 1) (or Kuril–Kamchatka arc; Nokleberg et al., 2000) is thought to delineate the Maastrichtian/Eocene–Miocene margin of the continent, and an East Kamchatka volcanic belt of Pliocene age is located further east (Parfenov

et al., 1993). This also matches the reconstruction of Akinin et al. (2009) who show a southward migration of the palaeo-Pacific subduction boundary across the Bering Sea region towards present-day subduction along the Aleutian arc. The terranes of Koryak and Kamchatka are of mostly oceanic affinity and accreted in the Late Cretaceous to Early Eocene, contemporaneous to the accretion of southern Alaskan terranes (Parfenov et al., 1993). Components of these terranes are also thought to have travelled from a southerly location, most likely with the plates of Panthalassa (e.g. Zonenshain et al., 1990). Nokleberg et al. (2000) however, support the notion of coeval singular/curve-linear arcs and subduction along the Siberian and NAM margins as opposed to arc migration across/with Panthalassa (with the exception of the Wrangellia Superterrane), and note that oblique subduction and strike-slip displacements between arc and cratons need to be considered in tectonic reconstructions.

Towards the south of the Kolyma–Omolon Superterrane and Chersky Range, deformation was due to the collision of the Okhotsk continental terrane (Fig. 1) along the Bilyakhan fault/suture with the Siberian passive margin. Deformation is inferred to have occurred from the Late Jurassic until ~119 Ma, some authors suggest that final deformation occurred after the collision and accretion of the adjacent Kolyma–Omolon Superterrane to the north (Parfenov, 1991; Parfenov et al., 1993; Prokopiev et al., 2009) whereas others suggest an earlier collision, along with the Viligia terrane (Fig. 2), around 230–208 Ma (Nokleberg et al., 2000). In a similar fashion to the terranes of the Kolyma–Omolon Superterrane, the Okhotsk terrane may have separated from Siberia by rifting and spreading, during the Devonian (Parfenov, 1991; Nokleberg et al., 2000; Prokopiev et al., 2009). The outboard margin along the palaeo-Pacific saw subduction and arc magmatism since at least the Devonian, including the Uda–Murgal arc (Prokopiev et al., 2009).

We reconstruct a north–northwestward-dipping subduction zone (under Siberia) along the palaeo-Pacific since at least the start of the Jurassic and incorporate south-southeastward trench jumps according to terrane and island-arc accretion. We reconstruct the Koni–Taigonos arc from the start of our reconstructions until 160.1 Ma, followed by the Uda–Murgal arc until 108.1 Ma, Okhotsk–Chukotka volcanic belt subduction until 67.1 Ma and the Kamchatka–Koryak subduction until southward stepping to the Aleutian arc around 55 Ma (Figs. 3–8) (e.g. Nokleberg et al., 2000; Sokolov et al., 2002, 2009). We link these arcs and subduction zones to those further east along the NAM margin in our preferred model, and via the Alazeya and Koyukuk–Nutesyn arcs in our alternative model (Figs. 4–8 and 10). Instead of incorporating a double subduction zone (Koyukuk–Nutesyn and Uda–Murgal) during the rotation of the AACM from 142.5 to 120.1 Ma, we have chosen a simple kinematic configuration whereby the Farallon–Izanagi–Cache Creek Ocean ridge propagates into the SAO. Once the SAO has been subducted under AACM the subduction zone along the northern-Pacific is restored. Our proposed locations of the convergent margin relative to present-day match those presented in Akinin et al. (2009). Collision of the Okhotsk/Viligia terranes (Fig. 2, Table 2) to the southern Kolyma–Omolon Superterrane and NE Asian margins is implied after the Kolyma–Omolon Superterrane collision until 120 Ma, and is in-board of the Uda–Murgal and Pacific subduction zones.

2.5. North Pacific/northern North American subduction

A complex history of subduction and exotic and native terrane accretion during the Mesozoic was also experienced further east along the Alaskan and NAM margin (see detailed summary in Plafker and Berg, 1994). The terranes of Alaska and northwestern NAM can be broadly separated into four terrane groups (modified from Nokleberg et al., 2000 and Colpron et al., 2007) (Fig. 2, Table 2): (1) The inboard passive and metamorphosed continental-margin and cratonal terranes, e.g. NAM Craton margin, Yukon–Tanana Upland, Cassiar and Kootenay terranes; (2) Arctic Alaska/continental margin and arc terranes

e.g. AACM and North Slope, Coldfoot, Seward, Ruby and the Nixon–Fork/Farewell (including the Dillinger and Mystic) terranes; (3) Insular terranes including Peninsular, Alexander, Wrangellia (comprising the Wrangellia Superterrane); (4) Intermontane terranes including the Yukon–Tanana, Stikinia, Quesnellia, Slide Mountain (oceanic) and Cache Creek (oceanic); and (5) outboard island-arc and subduction zone terranes that accreted in the Mid Jurassic to Cenozoic; Koyukuk, Angayucham (oceanic), Yakutat, Goodnews (oceanic) and Chugach terranes. The western-most outboard terranes linked to the Late Jurassic to mid-Cretaceous Nutesyn–Koyukuk arc and subduction of the SAO, are discussed earlier in Section 2.1.

While the most recent 200 million years is the focus of this paper, in order to explain the history of northern Panthalassa and NAM, both peripheral but important regions of the circum-Arctic, we find it necessary to attempt to reconcile the earlier Mesozoic and Palaeozoic history. Here, we separate the discussion and explanation of our plate model into subsections, loosely running forward in time, noting that much overlap between times and tectonic features is unavoidable, particularly concerning the highly debated Cache Creek Ocean.

2.5.1. The Yukon–Tanana Terrane and the Slide Mountain Ocean

The parautochthonous Yukon–Tanana Terrane was largely formed along the NAM margin from earlier arc magmatism that commenced around 385 Ma in the Devonian (e.g. Nelson et al., 2006). During the early Carboniferous from around 360 to 320 Ma, south–southwest directed slab-rollback along the western NAM margin and back-arc spreading lead to rifting of the Yukon–Tanana Terrane and the opening of an ~1300 km to 3000 km wide Slide Mountain Ocean (e.g. Plafker and Berg, 1994; Nokleberg et al., 2000; Nelson et al., 2006) (Fig. 9). Note, that the Slide Mountain Ocean was originally referred to as the Anvil Ocean (Tempelman-Kluit, 1979), but this designation erroneously correlated the Cache Creek and Slide Mountain terranes, and later as the Cache Creek Sea (Monger and Berg, 1987; Plafker and Berg, 1994). We suggest that this Late Devonian to Early Carboniferous rifting and seafloor spreading history of the Slide Mountain is contemporaneous with the opening the SAO and Oimyakon Ocean and furthermore that this widespread rifting event is best explained by a triple junction with one arm within the Slide Mountain Ocean, a second within the SAO and the third either the Oimyakon Ocean Basin or adjacent to the Wrangellia Superterrane (Fig. 9) (see below).

The Carboniferous Finlayson, Early Permian Klinkit and mid-Late Permian Klondike assemblages are often referred to as the magmatic arcs associated with stages of subduction of both “Panthalassa” and the Slide Mountain Ocean along the Yukon–Tanana Terrane (Nelson et al., 2006; Colpron et al., 2007; Colpron and Nelson, 2009). Additionally, two major island-arc systems, Stikinia and Quesnellia (Fig. 2), are commonly defined by their Late Triassic–Early Jurassic suite of plutonic, carbonate and volcanic rocks, but Devonian to Permian volcanics are also noted (e.g. Nokleberg et al., 2000). Northern portions of Stikinia and Quesnellia are penetrated and deformed, and may be included as stratigraphically and/or structurally overlying part of the Yukon–Tanana Terrane (e.g. Nokleberg et al., 2000). However, alternative non-NAM origins for Stikinia and Quesnellia exist (Johnston and Borel, 2007; see below). According to Nelson et al. (2006), the Pennsylvanian–Permian arc system of the eastern Yukon–Tanana Terrane and the northern Quesnellia arc consistently faced towards the west (subduction dipping towards the east). However, they suggest that arc polarity for the Stikinia arc from the Devonian and Pennsylvanian–Permian is towards the east (subduction dipping towards the west; also supported by Nokleberg et al., 2000), despite both arcs being connected to the Yukon–Tanana Terrane (Fig. 9).

Maximum width of the Slide Mountain Ocean was reached around the Early Permian before the cessation of back-arc spreading, a subduction zone jump and polarity reversal with subduction dipping towards the southwest around 280–260 Ma (Nokleberg et al., 2000) or 269–253 Ma (Nelson et al., 2006). Subsequent subduction along the

eastern margin of the Yukon–Tanana Terrane and closure of the Slide Mountain Ocean saw the accretion of the Yukon–Tanana Terrane and much of the Quesnellia arc to the NAM margin. Depending on the tectonic scenario, suggested timings of Yukon–Tanana–Quesnellia accretion range from the Late Permian (Nelson et al., 2006), 260–252 Ma (“Klondike” orogeny, Beranek and Mortenson, 2011), Mid-Permian to Late Triassic (Mortensen, 1992), “early Mesozoic” (Colpron et al., 2007) or 187–174 Ma (Mihalynuk et al., 1994). The point of accretion of the Yukon–Tanana Terrane is thought to be relatively close to its original location before Devonian rifting (Nelson et al., 2006; Colpron et al., 2007). In addition to subduction along the east margin of the Yukon–Tanana Terrane, Nokleberg et al. (2000) also reconstruct an additional subduction zone closer to the continental margin during the migration of the Stikinia–Quesnellia arc towards NAM (this double configuration is also shown in Nelson et al., 2006; Colpron and Nelson, 2009).

2.5.2. Stikinia and Quesnellia and the Cache Creek Ocean

The present-day geometry of the Yukon–Tanana–Quesnellia–Stikinia terranes is interpreted as a hairpin shape running from the more continent-proximal arm of the Quesnellia arc in the east/south, through the Yukon–Tanana Terrane with metamorphosed components of both Quesnellia and Stikinia, into the well-preserved Stikinia arc in the west. An additional ocean basin, separate to the Slide Mountain Ocean, with a distinct assemblage of exotic Late Permian Tethyan fauna is referred to as the Cache Creek Ocean (e.g. Coney et al., 1980; Nokleberg et al., 2000). Notably, the present-day Cache Creek terrane is enclosed between the Yukon–Tanana–Quesnellia–Stikinia terranes (Fig. 2), and it could therefore be assumed that the associated ocean lay only between the reconstructed arcs of Quesnellia and Stikinia. However, through a time-dependent consideration of connected plate boundaries and a detailed analysis of existing reconstructions, below, we identify the limitations of this interpretation and suggest that the plate to which the future Cache Creek terrane belonged can be extrapolated further outboard to the west, beyond that of the Stikinia to Quesnellia domain.

Mihalynuk et al. (1994) suggested that the present-day configuration of the Yukon–Tanana–Quesnellia–Stikinia terrane was due to oroclinal warping from a counter-clockwise rotation of Stikinia (relative to Quesnellia) isolating the Cache Creek Ocean from Panthalassa during the Late Triassic to Early Jurassic (beginning 235–208 Ma until 187–174 Ma). In this model, the timing of onset of oroclinal rotation is roughly contemporaneous with the timing of closure of the Slide Mountain Ocean. Their reconstructions show the east-dipping subduction of the Cache Creek Ocean under the Quesnellia section to an increasingly westward-dip under the Stikinia section. Closure and accretion of at least Yukon–Tanana and Quesnellia to the NAM margin is achieved by 187 Ma, and by inference also the Slide Mountain, with final collapse of a remnant Cache Creek Ocean and Stikinia by around 173 Ma (Mihalynuk et al., 2004). This timing is much later than more recent models based on U–Pb geochronology (e.g. Beranek and Mortenson, 2011), possibly due to a difference in timings based on accretion versus orogenic building.

By contrast, Colpron et al. (2007) acknowledge the oroclinal warping mechanism of Mihalynuk et al. (1994) but state and reconstruct the accretion of “the Yukon–Tanana Terrane, along with its juvenile arc cover (Harper Ranch, Quesnellia, and Stikinia)” to be early Triassic ~250 Ma. Significantly, even though Quesnellia is consistently reconstructed further east than Stikinia, the two arcs are continuously connected along strike, as is similarly shown in Nelson et al. (2006), Colpron and Nelson (2009) and Cocks and Torsvik (2011). The lack of a name beyond “Panthalassa” or delineation of a plate boundary further to the west of this subducting oceanic lithosphere (Cache Creek under Stikinia–Quesnellia) in many of these reconstructions (e.g. Mihalynuk et al., 1994; Nokleberg et al., 2000; Colpron et al., 2007), facilitates the simplest interpretation that the same oceanic plate extends to the west and south i.e. Cache Creek

Ocean. By inference the Stikinia and Quesnellia arcs also continued after Slide Mountain Ocean closure, leading to renewed east-dipping subduction under western Laurentia from the Late Triassic (Colpron and Nelson, 2009) and therefore suggesting subduction of the remaining Cache Creek Ocean or “Panthalassa” until Wrangellia Superterrane accretion.

There is significant disparity in the timing of initiation and cessation of subduction of both the Slide Mountain and Cache Creek oceans as well as the associated time of arc and terrane accretion. Part of this confusion might stem from original naming discrepancies of the adjacent oceanic components, diverse collision-related geochronological data, and subduction polarity-timing interpretations. Furthermore, the separation of the Farallon Plate from the Cache Creek Ocean, or any other missing ocean not discussed here, is unclear. Notably, in most models (e.g. Nokleberg et al., 2000; Nelson et al., 2006; Colpron et al., 2007; Colpron and Nelson, 2009), the Stikinia and Quesnellia arcs along with the Yukon–Tanana Terrane are consistently contiguous, despite the hair-pin style rotation and the observation of a distinct Cache Creek Ocean. Hence, the difference in the timing of accretion of the Yukon–Tanana–Quesnellia and Stikinia components should not be large or distinct, if separate at all, or perhaps best represented by a complex configuration as in the present-day western Pacific. If oroclinal warping was large enough to warrant a significantly delayed collision of Stikinia after Yukon–Tanana Terrane collision (contrary to the similar timing suggested by their reconstruction figures) or if oroclinal warping occurred after an initial phase of collision is unclear.

Seton et al. (2012), however, suggest that spreading occurred in the Cache Creek Ocean during Slide Mountain Ocean closure from 280 Ma until Yukon–Tanana–Quesnellia accretion at 230 Ma and that the Stikinia arc terrane did not accrete until 173 Ma. This interpretation therefore suggests that the Cache Creek Ocean was located between the clearly separated Yukon–Tanana–Quesnellia and Stikinia terranes, and therefore the Farallon Plate was located between Stikinia and the Wrangellia Superterrane. The Seton et al. (2012) model, however, fails to reconstruct the subduction zone and plate boundary along the Wrangellia Superterrane (see timing of magmatism below) and thus the inferred plate between the Wrangellia Superterrane and Stikinia is not adequately addressed. In other words, we argue that there is not a strong case to “rift” and separate the Stikinia segment from Yukon–Tanana–Quesnellia by a significant ocean (e.g. Seton et al., 2012).

The above reconstructions are in contrast to Nokleberg et al. (2000) who suggest subduction of the Cache Creek Ocean occurred on one side of the Yukon–Tanana–Quesnellia–Stikinia terrane from the Pennsylvanian to the Early Jurassic, therefore contemporaneous to the last of their timing of Yukon–Tanana Terrane rifting from NAM and opening of the Slide Mountain. On the other side of the Stikinia and Quesnellia arcs, the Slide Mountain Ocean is described to have been subducted only from the Early Jurassic, with subduction on either side of the Stikinia and Quesnellia arcs separated by a polarity reversal in the Early Jurassic. They also suggest that the Slide Mountain Ocean existed until 193–163 Ma when the connected Yukon–Tanana–Stikinia–Quesnellia terranes accreted and infer that subduction of the Cache Creek Ocean along the Wrangellia Superterrane (Talkeetna–Bonanza arc) occurred during the Late Triassic to Early Jurassic. In this model, due to the longevity of the Slide Mountain Ocean, the Cache Creek Ocean is labelled as the region south of the Wrangellia Superterrane, which could be confused with the Farallon Plate. Nevertheless, there appears to be a difference in tectonic models as to whether the Cache Creek Ocean was located strictly between the Yukon–Tanana–Quesnellia terranes and the Stikinia arc i.e. is just a product of enclosure by the suggested Stikinia rotation, or alternatively it is more broadly the area between the Yukon–Tanana Terrane and Wrangellia Superterrane. It could be a combination of both, with only the preservation of the Cache Creek Ocean that was obducted with associated oroclinal bending.

A complexity of our preferred model, and of those others to-date, is how to account for Permian Tethyan faunas of the Cache Creek Ocean; the approximate eastern extent of the Tethys was over ~19000 km away from the western Laurasian margin in the Permian. As an example, if a segment of ocean floor formed at around 300 Ma in the Tethyan realm and accreted to western Laurentia at 230 Ma, this requires a motion of ~27 cm/yr across the entirety of Panthalassa, which is an unreasonably fast spreading rate. We suggest that if the Permian Tethyan fauna are a necessary constraint on the model, the plate configuration might be better explained by a series of arc-backarcs and intraoceanic subduction zones that existed across northern Panthalassa, extending from the Tethys to western Laurasia. The incorporation of additional intra-oceanic subduction zones within Panthalassa e.g. Kutcho–Sitlika (Schiarizza et al., 1998) or Stuhini–Nicola (Johnston and Borel, 2007) may confine the Cache Creek Ocean to a smaller plate somewhere between our modelled Wrangellia Superterrane and Stikinia–Quesnellia.

Sigloch and Mihalynuk (2013) recently presented a novel interpretation of seismic tomography under NAM and suggest an alternative plate model that challenges the long-standing view of Andean-style continental subduction. Their revised plate model for selected timesteps labels a new “Mezcalera” Plate existing between Wrangellia and Stikinia–Quesnellia/NAM. The plate boundary complexity implied by their model including the polarity reversals, implications for origins of the plates and trenches, plate boundary continuation, relative plate motion and, significantly, the dynamics required to explain long-lived intra-oceanic trench stability provides a case-study for future investigation. On the other hand, Johnston and Borel (2007) suggest an alternative history for the Cache Creek, based largely on the assumption that a Tethyan origin for the Cache Creek terrane cannot be reconciled with a NAM-origin for the Stikinia–Quesnellia terrane. They suggest a migration rate of 11 cm/yr of the Cache Creek terrane from the Tethys towards eastern Panthalassa from 280 Ma, collision with a non-NAM derived Stikinia and Quesnellia arc at 230 Ma at a location some 10000–11000 km west of NAM, collision of these units to a pericratonic platform including the Cassiar terrane at 180 Ma and collision to the NAM margin around 150 Ma. As mentioned previously, how the Wrangellia Superterrane and arc fit into this reconstruction, as well as the continuation of these intraoceanic subduction zones that must span a significant portion of Panthalassa and implications for plate boundaries, is unclear. We stress that while alternative scenarios exist, future plate models should in a time-dependent sense specifically delineate plate boundaries, name the associated plates (beyond that of “Panthalassa”) and arcs, and consider the implications for relative plate motion, as is the novelty of our approach here.

2.5.3. Wrangellia Superterrane and the Cache Creek Ocean

The next major Mesozoic tectonic event along north-eastern Panthalassa margin was the accretion of the allochthonous Wrangellia Superterrane to NAM. The composite Wrangellia Superterrane includes four island arcs (Early Ordovician to Late Devonian Sicker arc, Pennsylvanian to Early Permian Skolai arc, Late Triassic to Early Jurassic Talkeetna–Bonanza arc and Late Jurassic to Mid-Cretaceous Gravina arc) and three sequences (Alexander, Peninsular and Wrangellia) which generally young from east to west (e.g. Nokleberg et al., 2000). Origins and motions of the several terranes and arcs of the Wrangellia Superterrane are varied and, due primarily to a lack of data and conflicting palaeomagnetic data, previous models have largely failed to address the time-dependent evolution of the early history of the Wrangellia Superterrane.

A component of the future Wrangellia Superterrane, the Alexander terrane is suggested to have originated from Baltica in the mid-Palaeozoic (e.g. Butler et al., 1997; Colpron and Nelson, 2009). For example, based primarily on palaeomagnetic data (e.g. Hillhouse and Grommé, 1984; Haeussler et al., 1992) Butler et al. (1997) suggested that the Alexander terrane rifted from Baltica in the Devonian and

migrated to 25–30°N latitude in the Permian (though also noted a possible eastern Gondwanan origin based on paleomagnetic uncertainty and Ediacaran arc-related rocks, see Colpron and Nelson, 2009). Furthermore, the Alexander terrane may have amalgamated with the Wrangellia terrane in the Mid-Pennsylvanian (Gardner et al., 1988), or the Talkeetna–Bonanza arc and Peninsula Terrane may have formed either on the combined Wrangellia–Alexander terrane or collided with it during the Permian to Late Jurassic (Trop and Ridgway, 2007 and references therein). Assuming the above northerly reconstructions, it is likely that the early tectonic history of the Wrangellia Superterrane is intimately linked to the opening of the Slide Mountain Ocean and SAO.

The above reconstructions for the Wrangellia Superterrane are also supported by Belasky et al. (2002), who offer a Permian reconstruction whereby the Wrangellia Superterrane is located further north (30°N) but along strike of the Stikinia and Eastern Klamath terranes. Alternatively, Colpron and Nelson (2009) invoke a “northwest sinistral passage mechanism” with sections of slab rollback linked via transform faults (see Section 2.1) to transport the Alexander terrane from Baltica towards Panthalassa. At the Pennsylvanian–Early Permian, the authors reconstruct the Wrangellia Superterrane further west and north (~30°N) but connected to the Yukon–Tanana–Stikinia terrane, and by the Late Permian–Early Triassic further increase the distance between the two terranes, with the Wrangellia Superterrane still located ~30°N. By the early Mesozoic, continued southward motion of the Wrangellia Superterrane is suggested by various authors (e.g. Plafker and Berg, 1994; Butler et al., 1997; Nokleberg et al., 2000; 12°N Trop et al., 2002; Trop and Ridgway, 2007 and references therein) with low palaeolatitudes (10–20°N) suggested by palaeomagnetic and geologic evidence during the Late Triassic to Early Jurassic (see Table 3 in Nokleberg et al., 2000 for detailed and synthesised palaeomagnetic data).

Assuming that the above interpretations are correct, a plate model must account for the relative southward motion of the Superterrane from Baltica in the mid-Palaeozoic to 10–20°N in the Triassic. In particular, it must explain a relative motion of the Wrangellia Superterrane from north of the Yukon–Tanana Terrane to outboard and to the southwest during this time. We suggest that the kinematics required to migrate the Wrangellia Superterrane in such a way, are best explained by an evolving triple junction and mid-ocean ridge spreading system (Fig. 9). Thus, a particular complexity in the mid-Phanerozoic history of northern Panthalassa is reconciling the motion of the Wrangellia Superterrane and the creation of the Cache Creek Ocean. Due to the evidence for a distinct ocean basin, the configuration of the Yukon–Tanana–Quesnellia–Stikinia assemblage and the arguments presented above, we suggest that the area between Yukon–Tanana–Stikinia–Quesnellia and the Wrangellia Superterrane (and perhaps a component of the area between Stikinia and Quesnellia during rotation) represents the Cache Creek Ocean.

If, however, the Wrangellia Superterrane remained along-strike and proximal to the Yukon–Tanana–Stikinia–Quesnellia terranes since the Permian, the consequences for plate boundaries and an intervening ocean basin (Cache Creek or other) radically differ to our preferred model. Here, we follow the majority of existing models, which clearly distinguish the evolution of the Wrangellia Superterrane, in both discussion and diagrammatic representation, from the Yukon–Tanana system (i.e. Insular versus Intermontane terranes e.g. Nokleberg et al., 2000; Colpron et al., 2007). Whether the inferred elongate Wrangellia Superterrane arc followed a longitudinal or latitudinal orientation during its evolution is unclear. Better constraints on palaeomagnetic data and the restoration of the Cenozoic dextral strike-slip motion (see below) will facilitate such reconstructions. In addition, the history of the Eastern Klamath terrane and the terranes of the future Kolyma–Omolon Superterrane (e.g. Omolon, Prikolyma) are likely key components to reconstructing the extent of this large rift setting.

To add to the uncertainty of this region, we find that one of the most significant implications for regional plate reconstructions is

the dip direction of the subduction zone along the Wrangellia Superterrane. Trop et al. (2002) describe the Wrangellia Superterrane to be an intraoceanic plateau setting from the Late Triassic to Middle Jurassic (230–180 Ma). Notably, this is in contrast to the timing of the Talkeetna–Bonanza arc of Nokleberg et al. (2000) (Late Triassic–Early Jurassic), who imply that subduction was occurring during this time. Nevertheless, Trop et al. (2002) suggest that this was followed from the Mid to Late Jurassic (179–160 Ma) by an intraoceanic subduction setting with northeast dipping subduction of the Farallon Plate along the Wrangellia Superterrane and a backarc basin located to the northeast. This intraoceanic subduction setting then evolved into a retroarc foreland basin from the Late Jurassic to Cretaceous (159–145 Ma), and was followed by a latest Late Jurassic–Early Cretaceous onset of collision with NAM (144–130 Ma). Gehrels et al. (2009 and references therein) present a detailed history of magmatism in the Coast Mountains batholith suggesting that following a Mid-Jurassic “juxtaposition of Alexander–Wrangellia against the outboard margin of Stikine and Yukon–Tanana,” the batholith evolved as a single west-facing magmatic arc (east-dipping subduction) since at least the Late Jurassic or Mid-Cretaceous (~155 Ma). Based on the timing of magmatism in the east and western portions of the batholith, they favour a model whereby sinistral motion juxtaposed the two previously along-strike portions around 120 Ma, and was complementary to a backarc “Gravina” and forearc setting (Monger et al., 1994), followed by final accretion of the Wrangellia Superterrane around 85 Ma.

This dominant north to northeast-dipping subduction under the southwest margin of the Wrangellia Superterrane is also presented in Nokleberg et al. (2000). However, these authors also state that the earlier “Talkeetna–Bonanza arc is interpreted as having formed from the Late Triassic and Early Jurassic subduction of part of the Cache Creek oceanic plate along the margin of the Wrangellia Superterrane” and furthermore that “the Stikinia–Quesnellia arc is interpreted as having formed during the Pennsylvanian, Permian, Late Triassic and Early Jurassic subduction of part of the Cache Creek oceanic plate along one margin” (before their polarity reversal and subduction of the Slide Mountain). In conjunction with the Yukon–Tanana–Quesnellia–Stikinia debate discussed above, we therefore interpret this statement by Nokleberg et al. (2000) to not disagree with our interpretation with the Cache Creek Ocean located between the Yukon–Tanana–Stikinia–Quesnellia terranes and the Wrangellia Superterrane. Due to the separation of the Wrangellia Superterrane and Stikinia–Quesnellia–YTT arc by Nokleberg et al. (2000), we argue that their statements actually suggest that the Cache Creek Ocean was subducted in a south–southwest dipping subduction zone along the eastern margin of the Wrangellia Superterrane from at least the Late Triassic to Early Jurassic.

Furthermore, if northeast-dipping subduction is to be inferred along the western margin of the Wrangellia Superterrane (i.e. subduction of the Farallon Plate) during its Early Jurassic history, it could be argued that such long-lived and extensive trench advance (in the order of at least 3000 km) is not a dominant process in any equivalent present-day setting (Schellart et al., 2008), whereas slab-roll back (trench retreat) from southwest-dipping subduction is kinematically more likely. In addition, an earlier northeast-dipping subduction model along the Wrangellia Superterrane (Farallon Plate subducted under the overriding plate of the Cache Creek Ocean) requires subduction to occur contemporaneously along the western NAM margin to be able to close the Cache Creek Ocean, of which evidence is not conclusive, but may be accounted for magmatism in Yukon–Tanana–Quesnellia–Stikinia terranes at least since 180–160 Ma (Gehrels et al., 2009).

In an attempt to satisfy the evidence for northeast-dipping subduction along the Wrangellia Superterrane since at least the Jurassic, strongly supported by numerous authors (e.g. Trop et al., 2002; Trop and Ridgway, 2007; Gehrels et al., 2009), we suggest an alternative history. We suggest that the Mid-Jurassic hiatus between the Talkeetna–Bonanza and Gravina arcs (Nokleberg et al., 2000)

represents a subduction polarity reversal facilitated by the proximity of the Wrangellia Superterrane to NAM. We therefore reconstruct a southwest directed subduction zone along the northeastern margin of the Wrangellia Superterrane as the Superterrane moved north within Panthalassa until around the Early Jurassic (185 Ma) (Fig. 4). During this time (200–185 Ma), the motion of the Wrangellia Superterrane is therefore dictated by the motion of the Farallon Plate and the Cache Creek Ocean is being subducted along the northeastern margin of the Superterrane. From the Early Jurassic a northeast directed subduction commenced along the western margin of the Wrangellia Superterrane as it approached NAM (Fig. 5). For simplicity we do not include the hiatus between the Talkeetna–Bonanza and Gravina arcs but rather switch polarity at 185 Ma. The opening of the Gravina back-arc during this final phase of subduction along the Wrangellia Superterrane is also possible, but we have not implemented this in our plate boundaries.

Timing of accretion of the Wrangellia Superterrane to the NAM margin has been dated around 145–130 Ma (Nokleberg et al., 2000; Trop et al., 2002) possibly with an earlier onset of collision around 159–144 Ma (Trop and Ridgway, 2007) or ~160–155 Ma (Colpron and Nelson, 2009). Alternatively, some models suggest a later period of accretion, with accretion of the Wrangellia Superterrane to Yukon–Tanana–Quesnellia–Stikinia terranes at ~105 Ma following the closure of a “Gravina–Kahiltna Ocean” basin (Clift et al., 2012), or ~85 after the “collapse” of the “Gravina” backarc basin (Gehrels et al., 2009), or even as late as the early Cenozoic (Plafker and Berg, 1994). We prefer a Late Jurassic timing for the onset of collision of the Wrangellia Superterrane at ~140 Ma. We note that this major collisional tectonic event is broadly contemporaneous with seafloor spreading in the adjacent Amerasia Basin. In addition, the link between the western Laurasian and intraoceanic subduction zones to the Koni–Taigonos and Uda–Murgal arcs along Siberia as well as the Koyukuk arc along the AACM is uncertain. Due to the episodic opposing polarities of the Talkeetna–Bonanza and Gravina arcs we suggest that the subduction zones were at least separated along strike from the Farallon–Izanagi–Cache Creek ridge by a transform fault (Figs. 3–6). This configuration, however, is difficult to account for when considering relative plate motions and associated plate boundaries. Future reconstructions should consider the indirect constraints from the motion of the Farallon Plate if the Wrangellia Superterrane is located on it (i.e. subduction of the Cache Creek under it), or vice-versa. In addition, implications for isochrons and the age of the ocean floor should be included. It is possible that an additional microplate(s) existed in this area to account for the intersection of subduction zones between the Wrangellia Superterrane and Siberian margin, albeit via transform, mid-ocean ridges or additional subduction zones.

Furthermore, there is a debate as to whether the Wrangellia Superterrane was accreted within 1000 km of its present location or 1000–5000 km further south (e.g. Irving et al., 1996; Keppie and Dostal, 2001; Stamatakos et al., 2001), with both models requiring some amount of dextral strike-slip motion. For example, a tectonic reconstruction at 193–163 Ma in Nokleberg et al. (2000) shows that the Wrangellia Superterrane may have been located at either 25°N or 45°N, or somewhere in between. We have applied the more northern-accretion location for the Wrangellia Superterrane (present-day) while still noting that post-Cretaceous dextral strike-slip migration should be included. We also note that the accretion of the Wrangellia Superterrane in the Late Jurassic–Early Cretaceous is contemporaneous with subduction along the Koyukuk–Nutesyn arcs, rotation of the AACM and opening of the Amerasia Basin. After the accretion of Wrangellia, the Kluane and Coast arcs are described to have existed along the southern margin of Alaska from the mid-Cretaceous, continuing possibly to the Palaeogene (75–56 Ma) and early Eocene (55–50 Ma) respectively (Plafker and Berg, 1994; Nokleberg et al., 2000). Again, how these subduction zones linked to the contemporaneous Okhotsk–Chukotka volcanic belt and Koryak–Kamchatka

subduction zones along NE Asia is uncertain but likely continuous due to the earlier rotation of continental fragments of the AACM. Around the Eocene, during the accretion of the Kula Plate and ridge, the northern Pacific subduction margin stepped southward from within the Bering Sea to the modern day Aleutian–Wrangell arc. The Aleutian–Wrangell arc, which continues for over 4000 km from southern Alaska to eastern Kamchatka, is intra-oceanic in the west and continental in the east (Nokleberg et al., 2000).

2.5.4. Summary

In summary, we adopt the generally accepted tectonic scenario of Slide Mountain Ocean opening from the Early Carboniferous (360 Ma) with slab roll back of an E–NE dipping subduction zone. With the maximum size of the Slide Mountain Ocean reached in the Permian, opening in the Slide Mountain was followed by a subduction polarity reversal and subduction jump to along the east margin of the Yukon–Tanana Terrane (Fig. 9). We primarily follow reconstructions with a timing of onset of west-dipping Slide Mountain subduction around 260 Ma until accretion of the Yukon–Tanana Terrane as well as both Stikinia and Quesnellia at 230 Ma (e.g. Nelson et al., 2006; Colpron et al., 2007; Beranek and Mortenson, 2011). We infer that counterclockwise rotation of the Stikinia arc relative to Quesnellia leading to the present-day configuration also occurred during this Slide Mountain Ocean closure. We note that such kinematics may have generated a complex subduction configuration with both east-dipping and west-dipping subduction zones and trench jumps. Following Colpron and Nelson (2009), we suggest the Wrangellia Superterrane was largely stationary at ~30°N between 300 Ma and 260 Ma until spreading in the Cache Creek Ocean during Slide Mountain Ocean subduction i.e. 260–230 Ma (Fig. 9). Perhaps the Cache Creek Ocean opened in a back-arc fashion during the westward dipping subduction of the Slide Mountain Ocean. Whether the relative southward and westward motion of the Wrangellia Superterrane and opening of the Cache Creek Ocean was contemporaneous with Slide Mountain Ocean opening or closure, or both, is unclear. After Yukon–Tanana–Quesnellia–Stikinia accretion at 260 Ma we reconstruct a subduction jump to the west of NAM, leading to renewed eastward dipping subduction of the Cache Creek Ocean. In order to subduct the Cache Creek Ocean, this subduction zone along NAM is required in tectonic reconstructions when the Farallon is being subducted under the Wrangellia Superterrane i.e. during NE-dipping subduction and trench advance along the Wrangellia Superterrane (185–140 Ma in our preferred model). We accrete the Wrangellia Superterrane to NAM at 140 Ma in its present-day relative location.

2.5.5. Cretaceous deformation

During the mid-Cretaceous, coastal terranes of Alaska and northern NAM are generally described to have undergone dextral strike-slip displacement (towards the northwest) along major faults including the Denali, Kaltag and Kobuck faults and smaller companion faults (e.g. Plafker and Berg, 1994 and references therein). The displacement was largely attributed to oblique convergence between the Kula Plate and NAM, but also due to the opening of the Central and North Atlantic. Estimates of the magnitude and timing of migration are highly debated, however, as noted by Colpron et al. (2007), while the latitudinal rotations are to be reconciled, the internal post-accretionary configuration of the terranes remains largely the same. In contrast to the older terrane and fault models, Redfield et al. (2007) invoke a “North Pacific Rim orogenic system” to suggest that crustal extrusion is largely driven by crustal flow rather than major strike-slip fault motion of rigid blocks. Furthermore, they suggest that the escape tectonics of the Alaska and northern NAM terranes also extend further west to the eastern margin of Kamchatka, including the Bering Block (Fig. 2). An overview by Ridgway and Flesche (2012) suggest that, among other data, a mantle convection model and lithospheric stress is consistent with, and do not preclude the hypothesis of Redfield et al. (2007). A summary of

the older terrane and fault model is provided in Plafker and Berg (1994), where some examples of displacement estimates include;

- (1) The Cassiar Terrane was displaced at least 450 km northward by dextral movement along the Tintina–Northern Rocky Mountain Trench Fault during the Late Cretaceous–Early Tertiary (Gabrielse, 1985; Plafker and Berg, 1994)
- (2) The Ruby and Angayucham terranes underwent a clockwise rotation of 135° relative to the continental margin in two phases during the opening of the Amerasia Basin and later in the Late Cretaceous–Early Tertiary (Plafker and Berg, 1994)
- (3) A 16–30° northward displacement of the Chugach terrane relative to the NAM craton occurred in the Late Cretaceous to Middle Eocene (Plumley et al., 1983; Plafker and Berg, 1994).
- (4) Plafker and Berg (1994) suggested that the Yakutat terrane was offset 180 km from the Chugach terranes in the late Paleocene or early Eocene and that an additional 600 km of dextral-slip northwestward displacement along the Queen Charlotte Fault to its present position occurred after the Oligocene.
- (5) A counter-clockwise bending of southwest Alaska of 45–60° between 65 and 50 Ma has been documented from geologic and palaeomagnetic evidence, possibly due to NAM–EUR convergence (Plafker and Berg, 1994).
- (6) This may have been contemporaneous with a Late Cretaceous–Early Tertiary 75° counter-clockwise rotation in the Farewell and Ruby terrane region (Plafker and Berg, 1994).
- (7) Gabrielse et al. (2006) suggested translation on the order of 860 km since the Cretaceous for the “intermontane” terranes (Colpron et al., 2007) including 450–900 km of dextral slip of the Yukon–Tanana Terrane (Gabrielse, 1985).

The incorporation and testing of post-accretionary deformation models of southern Alaska from at least the Late Cretaceous will be the focus of future deformation models. In our rigid plate model the terranes (Fig. 2) are kept in their relative locations and geometry as at present-day and therefore sometimes appear crossing plate boundaries (e.g. Figs. 4–6).

3. New plate model

To further converge on a robust history of the Mesozoic and Cenozoic circum-Arctic, we present a self-consistent, time-dependent and dynamically evolving plate tectonic model from the Early Jurassic (200 Ma) to present-day. Our model is based on a new type of global plate motion model (Seton et al., 2012; Gurnis et al., 2012) that includes topologically closed plate boundaries and is based on an extensive synthesis of geological and geophysical observations. This new generation of fully closed and time-dependent plate boundaries is a prerequisite for future geodynamic modelling in which plate motions and mantle convection can be coupled, providing an additional avenue for testing alternative plate models by comparing the modelled subduction history with tomographically imaged slab volumes in the mantle (e.g. Matthews et al., 2012).

We have created a simplified set of tectonic features for the Arctic at present-day, focusing on the AACM, the Kolyma–Omolon Superterrane, Alaska and northern NAM (Fig. 2, Table 2). We divide the present-day Arctic into major components that can be reconstructed back through time to their pre-rift and collisional configuration. The delineation of the features and terranes for this tectonic feature set was based on several datasets including gravity anomalies and derivatives (DNSCO8GRA Andersen et al., 2010; Circum-Arctic Mapping Project CAMP Gravity: Gaina et al., 2011), magnetics (CAMP Saltus et al., 2011; WDMAM), and geological mapping including fault and sedimentary succession mapping (Nokleberg et al., 1998b, 2000; Colpron et al., 2007; Harrison et al., 2011; Grantz et al., 2011a). Our tectonic feature set is in reasonable agreement with other tectonic maps based on geological surveys e.g. Zonenshain et al. (1990), Parfenov et al. (1993),

Plafker and Berg (1994), Nokleberg et al. (2000) and Sokolov et al. (2002).

We assign a Plate Identification Number (PID) to each of these digitised terranes (Table 2), which are embedded into a global plate model of relative plate motions. We base our reconstructions on the global plate motion model by Seton et al. (2012), but with significant changes to the circum-Arctic. The reconstructions for the opening of the Eurasia Basin from Anomaly 24 (~53 Ma), and the coupled motion of the Lomonosov Ridge, are based on the isochrons and rotations from Gaina et al. (2002). The rotations for the Siberian Craton are fixed to Eurasia (based on Srivastava and Roest, 1989; Gaina et al., 2002), which is a reasonable assumption for our reconstructions. Based on the rotational history of these terranes we construct polygons, in 1 Myr increments, which are composed of topological plate boundaries, including mid-ocean ridges, transform boundaries and subduction zones (Fig. 3). We use the open-source global plate reconstruction software GPlates (<http://www.gplates.org>; Boyden et al., 2011). The rotations, polygons and terranes of our preferred model can be freely downloaded and loaded into GPlates (ftp://earthbyte.org/papers/Shephard_etal_Arctic_plate_model). One aim of our model presented here is to provide the geoscience community with a base plate tectonic model for the circum-Arctic, which can be manipulated and refined according to user requirements or alternative tectonic reconstructions.

For the period 200–142.5 Ma we present two alternative models:

Model 1. “Convergent margin” (our preferred model)

Continuous subduction zone along northern Panthalassa running from Siberia (Koni–Taigonos and Uda–Murgal) to North America (and connected to Talkeetna–Bonanza and Gravina arcs via a mid-ocean ridge and transform boundary) (Figs. 4–8).

Model 2. “Embayment margin”

Koni–Taigonos and Uda–Murgal arc and subduction systems along Siberia are separate to subduction along the NAM margin, inclusion of Alazeya trench advance and Kolyma–Omolon Superterrane back-arc closure, continuous seafloor spreading linked to the Farallon–Izanagi–Cache Creek systems and early SAO subduction along Alazeya, pre-Oloy and pre-Koyukuk arcs (Fig. 10).

We have selected an absolute reference frame based on a hybrid hotspot and true polar wander-corrected (TPW) paleomagnetic reference frame which uses moving Indo-African hotspots between 100 Ma and present-day (O'Neill et al., 2005) and a true polar wander-corrected palaeomagnetic frame for earlier times (Steinberger and Torsvik, 2008). The choice of an absolute reference frame, which describes the motion of plates relative to a fixed point or “frame,” holds particular implications for palaeo-plate velocities, the location of palaeo-plate boundaries and predicted mantle structure, especially at higher latitudes (Shephard et al., 2012). Absolute reference frames may be based on hotspot tracks, with hotspots either assumed as fixed (e.g. Morgan, 1984; Müller et al., 1993) or moving (e.g. Steinberger, 2000a; Dubrovine et al., 2012), as well as palaeomagnetic data, with or without corrections of true-polar wander (e.g. Torsvik et al., 2008; Steinberger and Torsvik, 2010). Fig. 11 shows a comparison between four absolute reference frames; our base hybrid moving hotspot and TPW model (TPW), a palaeomagnetic model (PMG) (Torsvik et al., 2008), a new moving hotspot model which only goes back as far as 124 Ma (DBV) (Dubrovine et al., 2012) and a subduction reference frame (SUB) (Van der Meer et al., 2010), which is similar to the TPW model but with a longitudinal correction applied. Focusing on the northern hemisphere, differences in palaeo-plate boundary locations are greatest further back in time. When comparing the SUB with the TPW at 200 Ma, we find up to ~800 km longitudinal difference between the two models in the polar latitudes, with the offset increasing towards the equator. Comparing the TPW and PMG models shows up to ~1000 km difference in longitude and 2000 km in latitude with maximum offset along the western NAM margin. At 150 Ma the TPW and

PMG models are largely similar with up to 300 km offset predicted in the polar latitudes. After 100 Ma the TPW and PMG models are the same, with up to ~1500 km difference in longitude between them and the SUB reference frame. A comparison between the DBV model and the TPW/PMG model at 100 Ma shows the DBV plate boundaries located further north and east in the polar latitudes by around 500 km and by the same amount to the south and west by 50 Ma.

This uncertainty in absolute reference frames holds implications in our interpretations of seismic tomography because structures observed in the mantle could be attributed to different subduction zones on the surface. Furthermore, the correlation of mantle heterogeneity and plate boundaries is also complicated by the potential lateral displacement of subducted slabs, sinking rates and stalling slabs in the transition zone. We attempt to avoid this uncertainty by also considering the relative positioning of slab bodies rather than their absolute locations.

4. Mantle structure from seismic tomography

While most models of seismic tomography, both P and S wave, are not as robust under the circum-Arctic as other regions of the globe, they image key mantle features that can be linked to our plate kinematic model. Here, assuming vertical slab sinking, we compare the modelled mantle structure of five S-wave tomography models (Grand, 2002; Montelli et al., 2006; Simmons et al., 2007; Gypsum S Simmons et al., 2010; S40RTS Ritsema et al., 2010) and one P-wave model (MITP 08 Li et al., 2008) to our predicted palaeo-subduction zones. Primarily due to source and receiver limitations for high latitudes, we find that S-wave tomography models are generally better resolved than P-wave tomography models under the circum-Arctic. Fig. 12 shows the locations of our selected vertical cross-sections which were chosen to sample the sites of subduction zones as predicted in our plate model between 200 Ma and present-day. Estimates of average slab sinking rates in the mantle generally range between 1 and 2 cm/yr based on seismic tomography and mantle convection modelling (e.g. Lithgow-Bertelloni and Richards, 1998; van der Voo et al., 1999; Hafkenscheid et al., 2006; Schellart et al., 2009). For example, using a global average sinking rate of 1.5 cm/yr a slab subducted at 80 Ma would be expected around 1200 km depth, 100 Ma at 1500 km, 140 Ma at 2100 km and 200 Ma at the CMB. However, this rate is dependent on modelling considerations including mantle viscosity (e.g. Hafkenscheid et al., 2006; Goes et al., 2008) and slab stagnation (e.g. Fukao et al., 2009; Sigloch, 2011), lateral slab motion (Bunge et al., 1997; Steinberger, 2000b) and the history of subduction (Steinberger, 2000b).

4.1. Circum-Arctic

A vertical section (Fig. 13. Latitude 65°N, longitude 140°E–150°W) through the subduction zone along western Panthalassa shows a major longitudinally-extensive anomalously fast structure (a) between 1500 and 2500 km depth in all models. This could be interpreted to be Jurassic slabs of Panthalassa (Izanagi Plate) subducted along a predominantly westward-migrating subduction zone (Figs. 3, 12). A second smaller anomalously fast region (b) is shown lying in the transition zone (440–660 km depth) under ~160–170°E longitude which is likely resultant from later subduction (Izanagi and Pacific plates) into a more stable, or south–southeastern migrating subduction zone (Figs. 3, 12). This transition zone anomaly corresponds to an inferred stagnated Pacific slab behind the Aleutian arc also noted in a higher resolution tomography model by Zhao et al. (2010). Comparing absolute reference frames through this latitude, between 200 and 150 Ma the plate boundaries of the SUB, TPW and PMG are located from west to east respectively, with the PMG being significantly offset at 200 Ma. We argue that the bulk of the slab (a) through this latitude is located between 175°E to 150°W which best suits the TPW or SUB reference frame

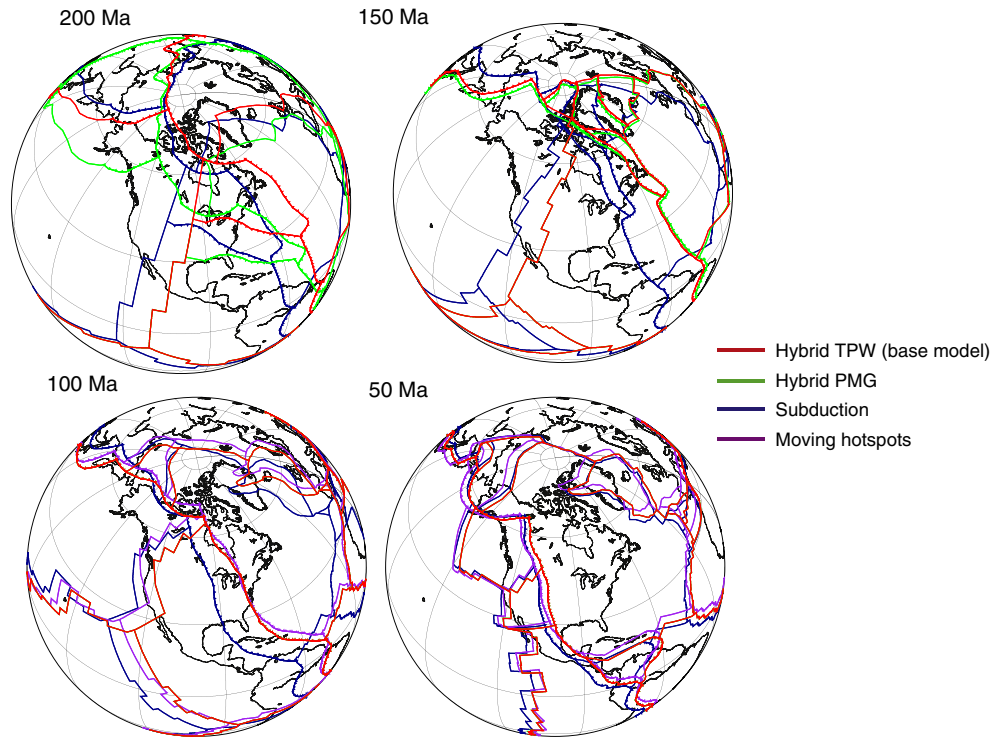


Fig. 11. Comparison of palaeo-plate boundaries, red, for our plate model, based on a hybrid moving hotspot and TPW corrected frame (O'Neill et al., 2005; Steinberger and Torsvik, 2008), and three alternative absolute reference frames at 200 Ma, 150 Ma, 100 Ma and 50 Ma. Green, a palaeomagnetic model of Torsvik et al. (2008); blue, a subduction reference frame of Van der Meer et al. (2010) and purple, for moving hotspot model of Dubrovine et al. (2012) (only back to 124 Ma). Present-day coastlines included in light grey for reference.

but is too far west to fit the PMG frame at 200 Ma. The significant north-westward motion of this PMG boundary (over 2500 km) between 200 and 150 Ma is arguably very fast.

Three latitudinal profiles (60–90°N) were chosen to image the western (Fig. 14. Longitude 180°E), central (Fig. 15. Longitude 140°W) and eastern (Fig. 16. Longitude 100°W) segments of the

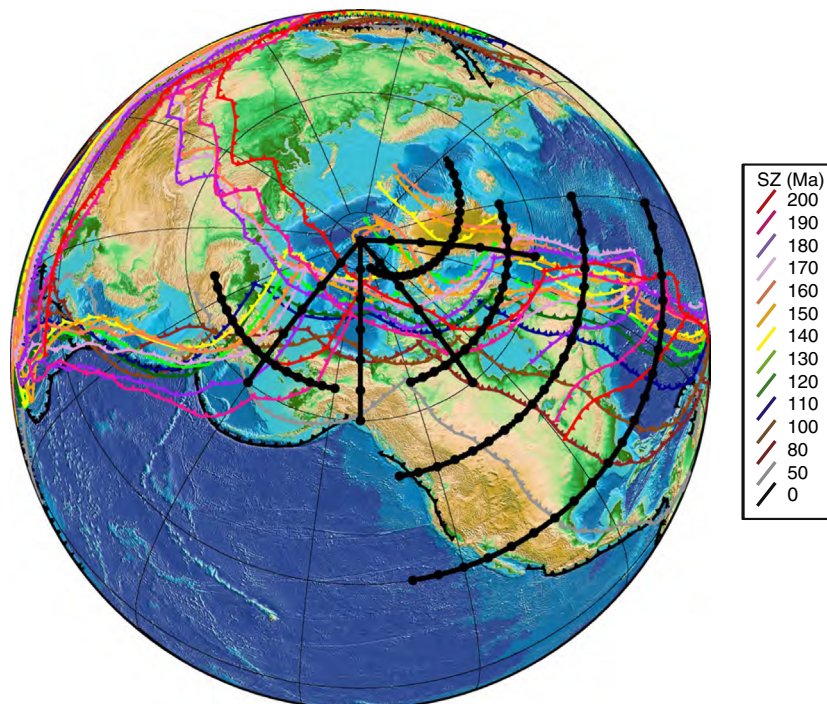


Fig. 12. Location of vertical profiles through seismic tomography models (Figs. 13–21), black with circles, superimposed on subduction zone locations as predicted by our preferred plate model, colour coded, between 200 and 0 Ma, see inset, and projected onto present-day topography (ETOPO2) for reference.

northern Panthalassa margin including the Koni–Taigonos and Uda–Murgal arcs (Figs. 4–6). All three profiles through the tomography models show significant anomalously fast material throughout the mantle, in particular between 1000 and 2500 km depth (c) and along the CMB (d). Both of these slab features are likely the same longitudinally-extensive slabs across the same three profiles. We interpret the (c) anomalies to be linked to the subduction along the Mesozoic northern Panthalassa margin (Farallon, Cache Creek Ocean and Izanagi) and may be the same as imaged in Fig. 13 (slab a). Our interpreted slab (c) at least in the central profile (Fig. 15) broadly matches the >1500 km deep “Beaufort” slab interpreted by Van der Meer et al. (2010) to be related to the early-mid Mesozoic Alazeya arc and subduction from approximately 214–154 Ma. However, Van der Meer et al. (2010) also interpreted an adjacent but shallower (~1000–1500 km) “Chukchi slab” under the Eastern Siberian Shelf to be related to Late Jurassic (154–110 Ma) Koyukuk arc subduction. Based on our plate model we suggest that their “Chukchi” slab is too far west to be subducted at the Koyukuk arc but instead is related to Panthalassa subduction. This “Chukchi” slab also broadly matches slab (c) from the western profile (Fig. 14) and based on our correlation of slab (c) between Figs. 14 and 16, the Beaufort and Chukchi slabs might in fact be the same i.e. Panthalassa-related subduction. However, because the “Chukchi” is shallower than the “Beaufort” slab, it might represent a younger phase of subduction of the Farallon/Cache Creek Ocean/Izanagi plates. Some of the deepest slabs in the western profile (slab d, Fig. 14) may include some of the subducted Monghol–Okhotsk Ocean. Furthermore, in the eastern profile (Fig. 16) it could be argued that a second semi-detached slab (e) (compared to the dominant anomaly, c, further south) can be imaged between 1000 and 1500 km depth under 75–85°N. This feature might be related to subduction of the Oimyakon Ocean or SAO due to its northerly location relative to our predictions of palaeo-plate boundaries. At these longitudes, from 150 to 50 Ma, the latitudinal discrepancy between the four absolute reference frames is minimal (less than 5°). However, it should be noted that the deepest slab material (d) does continue as far south as 60°N which may arguably be better explained by the more southerly PMG plate boundary between at least 200 and 150 Ma.

The mantle structure, as modelled by seismic tomography, along 65°N displays significant heterogeneity (Fig. 17). We suggest that the major fast anomaly between 1000 and 2000 km (f) in the west of the profile (120°W to 80°W longitude) corresponds to Farallon and Cache Creek Ocean subduction along the Uda–Murgal arc and northernmost NAM margins, as also interpreted from Fig. 16 (slab c). It may, however, correspond to the northern edge of the younger, well-defined, Farallon slab (see Section 4.2). Further east under 70°W to 40°W longitude is another, smaller but arguably separate and fast anomaly (g) lying horizontally around 1500 km depth. Due to its more easterly location we suggest that this slab might correspond to subducted Cache Creek Ocean or even SAO subduction along the Koyukuk arc. If this slab (maximum depth of slab, 1500 km) is associated with subduction around 150–130 Ma, as suggested by our plate model, the average sinking rate implied is ~1–1.2 cm/yr. This rate is similar to the sinking rate implied in Van der Meer et al. (2010) (1 cm/yr) who used a similar methodology. Conversely, if an upper-value average sinking rate of 2 cm/yr is implied, the age of this slab would be around 75 Ma. This slab is over 1000 km east from the nearest subduction zone at that time based on our plate model and regardless of the absolute reference frame (Fig. 11). A comparison between absolute reference frames along this latitude is relatively similar for times younger than 100 Ma, however, for 200–150 Ma the offset of subduction zones is quite large and is difficult to robustly analyse.

Figs. 18 and 19 were selected to best image slabs associated with the subduction of the SAO along the Oloy and Koyukuk–Nutesyn arc and subduction zones. The longitudinal profile (50°W Fig. 18) shows an upper and mid-mantle anomaly (h) between 440 and

1800 km and might match the eastern mid-mantle slab imaged in Fig. 17 (slab g). This slab (h) might be a remnant of the South Anuyi Ocean as subducted along the Koyukuk–Nutesyn subduction zones or even the Cache Creek Ocean or Farallon plates along the Uda–Murgal subduction zone. The proximity of this slab to both subduction zones makes it difficult to assign to either subduction system, however, the slab feature does extend further to 40°W and 30°W in most seismic tomography models suggesting that it might be more related to South Anuyi Ocean subduction (see slab k, below). Furthermore, a second phase of slab subduction might be inferred from the transition zone smearing in the Gypsum S, S4ORTS and Simmons S models. In nearly all tomography models, there is a fast anomaly (i) lying along the lowermost mantle under 80–90°N. This slab is likely the same as the high latitude slab imaged in Figs. 14–16 (slab d). Furthermore, its continuation across the pole (e.g. identified at both 180°W and 50°W longitude) lends to the interpretation that this slab is further north than the circum-Panthalassa subduction zones and could therefore be related to subduction of the Oimyakon Ocean Basin, or the SAO along the Oloy arc. Alternatively, this slab may also be related to older Mongol–Okhotsk subduction. A comparison of absolute reference frames under the north geographic pole (Fig. 10) illustrates that the subduction zones predicted in this area are largely similar between the different absolute reference frames.

A complicated mantle structure is represented in Fig. 19; there is a major anomaly (j) between 1000 and 1500 km primarily in the north–northwest of the profile between 120°W and 80°W longitude. This slab likely matches the northern anomaly imaged in Fig. 16 (slab e, eastern Uda–Murgal), which was tentatively interpreted as either SAO slab subducted along the Oloy subduction zone, or Panthalassa slab. Furthermore this slab feature may be distinct from slab material (k) located primarily between 440 and 1100 km in the east of the profile between 60°W and 30°W longitude. This slab (k) may also represent SAO material subducted along the Koyukuk–Nutesyn arc (as also imaged as (h) in Fig. 18 and possibly an extension of (g) in Fig. 17). Based on our preferred plate model, we argue that the slab's far northern and eastern location precludes it being Panthalassa slab material and therefore is evidence for SAO subduction under the AACM. Its relatively shallow depths, however, suggest a more recent subduction history. For example, taking a maximum slab depth of 1100 km and age range of 150–130 Ma the implied average sinking rate is ~0.73–0.85 cm/yr. Conversely, a rate of 1 cm/yr implies an age of 110 Ma and a rate of 2 cm/yr implies an age of 55 Ma. At 110 Ma the closest subduction zones of that age based on our base plate model are over 1000 km away and at 55 Ma are over 3000 km to the west. Importantly, a comparison of absolute reference frames in the high Arctic at 200 and 150 Ma (region of Figs. 18 and 19) shows that our base TPW model consistently predicts a subduction zone the furthest east and north compared to PMG or SUB. Therefore, because slab (k) is imaged as far east as 30°W it cannot be sufficiently accounted for, based on the absolute reference frames compared here, by a subduction zone later than the Late Jurassic. Despite implying a relatively slow sinking rate, we suggest that the location of this slab under Greenland is best explained by SAO subduction associated with the opening of the Amerasia Basin. There is also slab material along the CMB (l) which might be related to older SAO, Monghol–Okhotsk or Panthalassa subduction (correlates with slab e of Fig. 18). However, in the S4ORTS and Montelli S tomography models this lower mantle/CMB material also extends further east than our modelled Panthalassa boundaries and may be linked to SAO subduction.

4.2. North America

Numerous studies based on high-resolution seismic tomography models under western North America have recently been published, and to a large degree they consistently image the major features of

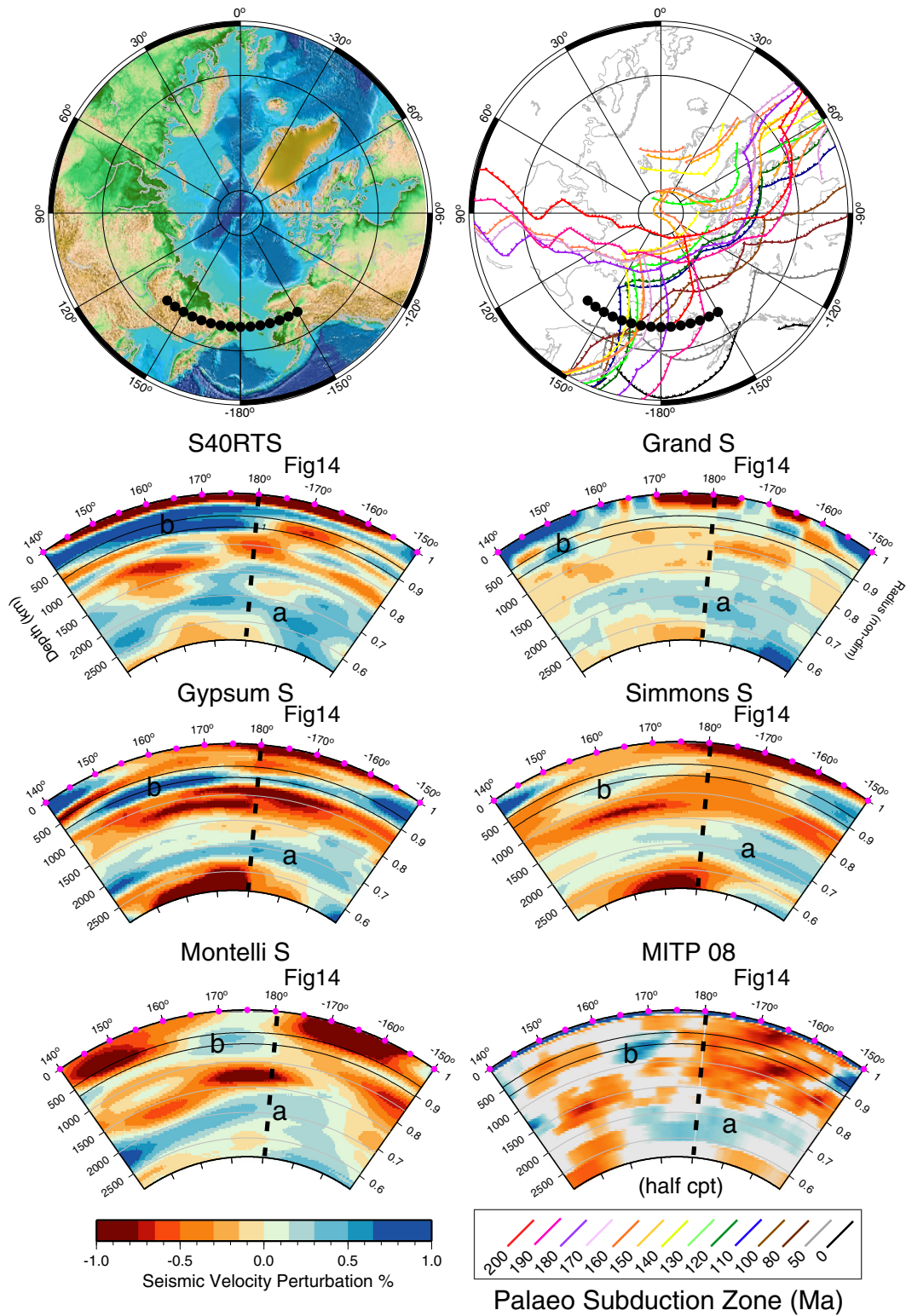


Fig. 13. Vertical cross-section (1) along reconstructed western Panthalassa and East Monghol–Okhotsk boundaries through five S-wave and one P-wave seismic tomography models. Latitude: 65°N, longitude 140°E–150°W, shown as black line with circles on stereographic maps, see inset for legend. Long dashed line through the vertical cross-sections corresponds to intersection with Fig. 14. Interpreted slab feature (a) likely represents post-Jurassic subducted Izanagi slabs and (b) interpreted to represent younger Izanagi and Pacific slabs stalled in the transition zone.

the regional mantle structure including a fragmented system of slabs (Becker, 2011; Pavlis et al., 2012; Sigloch, 2011). However, the timing, mechanism and tectonic implications of the fragmented lower mantle slabs under NAM are still debated. Here, we provide a brief overview of key features in the context of linking the circum-Arctic to the

eastern Panthalassa systems during the Jurassic, noting the listed references for further discussion.

It is generally assumed that prior to 80 Ma and the Laramide Orogeny, the Farallon Plate was subducting and arc magmatism occurred along the entire margin of western North America (Dickinson,

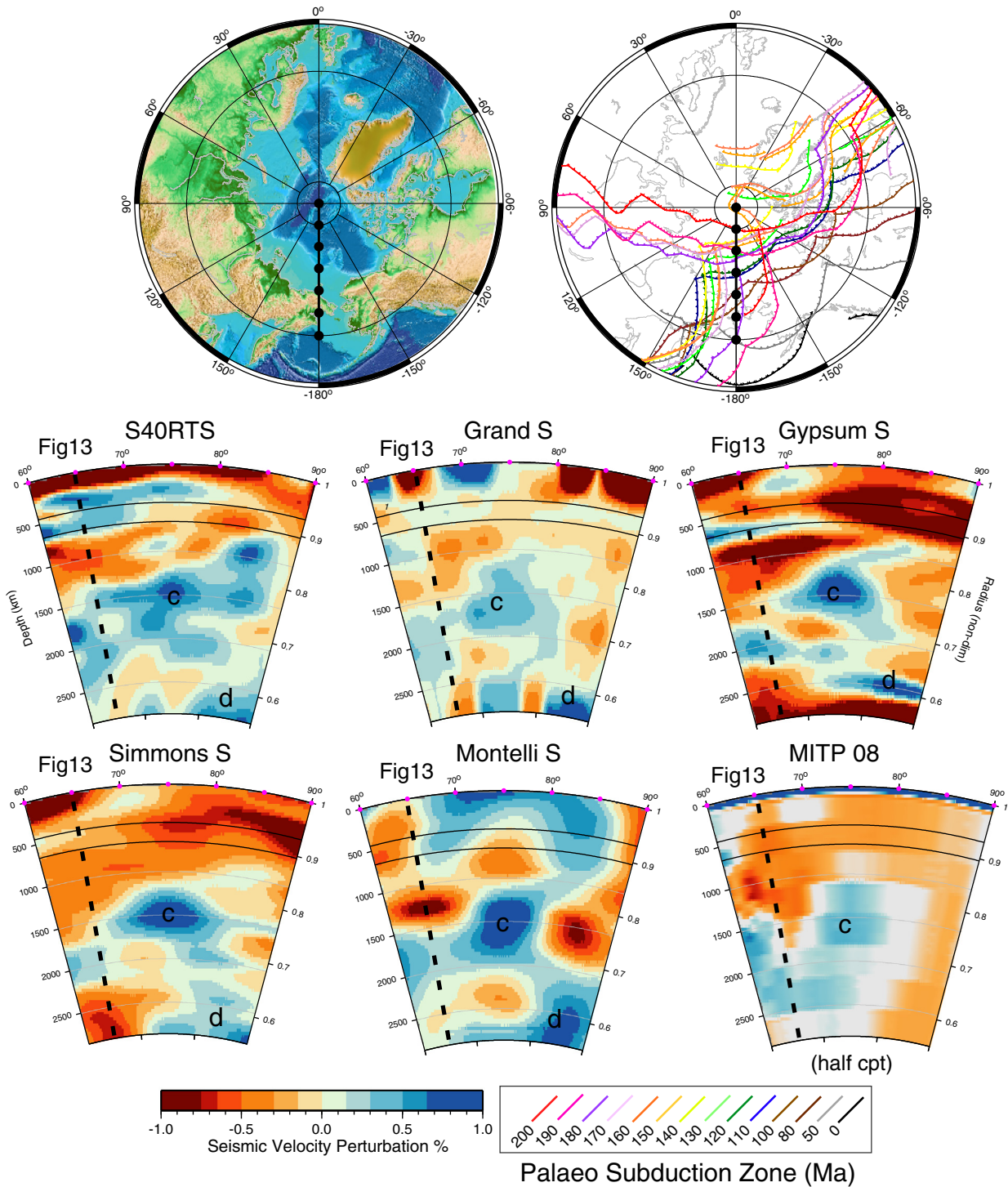


Fig. 14. Vertical cross-section (2) along reconstructed northern Panthalassa and western Uda–Murgal arc boundaries through five S-wave and one P-wave seismic tomography models. Latitude: 60–90°N, longitude 180°E, shown as black line with circles on stereographic maps, see inset for legend. Long dashed line through the vertical cross-sections corresponds to intersection with Fig. 13. Slab features (c) and (d) interpreted as subducted Jurassic Farallon, Izanagi and Cache Creek Ocean slabs, with (d) possibly subducted Mongol–Okhotsk subduction. Slab (c) likely matches slab (a) in Fig. 13. The apparent thickness of some seismic tomography anomalies e.g. our interpreted slab (c), might be related to the resolution of the tomography model, slab advection and thermal dissipation, folded slabs or the convergence of slabs from multiple/adjacent subduction zones.

2004). The robustly imaged “Farallon” slab located under eastern NAM throughout the lower mantle is widely thought to represent this eastward-subducted Farallon lithosphere. However, timings of the deepest parts of this slab are debated, ranging from the Early Jurassic through to the Cretaceous (~194–60 Ma) (Van der Meer et al., 2010), 120–85 Ma or older (Ren et al., 2007) younger than 100 Ma (Grand et al., 1997), older than 150 Ma (Sigloch et al., 2008). Alternatively, this slab may instead correspond to subduction

along a long-lived stable intra-oceanic subduction zone, with the base of the slab being significantly older than 140 Ma (Sigloch and Mihalynuk, 2013). Furthermore, the kink in the slab around 50°N has previously been attributed to flat slab subduction and/or a break in the Kula Plate (Bunge and Grand, 2000; Ren et al., 2007) occurring at least before 80 Ma (Sigloch, 2011) or a separate but along-strike system of stable intra-oceanic subduction (Sigloch and Mihalynuk, 2013). A comparison of absolute reference frames (Fig. 11) shows

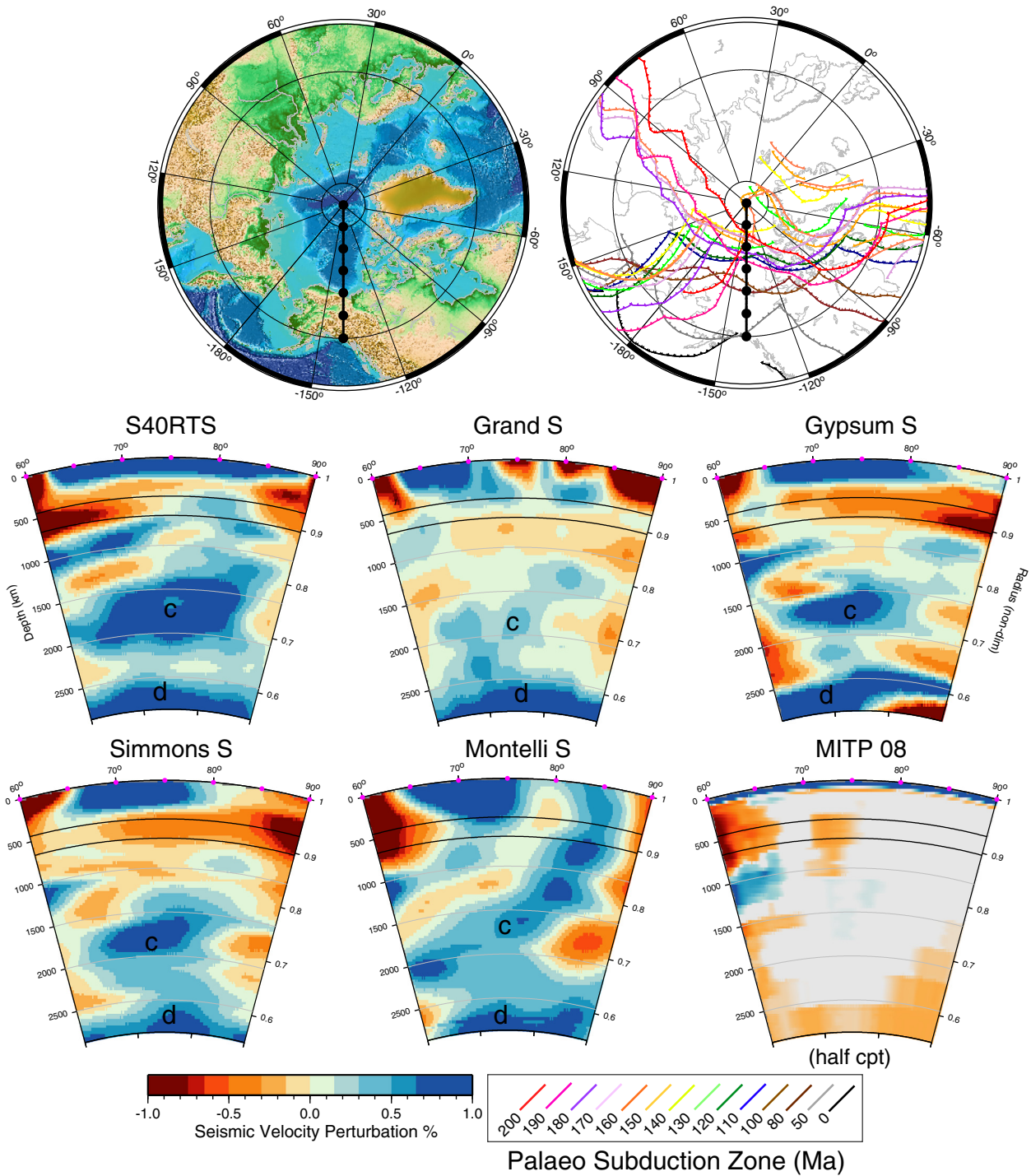


Fig. 15. Vertical cross-section (3) along reconstructed northern Panthalassa and central Uda–Murgal arc boundaries through five S-wave and one P-wave seismic tomography models. Latitude: 60–90°N, longitude 140°W, shown as black line with circles on stereographic maps, see inset for legend. Slabs (c) and (d) interpreted as subducted Jurassic Farallon, Izanagi and Cache Creek Ocean slabs, (c) likely matches slab (a) in Fig. 13. The massive fast anomalies in the upper mantle (see also Figs. 16–18) are likely a function of the resolving power of the tomographic models, source–receiver limitations and disparity in sampling of some mantle regions by direct waves, the uncertain effects of the crust on surface-wave dispersion, location of slices adjacent to shields and that some transition zone anomalies might be extended into shallower mantle depths (e.g. Grand, 2002).

that the bulk of the Farallon slab (m) (90–60°W) is best explained by the location of the western Laurentian margin of the PMG, TPW and DBV models between 150 and 100 Ma. Due to the longitudinal correction of the SUB model, the SUB subduction zone along NAM coincides with this slab for earlier times (200–150 Ma), however, this longitudinal shift does not fit their interpretation of slabs related to the Wrangellia Superterrane (see below).

Figs. 20 and 21 capture the mantle structure under the northeastern margin of Panthalassa (50°N and 30°N latitude) associated with subduction between at least 200 Ma and present-day. Here we discuss four main slab features. Based on our plate model, the main fast anomaly (m) in the centre of Fig. 20 between 1000 and at least 2000 km depth is interpreted to be the Farallon slab, as in most previous studies. Using the imposed absolute reference frame we note

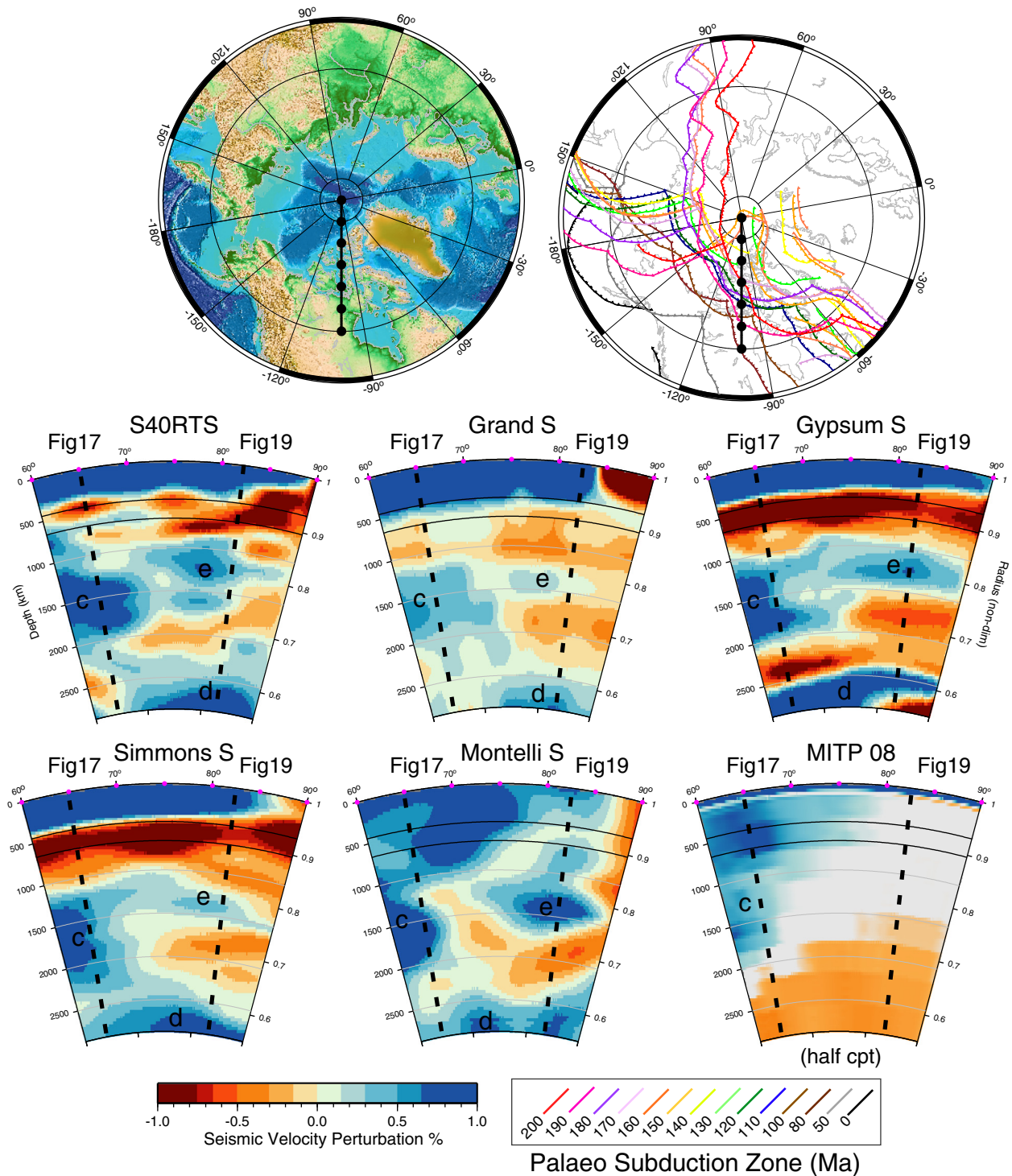


Fig. 16. Vertical cross-section (4) along reconstructed northern Panthalassa and eastern Uda–Murgal arc boundaries through five S-wave and one P-wave seismic tomography models. Latitude: 60–90°N, longitude 100°W, shown as black line with circles on stereographic maps, see inset for legend. Long dashed lines through the vertical cross-sections correspond to intersection with Figs. 17 and 19. Slab features (c) and (d) interpreted as subducted Jurassic Farallon, Izanagi and Cache Creek Oceanic slabs, (c) likely matches slab (a) in Fig. 13. Northerly slab (e) possibly related to subduction of the Oimyakon or SAO.

that the majority of this slab is located further west of the 110 Ma western NAM plate margin, suggesting that it is likely related to younger subduction.

Further west, under 130–120°W longitude, a slab anomaly (n) at similar depths to the Farallon slab may be distinguished. It corresponds to the “Idaho” slab of Van der Meer et al. (2010, 2012) who suggested that it represents eastward-dipping Farallon/Panthalassa lithosphere from mid-late Mesozoic (~186–92 Ma) along an intra-

oceanic arc, possibly the northern part of the Wrangellia arc. The “Idaho” slab has been interpreted by these authors to be located at the same depths as another slab, “Socorro,” located further south under Central America. Van der Meer et al. (2010) suggest that this mid-mantle “Socorro” slab is also related to an eastward-dipping intra-oceanic subduction zone of the Jurassic–Cretaceous (~186–92 Ma), possibly a southern component of the Wrangellia Superterrane. However, based on our plate model, Fig. 11 shows that between 200 and

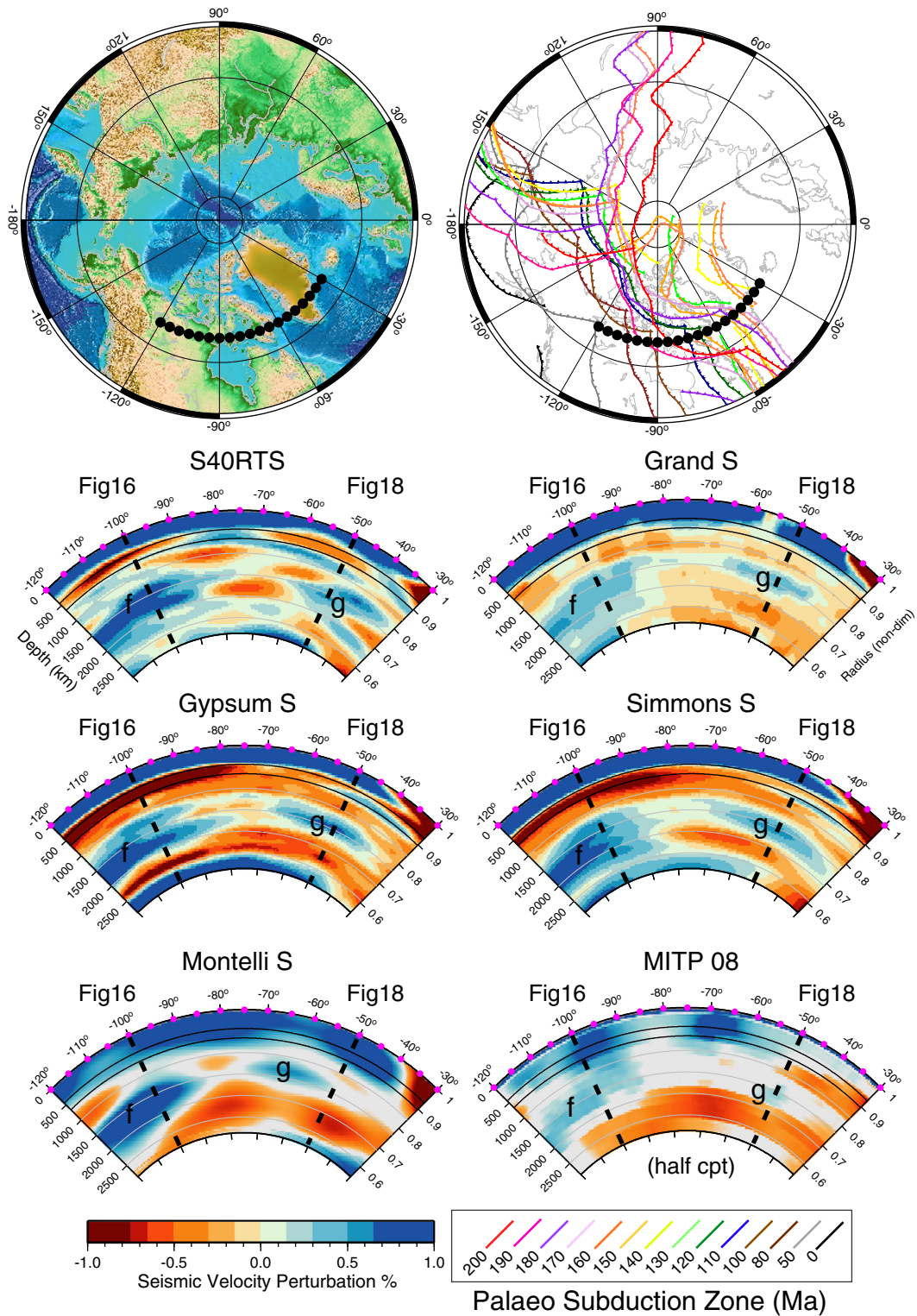


Fig. 17. Vertical cross-section (6) along reconstructed northern Panthalassa and Uda–Murgal arc boundaries through five S-wave and one P-wave seismic tomography models. Latitude: 65°N, longitude 120–30°W, shown as black line with circles on stereographic maps, see inset for legend. Long dashed lines through the vertical cross-sections correspond to intersection with Figs. 16 and 18. Interpreted slab (f) as Farallon and Cache Creek Ocean subduction along the Koni–Taigonos and Uda–Murgal subduction zones, may correspond to slab (c) in Fig. 14. Slab (g) interpreted as Cache Creek Ocean or SAO slabs subducted along the Oloy subduction zone, see slab (h) Fig. 18.

150 Ma the Wrangellia Superterrane predicted by the SUB frame is closer to a maximum western reach of 100°W (100°–70°W) which is inconsistent with their interpretation. Van der Meer et al. (2012) imply that the Wrangellia Superterrane was still intraoceanic at 130 Ma, located 3000 km offshore of NAM, which is not supported by geological evidence. Even if a later Wrangellia Superterrane accretion time is imposed

(e.g. 80 or 100 Ma), the NAM boundary for the SUB reference frame is still too far east (100°W) to be attributed to this slab. In contrast to this interpretation, we argue that our modelled age of Wrangellia Superterrane arc activity (at least 200–140 Ma) and location of the Superterrane means that subducted slabs from this subduction zone are expected to be closer to 60°W longitude (or 90°W at most) rather

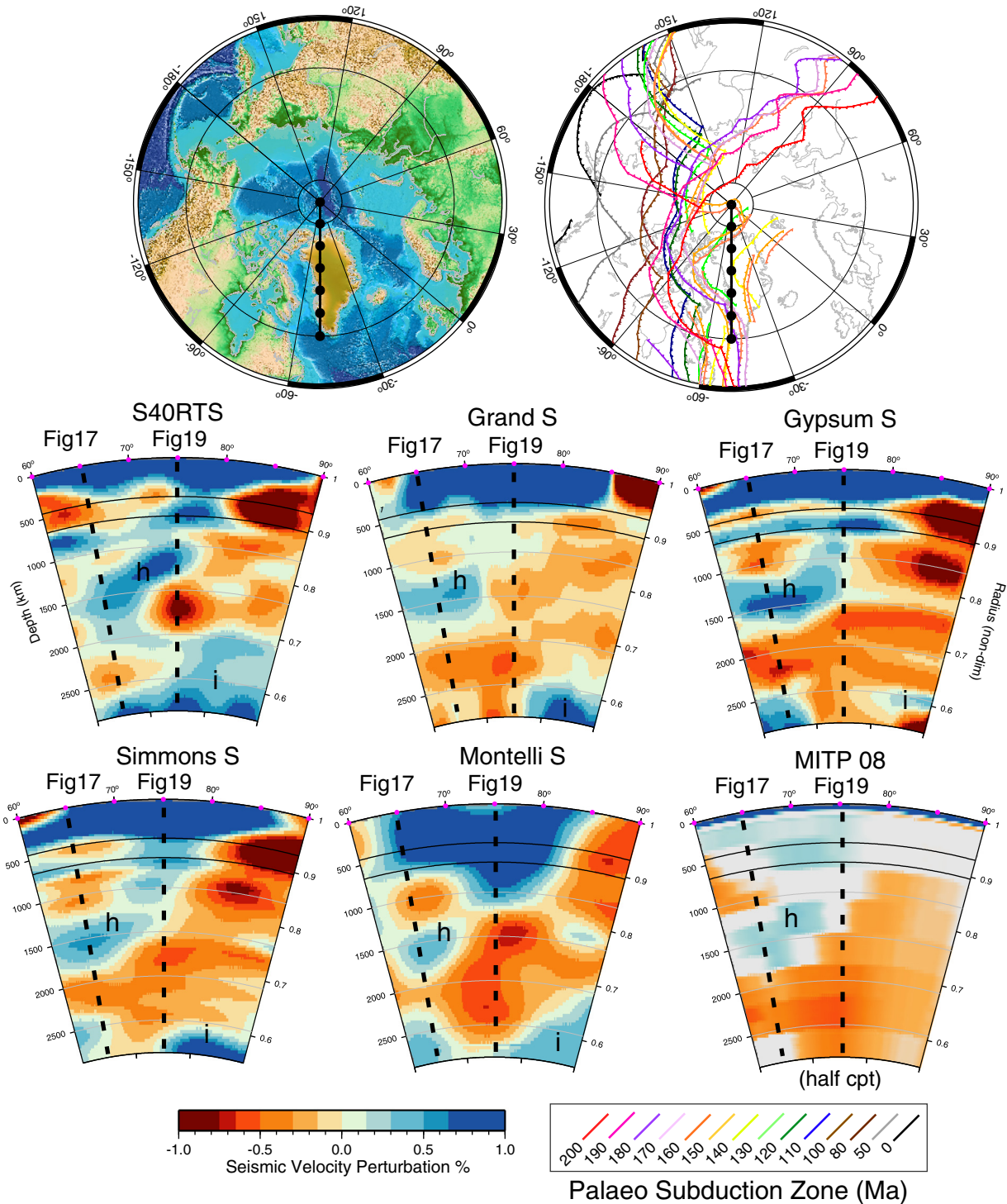


Fig. 18. Vertical cross-section (7) along reconstructed Oloy arc boundaries through five S-wave and one P-wave seismic tomography models. Latitude: 60–90°N, longitude 50°W, shown as black line with circles on stereographic maps, see inset for legend. Long dashed lines through the vertical cross-sections correspond to intersection with Figs. 17 and 19. Slab feature (h) interpreted as SAO slab subducted along Oloy or Koyukuk subduction zones, possibly matching slab (g) from Fig. 17. Northern and eastern location of slab (i) suggests link to Oimyakon Ocean or SAO subduction.

than the 130–120°W of the “Idaho slab.” We therefore prefer the interpretation that the western mid-mantle “Idaho” slab (n) is interpreted as either Cenozoic Farallon slab (Sigloch et al., 2008, “S2”) or Cretaceous Kula or Izanagi slab (Ren et al., 2007). As an alternative, Sigloch (2011) noted that this slab (“Cascadia Root”) is connected to the present-day Cascadia trench and attribute it to an intra-oceanic Siletzia subduction system, which accreted to NAM around 50 Ma.

We have identified anomalous material lying along the CMB (o) in nearly all tomographic models, located under the main Farallon slab (m). Based on its longitudinally variable extent depending on tomography model, we cautiously suggest that it may match subducted Cache Creek Ocean and/or Farallon lithosphere along the Talkeetna-Bonanza and Gravina arcs, or possibly older remnant Slide Mountain Ocean slab from earlier Stikinia-Quesnellia subduction (Figs. 3–6,

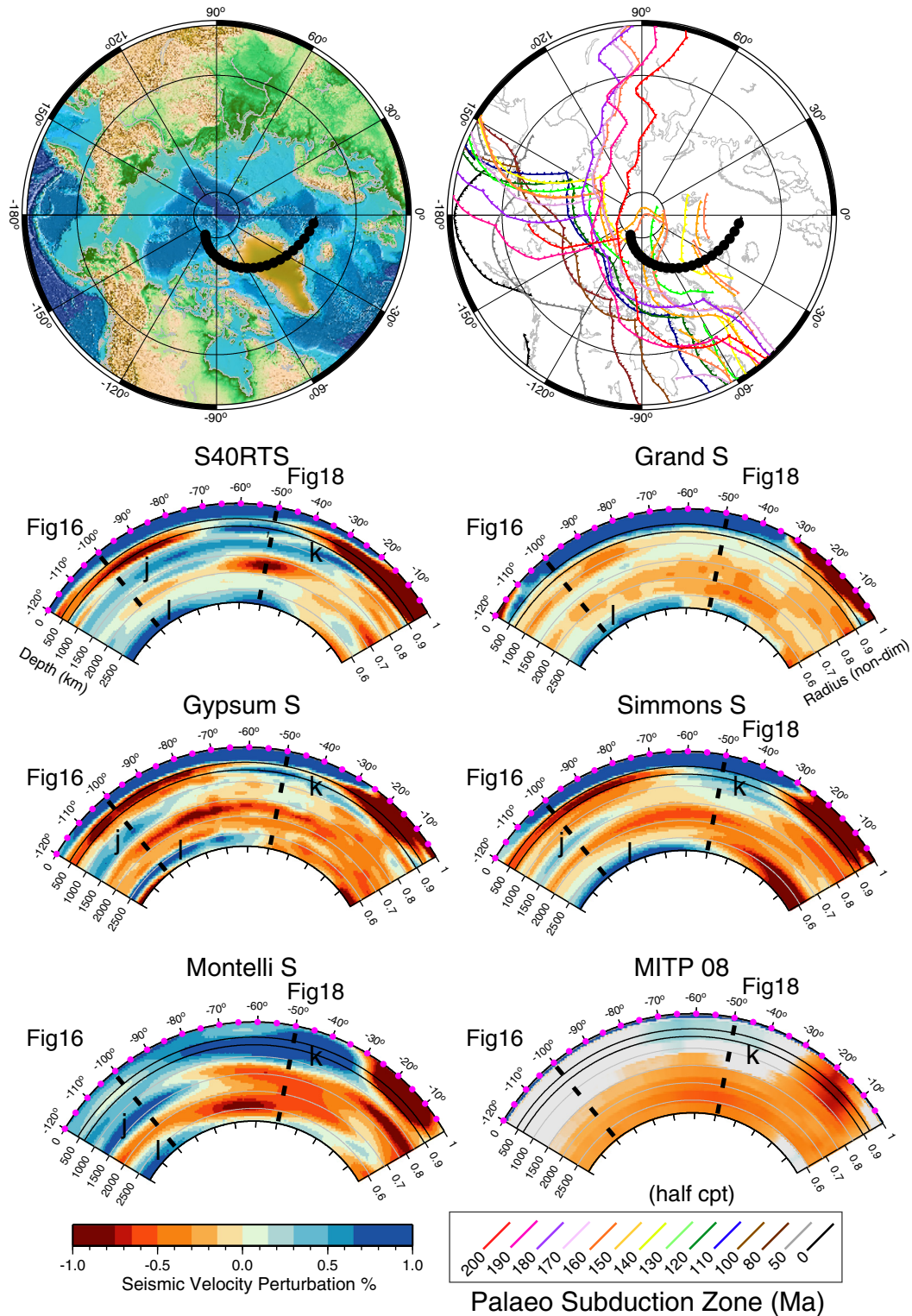


Fig. 19. Vertical cross-section (8) along reconstructed Oloy and Koyukuk–Nutesyn arc boundaries through five S-wave and one P-wave seismic tomography models. Azimuthal 120°W, 85°N azimuth 98 distance 120°, shown as black line with circles on stereographic maps, see inset for legend. Long dashed lines through the vertical cross-sections corresponds to intersection with Figs. 16 and 18. Slab (j) interpreted as Panthalassa or SAO slabs, see slab (e) of Fig. 16. Slab (k) interpreted as SAO subducted along the Koyukuk arcs (as in Figs. 17 and 18). Slab (l) likely older SAO or Panthalassa subduction.

9). Moving further east of the dominant Farallon slab, additional slab material can be identified in the mid and lower mantle under ~55–30°W (p). A profile through 30°N (Fig. 21) also shows this eastern slab material under the western Atlantic and seems to extend from various depths throughout the lower mantle depending on tomography model. These (p) slabs are arguably deeper in the 30°N section

than the 50°N section, suggesting oldest subduction to the south and would complement a north–northeasterly migrating subduction zone. Based on our preferred model, the longitude of this (p) slab suggests that it is related to subduction of the Cache Creek Ocean along western Laurentia or parts of the Cache Creek Ocean or Farallon Plate along the Wrangellia Superterrane, or a component of both.

However, contrary to what might be expected, an orthogonal transect through the modelled northeastward migrating Wrangellia Superterrane does not yield a robust slab, illustrating the complexity and uncertainty in the reconstructions of this terrane. The maximum depth of the (p) anomaly at 30°N is the CMB which matches an ~1.5 cm/yr average sinking rate of a slab subducted at 190 Ma. At 50°N the maximum depth of (p) is highly dependent on the tomography model used and may be particularly poorly resolved. However, for the Gypsum S model, the maximum depth is ~2000 km and for a slab subducted between 170 and 140 Ma a

sinking rate of 1.2–1.4 cm/yr is estimated. We argue that these rates are reasonable and fit with our suggested Wrangellia Superterrane history.

A comparison of the TPW and PMG absolute reference frames at 200 Ma along the NAM/Wrangellia Superterrane boundaries indicates a large southern and western offset of the PMG model (~1000 km longitude and ~2000 km latitude) until 150 Ma; after that time the models are similar. As also mentioned for the northwest Panthalassan margin (Fig. 13), this offset of the PMG model between 200 and 150 Ma points to an arguably fast net northeastward motion of the NAM margin based

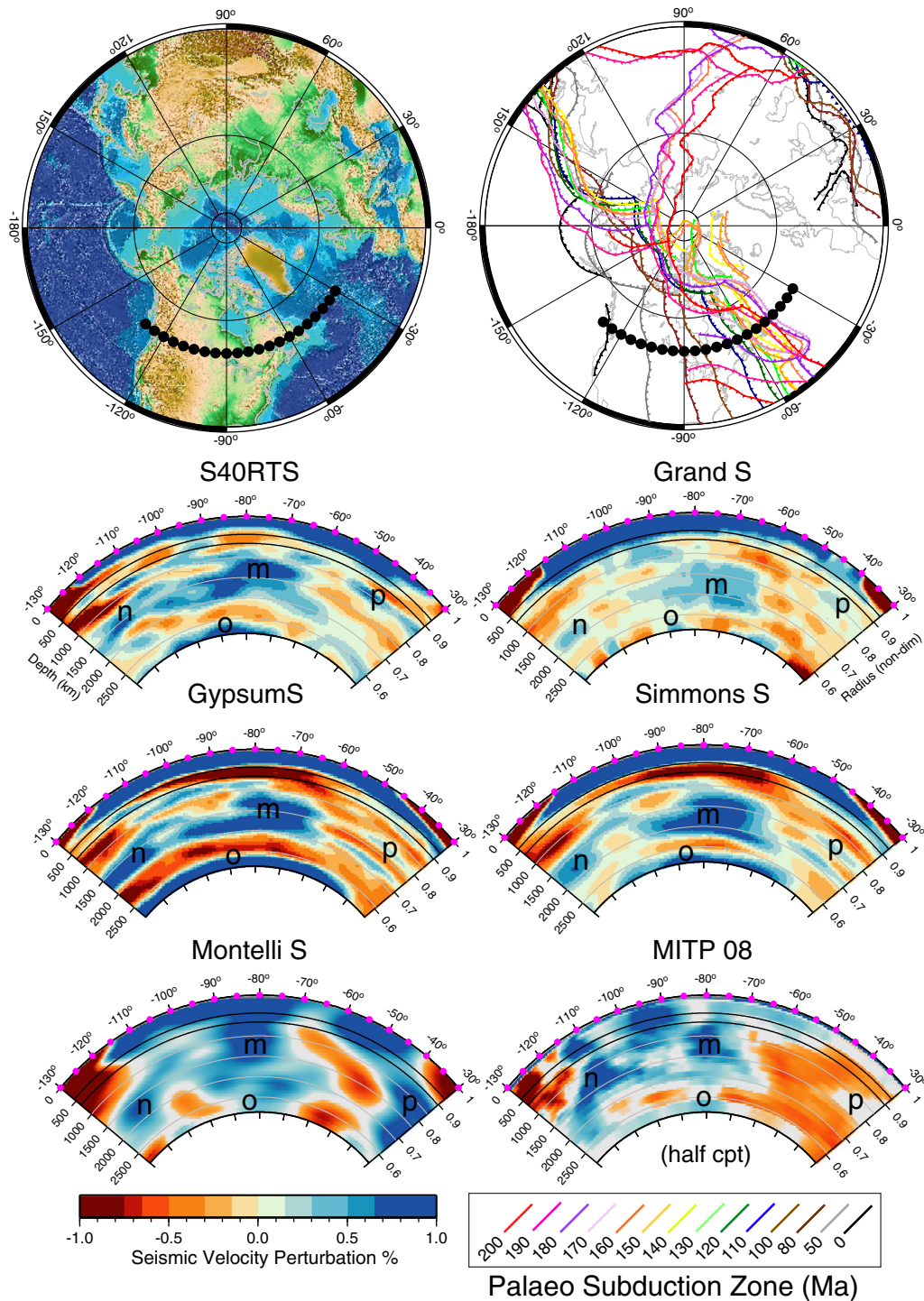


Fig. 20. Vertical cross-section (9) along reconstructed eastern Panthalassa and Wrangellia arc boundaries through five S-wave and one P-wave seismic tomography models. Latitude: 50°N, longitude 160–30°W, shown as black line with circles on stereographic maps, see inset for legend. Interpreted slab features (m) as Farallon slab and (n) as either Cretaceous Kula or Farallon slab or Cenozoic Farallon slab. Slab (o) along the CMB is interpreted as Cache Creek Ocean subducted along Wrangellia Superterrane or possibly older slabs and (p) alternatively, as slabs subducted along a northward migrating Wrangellia Superterrane or along a coeval subduction zone along Laurasia.

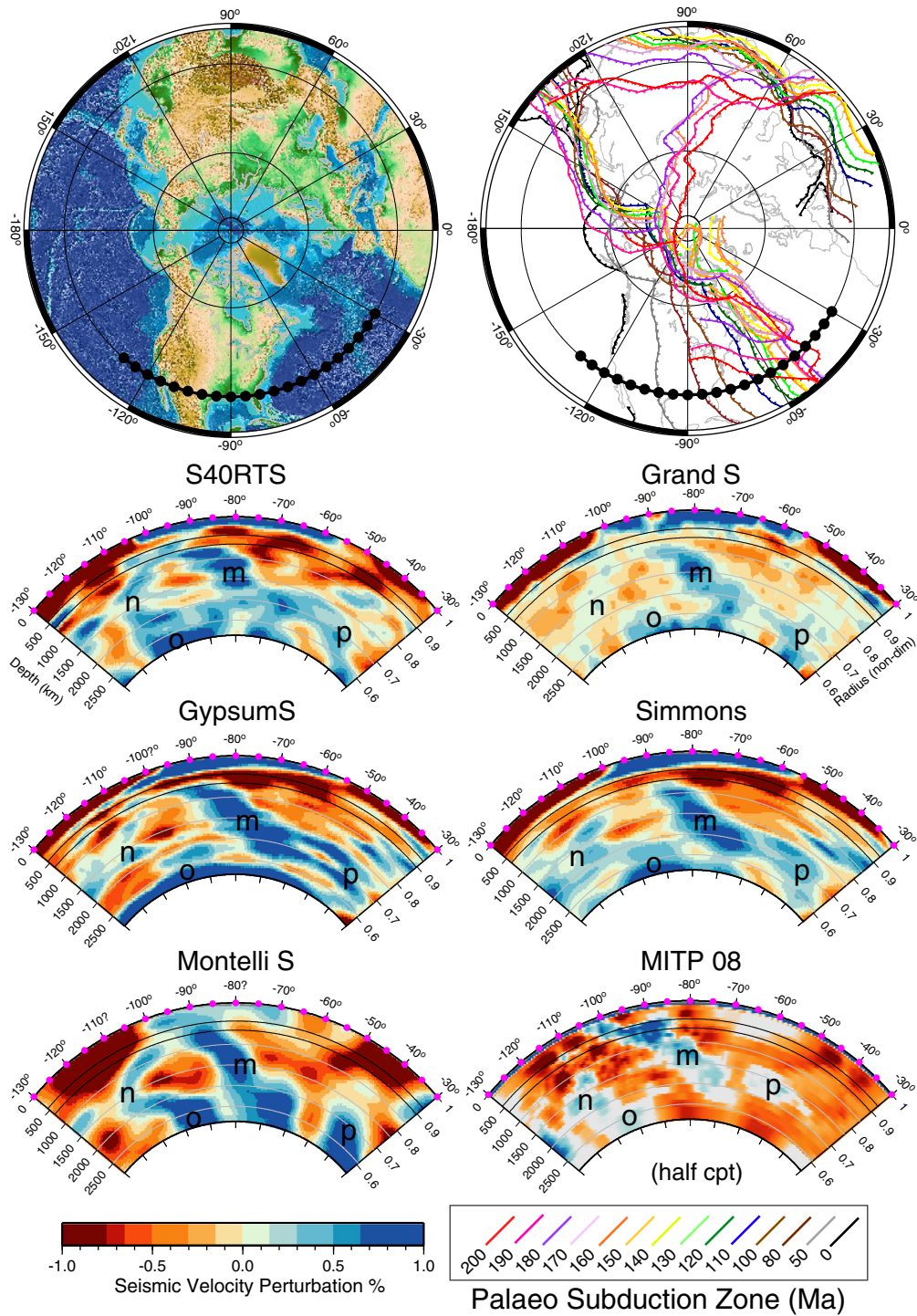


Fig. 21. Vertical cross-section (10) along reconstructed eastern Panthalassa and Wrangellia arc boundaries through five S-wave and one P-wave seismic tomography models. Latitude: 30°N, longitude 160–30°W, shown as black line with circles on stereographic maps, see inset for legend. Interpreted slab features as in Fig. 12, but note that slab (p) is imaged at deeper depths at this latitude compared to 50°N.

on the PMG model. We argue that this PMG–TPW discrepancy cannot be discerned through our tomography analysis, however, we suggest that the eastern location of the anomaly (p) is best explained by the TPW model. Interestingly, the southern portion of the Farallon slab (south of the 50°N kink) corresponds approximately with the predictions of the Wrangellia Superterrane during 200–150 Ma based on the PMG reference frame (or SUB frame but note the self-inconsistencies mentioned above). However, the broad eastward-dip and volume of

the slab is better explained by the more conventional interpretation of post-100 Ma Farallon slab.

The “Trans-Americas” slab of Van der Meer et al. (2010) located further south and offshore of Central America was interpreted to represent westward-dipping and eastward-migrating early Mesozoic (~219–178 Ma) intra-oceanic subduction, possibly from along the Stikinia–Quesnellia arc or along the western margin of Laurentia. Similarly, their “Wichita” slab located in the lower mantle under

central-eastern NAM was also interpreted to be intraoceanic subduction (~219–178 Ma) possibly along the Stikinia–Quesnellia arc. However, we suggest the youngest Stikinia–Quesnellia (Slide Mountain Ocean) slab to be/have been located not significantly further west than the later Wrangellia subduction (see Section 2.5). Furthermore, in our model the Stikinia–Quesnellia arc accreted at 230 Ma and is unlikely to be robustly imaged in seismic tomography. We note that this interpretation is based on our early accretion of the Yukon–Tanana–Quesnellia–Stikinia terranes, however, it is possible that if the Stikinia arc accreted later (e.g. 172 Ma as in Seton et al., 2012) this subduction zone may account for slabs (o), or possibly (p). However, this interpretation would question our reconstruction of the Cache Creek Ocean as being located between the Wrangellia Superterrane and Yukon–Tanana–Quesnellia–Stikinia terranes (see Section 2.5). Nevertheless, we therefore expect that slabs in the central and western Atlantic Ocean correlate to such Mesozoic intra-oceanic subduction zones whereas the slabs further west most likely point to younger subduction or possibly missing Cenozoic intraoceanic subduction.

5. Conclusions

We have created a refined tectonic model of the circum-Arctic since the beginning of the Jurassic, and importantly, generated time-dependent and topologically closed plate boundaries. Our plate tectonic model incorporates an extensive synthesis of published geological and geophysical data as well as an analysis of global seismic tomography and a comparison of absolute reference frames.

Our comparison of seismic tomography has shown that seismically fast anomalies underlying the present-day circum-Arctic and NAM can be linked to post-Jurassic subduction zones of our plate model. Our interpretation differs for much of the circum-Arctic and NAM as compared to other recent tomography studies (Van der Meer et al., 2010, 2012). Independent of the absolute reference frame imposed, we are arguably able to discriminate between slabs related to Panthalassa and those related to a more northerly and easterly subduction system(s). In particular, we suggest that tomography anomalies under present-day Greenland and the Canadian Arctic Islands may be explained by the Jurassic destruction of the SAO. We note that the current resolution of seismic tomography precludes a more detailed analysis of subduction kinematics including polarity reversals, slab stagnation and the existence of smaller or short-lived subduction zones (e.g. Oimyakon Ocean under the Uyandina–Yasachnaya subduction zone or Kobuk Sea under the Koyukuk subduction zone), and limits a tighter constraint on the timing of onset and cessation of subduction.

Here, for the first-time, we present a model for a defined Cache Creek Ocean Plate, located between the Wrangellia Superterrane and the Yukon–Tanana–Quesnellia–Stikinia terranes, the latter of which accreted to the western NAM margin around 230 Ma. Assuming a north (30°N) to south (10–20°N) migration of the Wrangellia Superterrane between the Permian and Mid Triassic, we suggest that the Cache Creek Ocean opened during Slide Mountain Ocean closure (260–230 Ma). Furthermore, we reconstruct a subduction polarity reversal along the Wrangellia Superterrane, with an early phase of slab roll back, followed by trench advance as the Superterrane approached the North American margin. This north–northeastward migration of the Wrangellia Superterrane is arguably supported by a northerly-shallowing slab in the western Atlantic as interpreted from global seismic tomography. We also suggest that a mid-Palaeozoic triple-junction can explain the broadly contemporaneous opening of the Slide Mountain Ocean, Oimyakon Basin and South Anuyi Ocean.

For the Amerasia Basin, we present a new multi-stage three-plate model accounting for recently published geophysical data while building upon the large body of published geological observations. We support the reconstruction of a “windshield” wiper model for the Canada Basin with seafloor spreading between 142.5 and 126 Ma (Alvey et al., 2008). New aeromagnetic data supporting an orthogonal rifting and

opening to the Lomonosov Ridge is incorporated for the more northerly regions (Døssing et al., 2013). Based on rates of seafloor spreading of 2.2–7.7 cm/yr (Døssing et al., 2013), we suggest that seafloor spreading occurred in the Makarov and Podvodnikov basins for at least 20 Myr, from 142.5 to 120 Ma. We initiate basin-wide rifting from 195 Ma (Grantz et al., 2011b), noting that this onset may be younger, however, earlier timings for the onset of seafloor spreading exist and may explain apparently conflicting sediment and palaeogeography studies (e.g. Miller et al., 2006, 2008). We emphasise that the AACM cannot be rotated as a single, rigid fragment as also suggested by others (e.g. Funck et al., 2011; Miller et al., 2006). Our timing of opening within the Amerasia Basin, including either rifting or seafloor spreading, or both, is slightly earlier than other rotational models (e.g. Lawver et al., 2002; Alvey et al., 2008; Grantz et al., 2011b), and may better reconcile the Siberian affinities and pre-Tithonian SAO subduction timings for the AACM as presented in Miller et al. (2006, 2008). While we present a plate model with rifting orthogonal to the Lomonosov Ridge, we suggest that a component of younger strike slip along the SAZ and extension parallel to the Lomonosov Ridge, perhaps related to younger HALIP activity and emplacement of the Alpha–Mendeleev Ridge or the opening of the Atlantic, is not precluded. The initial collision between the AACM and NE Siberia may have been orthogonal with a final stage of oblique slip accompanied by transpression and strike-slip faults along the South Anuyi Suture, as suggested by Sokolov et al. (2002). This may account for the western continuation of the South Anuyi Suture being poorly defined. Further work to account for seemingly contrasting regional observations for the opening of the Amerasia Basin may be achieved through plate deformation models that build upon our regional rigid plate model.

We acknowledge that there are many aspects to our Jurassic reconstructions that remain to be further constrained, and suggest that some of the most important considerations for future plate tectonic reconstructions include:

- (1) Discerning the longevity of subduction and seafloor spreading on both the northern and/or southern margins of the SAO.
- (2) Whether subduction along the Siberian (Kedon and Uda–Murgal arcs) and NAM (Western Laurentian) subduction zones were linked for all or part of time since the Triassic. Therefore, addressing if the SAO was located behind a continuous subduction zone or if there was an “embayment” style geometry.
- (3) Constraining the timing and mechanism of Cache Creek Ocean opening and closure – whether our interpretation of its location between Wrangellia and the Yukon–Tanana–Laurentian margin is correct.
- (4) Kinematically constraining reconstructions of the Yukon–Tanana, Quesnellia and Stikinia terranes and the Wrangellia Superterrane since at least the Permian until their accretion.
- (5) Developing more regional-specific deformation models accounting for conflicting regional observations e.g. the Laptev Sea, Amerasia Basin, western Siberia.
- (6) Constraining timing and rates of rifting and seafloor spreading within the Amerasia Basin, the nature of the underlying crust and timing of the Alpha–Mendeleev Ridge as well as accounting for the deformation of the tectonic blocks involved.

Plate outlines, rotations and static terrane polygons for our preferred model are available at ftp://earthbyte.org/papers/Shephard_et_al_Arctic_plate_model.

Supplementary data to this article can be found online at <http://dx.doi.org/10.1016/j.earscirev.2013.05.012>.

Acknowledgements

GES, RDM and MS were supported by Australian Research Council (ARC) grant FL0992245, ARC Linkage grant LP0989312 and ARC

Discovery grant DP0987713. We would like to thank Ron Blakey and an anonymous reviewer for their helpful comments on the manuscript, Mitchell Mihalynuk for insightful discussions about the Cache Creek Ocean and Trond Torsvik for providing the rotations for the subduction reference frame.

References

- Akinin, V.V., Miller, E.L., Wooden, J.L., 2009. Petrology and geochronology of crustal xenoliths from the Bering Strait region: linking deep and shallow processes in extending continental crust. In: Miller, R.B., Snoke, A.W. (Eds.), *Crustal Cross-sections from the Western North American Cordillera and Elsewhere: Implications for Tectonic and Petrologic Processes*. Special Paper, 456. The Geological Society of America, Boulder, Colorado.
- Alvey, A., Gaina, C., Kusznir, N.J., Torsvik, T.H., 2008. Integrated crustal thickness mapping and plate reconstructions for the high Arctic. *Earth and Planetary Science Letters* 271, 310–321.
- Andersen, O.B., Knudsen, P., Berry, P., 2010. The DNSC08GRA global marine gravity field from double retracked satellite altimetry. *Journal of Geodesy* 84 (3). <http://dx.doi.org/10.1007/s00190-009-0355-9>.
- Becker, T.W., 2011. On recent seismic tomography for the western United States. *Geochemistry, Geophysics, Geosystems* 13 (1), Q01W10. <http://dx.doi.org/10.1029/2011GC003977>.
- Belasky, P., Stevens, C.H., Hanger, R.A., 2002. Early Permian location of western North American terranes based on brachiopod, fusulinid and coral biogeography. *Palaeogeography, Palaeoclimatology, Palaeoecology* 179, 245–266.
- Beranek, L.P., Mortenson, J.K., 2011. The timing and provenance record of the Late Permian Klondike orogeny in northwestern Canada and arc-continent collision along western North America. *Tectonics* 30, TC5017. <http://dx.doi.org/10.1029/2010TC002849>.
- Blodgett, R.B., Rohr, D.M., Boucot, A.J., 2002. Paleozoic links among some Alaskan accreted terranes and Siberia based on megafossils. In: Miller, E.L., Grantz, A., Klemperer, S.L. (Eds.), *Tectonic Evolution of the Bering Shelf–Chukchi Sea–Arctic Margin and Adjacent Land Masses*. Special Papers, vol. 360. Geological Society of America, Boulder, Colorado, pp. 273–290.
- Boyden, J.A., Müller, R.D., Gurnis, M., Torsvik, T.H., Clark, J.A., Turner, M., Ivey-Law, H., Watson, R.J., Cannon, J.S., 2011. Next-generation plate-tectonic reconstructions using GPlates. In: Keller, G.R., Barz, C. (Eds.), *Geoinformatics: Cyberinfrastructure for the Solid Earth Sciences*. Cambridge University Press, pp. 95–114.
- Brozina, J.M., Childers, V.A., Lawver, L.A., Gahagan, L.M., Forsberg, R., Faleide, J.I., Eldholm, O., 2003. New aerogeophysical study of the Eurasia Basin and Lomonosov Ridge: implications for basin development. *Geology* 31 (9), 825–828.
- Bunge, H.-P., Grand, S., 2000. Mesozoic plate-motion history below the northeast Pacific Ocean from seismic images of the subducted Farallon slab. *Nature* 405, 337–340.
- Bunge, H.-P., Richards, M.A., Baumgardner, R.A., 1997. A sensitivity study of three dimensional spherical mantle convection at 10exp8 Rayleigh number: effects of depth-dependent viscosity, heating mode and an endothermic phase change. *Journal of Geophysical Research* 102, 11991–12007.
- Butler, R.F., Gehrels, G.E., Bazard, D.R., 1997. Paleomagnetism of Paleozoic strata of the Alexander terrane, southeastern Alaska. *GSA Bulletin* 109 (10), 1372–1388.
- Carey, S.W., 1958. The tectonic approach to continental drift. In: Carey, S.W. (Ed.), *Continental Drift: A Symposium*. Tasmania University, Hobart, Australia, pp. 177–355.
- Clift, P.D., Ware, N.M., Amato, J.M., Pavlis, T.L., Hole, M.J., Worthman, C., Day, E., 2012. Evolving heavy mineral assemblages reveal changing exhumation and trench tectonics in the Mesozoic Chugach accretionary complex, south-central Alaska. *GSA Bulletin* 124, 989–1006. <http://dx.doi.org/10.1130/B30594.1>.
- Cochran, J.R., Edwards, M.H., Coakley, B.J., 2006. Morphology and structure of the Lomonosov Ridge, Arctic Ocean. *Geochemistry, Geophysics, Geosystems* 7 (5), Q05019. <http://dx.doi.org/10.1029/2005GC001114>.
- Cocks, L.R.M., Torsvik, T.H., 2011. The Paleozoic geography of Laurentia and western Laurussia: a stable craton with mobile margins. *Earth-Science Reviews* 106, 1–51.
- Coffin, M.F., Eldholm, O., 1994. Large igneous provinces: crustal structure, dimensions and external consequences. *Reviews of Geophysics* 32, 1–36.
- Colpron, M., Nelson, J.L., 2009. A Palaeozoic Northwest Passage: incursion of Caledonian, Baltican and Siberian terranes into eastern Panthalassa, and the early evolution of the North American Cordillera. In: Cawood, P.A., Kröner, A. (Eds.), *Earth Accretionary Systems in Space and Time*. The Geological Society, London, Special Publications, vol. 318, pp. 273–307.
- Colpron, M., Nelson, J.L., Murphy, D.C., 2007. Northern Cordilleran terranes and their interactions through time. *GSA Today* 17, 4–10.
- Coney, P.J., Jones, D.L., Monger, J.W.H., 1980. Cordilleran suspect terranes. *Nature* 288, 329–333.
- Dickinson, W.R., 2004. Evolution of the North American Cordillera. *Annual Review of Earth and Planetary Sciences* 32, 13–45. <http://dx.doi.org/10.1146/annurev.earth.32.101802.120257>.
- Didenko, A.N., Bondarenko, G.Y., Sokolov, S.D., Kravchenko-Berezhnoy, I.R., 2002. Jurassic–Cretaceous history of the Omolon massif, northeastern Russia: geologic and paleomagnetic evidence. In: Miller, E.L., Grantz, A., Klemperer, S.L. (Eds.), *Tectonic Evolution of the Bering Shelf–Chukchi Sea–Arctic Margin and Adjacent Land Masses*. Special Papers, vol. 360. Geological Society of America, Boulder, Colorado, pp. 225–241.
- Døssing, A., Jackson, H.R., Matzka, J., Einarsson, I., Rasmussen, T.M., Olesen, A.V., Brozina, J., 2013. The origin of the Amerasia Basin and the High Arctic Large Igneous Province – results of new aeromagnetic data. *Earth and Planetary Science Letters* 363, 219–230.
- Dove, D., Coakley, B., Hopper, J., Kristoffersen, Y., the HLY0503 Geophysics Team, 2010. Bathymetry, controlled source seismic and gravity observations of the Mendeleev ridge: implications for ridge structure, origin, and regional tectonics. *Geophysical Journal International* 183, 481–502. <http://dx.doi.org/10.1111/j.1365-246X.2010.04746.x>.
- Drachev, S.S., Savostin, L.A., Groshev, V.G., Bruni, L.E., 1998. Structure and geology of the continental shelf of the Laptev Sea, Eastern Russian Arctic. *Tectonophysics* 298, 357–393.
- Drachev, S.S., Malyshev, N.A., Nikishin, A.M., 2010. Tectonic history and petroleum geology of the Russian Arctic Shelves: an overview. In: Vining, B.A., Pickering, S.C. (Eds.), *Petroleum Geology: From Mature Basins to New Frontiers – Proceedings of the 7th Petroleum Geology Conference*, pp. 519–619. <http://dx.doi.org/10.1144/0070591>.
- Dubrovine, P.V., Steinberger, B., Torsvik, T.H., 2012. Absolute plate motions in a reference frame defined by moving hotspots in the Pacific, Atlantic and Indian oceans. *Journal of Geophysical Research: Solid Earth* 117. <http://dx.doi.org/10.1029/2011JB009072>.
- Dumoulin, J.A., Harris, A.G., Gagiev, M., Bradley, D.C., Repetski, J.E., 2002. Lithostratigraphic, conodont, and other faunal links between lower Paleozoic strata in northern and central Alaska and northeastern Russia. In: Miller, E.L., Grantz, A., Klemperer, S.L. (Eds.), *Tectonic Evolution of the Bering Shelf–Chukchi Sea–Arctic Margin and Adjacent Land Masses*. Special Papers, vol. 360. Geological Society of America, Boulder, Colorado, pp. 291–312.
- Embry, A.F., 1990. Geological and geophysical evidence in support of the hypothesis of anti-clockwise rotation of northern Alaska. *Marine Geology* 93, 317–329.
- Embry, A., 1991. Mesozoic history of the Arctic Islands. *Geology of the Inuitian Orogen and Arctic Platform of Canada and Greenland*. *Geology of Canada* 3, 369–433.
- Franke, D., Hinz, K., Oncken, O., 2001. The Laptev Sea Rift. *Marine and Petroleum Geology* 18, 1083–1127.
- Franke, D., Reichert, C., Damm, V., Piepjohn, K., 2008. The South Anuyi suture, North-east Arctic Russia, revealed by offshore seismic data. *Norwegian Journal of Geology* 88, 189–200.
- Fukao, Y., Obayashi, M., Nakakuki, T., the Deep Slab Project Group, 2009. Stagnant slab: a review. *Annual Review of Earth and Planetary Sciences* 37, 19–46. <http://dx.doi.org/10.1146/annurev.earth.36.031207.124224>.
- Funck, T., Jackson, H.R., Shimeld, J., 2011. The crustal structure of the Alpha Ridge at the transition to the Canadian Polar Margin: results from a seismic refraction experiment. *Journal of Geophysical Research* 116, B12101. <http://dx.doi.org/10.1029/2011JB008411>.
- Gabrielse, H., 1985. Major dextral transcurrent displacements along the Northern Rocky Mountain Trench and related lineaments in north-central British Columbia. *Geological Society of America Bulletin* 96, 1–14.
- Gabrielse, H., Murphy, D.C., Mortensen, J.K., 2006. Cretaceous and Cenozoic dextral orogen-parallel displacements, magmatism, and paleogeography, north-central Canadian Cordillera. In: Haggart, J.W., Enkin, R.J., Monger, J.W.H. (Eds.), *Paleogeography of the North American Cordillera: Evidence for and Against Large-scale Displacements*. Geological Association of Canada, Special Paper, vol. 46, pp. 255–276.
- Gaina, C., Roest, W.R., Müller, R.D., 2002. Late Cretaceous–Cenozoic deformation of northeast Asia. *Earth and Planetary Science Letters* 197, 273–286.
- Gaina, C., Werner, S.C., Saltus, R., Maus, S., the CAMP-GM Group, 2011. Circum-Arctic mapping project: new magnetic and gravity anomaly maps of the Arctic. In: Spencer, A.M., Embry, A.F., Gautier, D.L., Stoupakova, A.V., Sørensen, K. (Eds.), *Arctic Petroleum Geology*. Geological Society, London, Memoirs, vol. 35, pp. 39–48. <http://dx.doi.org/10.1144/M35.3> (Chapter 3).
- Gardner, M.C., Bergman, S.C., Cushing, G.W., MacKevett Jr., E.M., Plafker, G., Campbell, R.B., Dodds, C.J., McClelland, W.C., Mueller, P.A., 1988. Pennsylvanian pluton stitching of Wrangellia and the Alexander terrane, Wrangell Mountains, Alaska. *Geology* 16, 967–971.
- Gehrels, G., Rusmore, M., Woodsworth, G., Crawford, M., Andronicos, C., Hollister, L., Patchett, J., Ducea, M., Butler, R., Klepeis, K., Davidson, C., Friedman, R., Haggart, J., Mahoney, B., Crawford, W., Pearson, D., Girardi, J., 2009. U–Th–Pb geochronology of the Coast Mountains batholith in north-coastal British Columbia: constraints on age and tectonic evolution. *GSA Bulletin* 121 (9/10), 1341–1361. <http://dx.doi.org/10.1130/B26404.1>.
- Goes, S., Capitanio, F.A., Morra, G., 2008. Evidence of lower-mantle slab penetration phases in plate motions. *Nature* 451 (7181), 981–984. <http://dx.doi.org/10.1038/nature06691>.
- Golonka, J., 2011. Phanerozoic palaeoenvironment and palaeolithofacies maps of the Arctic region. In: Spencer, A.M., Embry, A.F., Gautier, D.L., Stoupakova, A.V., Sørensen, K. (Eds.), *Arctic Petroleum Geology*. Geological Society, London, Memoirs, vol. 35, pp. 79–129. <http://dx.doi.org/10.1144/M35.6> (Chapter 6).
- Grand, S., 2002. Mantle shear-wave tomography and the fate of subducted slabs. *Philosophical Transactions of the Royal Society of London, Series A: Mathematical, Physical and Engineering Sciences* 360 (1800), 2475–2491.
- Grand, S.P., van der Hilst, R.D., Widiyantoro, S., 1997. Global seismic tomography: a snapshot of convection in the Earth. *GSA Today* 7, 1–7.
- Grantz, A., May, S.D., Taylor, P.T., Lawver, L.A., 1990. Canada Basin. In: Grantz, A., Johnson, G.L., Sweeney, J.F. (Eds.), *The Arctic Ocean Region*. *Geology of North America*, vol. L. Geological Society of America, Boulder, Colorado, pp. 379–402.
- Grantz, A., Clark, D.L., Phillips, R.L., et al., 1998. Phanerozoic stratigraphy of Northwind Ridge, magnetic anomalies in the Canada Basin, and the geometry and timing of rifting in the Amerasia Basin, Arctic Ocean. *GSA Bulletin* 110 (6), 801–820.
- Grantz, A., Scott, R.A., Drachev, S.S., Moore, T.E., Valin, Z.C., 2011a. Map showing the sedimentary successions of the Arctic Region (58–64° to 90°N) that may be prospective for hydrocarbons. In: Spencer, A.M., Embry, A.F., Gautier, D.L., Stoupakova, A.V.,

- Sørensen, K. (Eds.), *Arctic Petroleum Geology*. Geological Society, London, Memoirs, vol. 35, pp. 17–37. <http://dx.doi.org/10.1144/M35.2> (Chapter 2).
- Grantz, A., Hart, P.E., Childers, V.A., 2011b. Geology and tectonic development of the Amerasia and Canada Basins, Arctic Ocean. In: Spencer, A.M., Embry, A.F., Gautier, D.L., Stoupakova, A.V., Sørensen, K. (Eds.), *Arctic Petroleum Geology*. Geological Society, London, Memoirs, vol. 35, pp. 771–799. <http://dx.doi.org/10.1144/M35.50> (Chapter 50).
- Gurnis, M., Turner, M., Zahirovic, S., DiCaprio, L., Spasojevic, S., Müller, R., Boyden, J., Seton, M., Manea, V., Bower, D., 2012. Plate tectonic reconstructions with continuously closing plates. *Computers and Geosciences* 38, 35–42.
- Haeussler, P.J., Coe, R.S., Onstott, T.C., 1992. Paleomagnetism of the Late Triassic Hound Island Volcanics: revisited. *Journal of Geophysical Research* 97, 19617–19639.
- Hafkenscheid, E., Wortel, M.J.R., Spakman, W., 2006. Subduction history of the Tethyan region derived from seismic tomography and tectonic reconstructions. *Journal of Geophysical Research* 111, B08401. <http://dx.doi.org/10.1029/2005JB003791>.
- Halgedahl, S., Jarrard, R., 1987. Paleomagnetism of the Kuparuk River Formation from oriented drill core: evidence for rotation of the North Slope block. In: Tailleux, L., Weimer, P. (Eds.), *Alaskan North Slope Geology: Pacific Section. Society of Economic Paleontologists and Mineralogists*, vol. 50, pp. 581–620.
- Harris, D.B., Toro, J., Prokopyev, A.V., 2012. Detrital zircon U–Pb geochronology of Mesozoic sandstones from the Lower Yana River, northern Russia. *Lithosphere* 5 (1), 98–108. <http://dx.doi.org/10.1130/L250.1>.
- Harrison, J.C., St-Onge, M.R., Petrov, O., Strel'nikov, S., Lopatin, B., Wilson, F., Tella, S., Paul, D., Lynds, T., Shokalsky, S., Hults, C., Bergman, S., Jepsen, H.F., Solli, A., 2011. Geological Map of the Arctic; Geological Survey of Canada, Map 2159A, Scale 1:5000000.
- Hillhouse, W., Grommé, C.S., 1984. Northward displacement and accretion of Wrangellia: new paleomagnetic evidence from Alaska. *Journal of Geophysical Research* 89, 4461–4477.
- Irving, E., Wynne, P.J., Thorkelson, D.J., Schiarizza, P., 1996. Large (1000 to 4000 km) northward movements of tectonic domains in the northern Cordillera, 83 to 45 Ma. *Journal of Geophysical Research* 101, 17901–17916.
- Johnston, S.T., Borel, G.D., 2007. The odyssey of the Cache Creek terrane, Canadian Cordillera: implications for accretionary orogens, tectonic setting of Panthalassa, the Pacific superswell, and the break-up of Pangea. *Earth and Planetary Science Letters* 253, 415–428.
- Katkov, S.M., Miller, E.L., Toro, J., 2010. Structural assemblies and age of deformation in the Western Sector of the Anyui–Chukotka Fold System, Northeastern Asia. *Geotectonics* 44 (5), 424–442.
- Keppie, J.D., Dostal, J., 2001. Evaluation of the Baja controversy using paleomagnetic and faunal data, plume magmatism and piercing points. *Tectonophysics* 339, 427–442.
- Kerr, J.W., 1981. Evolution of the Canadian Arctic Islands: a transition between the Atlantic and Arctic Oceans. In: Nairn, M., Churkin, M., Stehli, F.G. (Eds.), *Ocean Basins and Margins. The Arctic Ocean*, vol. 5. Springer, New York, pp. 105–199.
- Kos'ko, M., Cecile, M., Harrison, J., Ganelin, V., Kandoshko, N., Lopatin, B., 1993. Geology of Wrangel Island, between Chukchi and eastern Siberian seas, northeastern Russia. Geological Survey of Canada, Bulletin 461.
- Kuzmichev, A.B., 2009. Where does the South Anyui suture go in the New Siberian islands and Laptev Sea? Implications for the Amerasia basin origin. *Tectonophysics* 463, 86–108.
- Kuzmin, M.I., Yarmolyuk, V.V., Kravchinsky, V.A., 2010. Phanerozoic hot spot traces and paleogeographic reconstructions of the Siberian continent based on interaction with the African large low shear velocity province. *Earth-Science Reviews* 102, 29–59.
- Lane, L.S., 1997. Canada Basin, Arctic Ocean: evidence against a rotational origin. *Tectonics* 16, 363–387.
- Lawver, L.A., Scotese, C.R., 1990. A review of tectonic models for the evolution of the Canada Basin. In: Grantz, A., Johnson, L., Sweeney, J.F. (Eds.), *The Geology of North America. The Arctic Ocean Region*, vol. L. The Geological Society of America.
- Lawver, L.A., Grantz, A., Gahagan, L.M., 2002. Plate kinematic evolution of the present Arctic region since the Ordovician. In: Miller, E.L., Grantz, A., Klemperer, S.L. (Eds.), *Tectonic Evolution of the Bering Shelf–Chukchi Sea–Arctic Margin and Adjacent Land Masses. Special Papers*, 360. Geological Society of America, Boulder, Colorado, pp. 333–358.
- Lawver, L.A., Gahagan, L.M., Norton, I., 2011. Palaeogeographic and tectonic evolution of the Arctic region during the Paleozoic. In: Spencer, A.M., Embry, A.F., Gautier, D.L., Stoupakova, A.V., Sørensen, K. (Eds.), *Arctic Petroleum Geology*. Geological Society, London, Memoirs, vol. 35, pp. 61–77. <http://dx.doi.org/10.1144/M35.5> (Chapter 5).
- Laxon, S., McAdoo, D., 1994. Arctic Ocean gravity field derived from ERS-1 satellite altimetry. *Science* 265, 621–624. <http://dx.doi.org/10.1126/science.265.5172.621>.
- Layer, P.W., Newberry, R., Fujita, K., Parfenov, L., Trunilina, V., Bakharev, A., 2001. Tectonic setting of the plutonic belts of Yakutia, northeast Russia, based on 40A/39Ar geochronology and trace element geochemistry. *Geology* 29 (2), 167–170.
- Lebedeva-Ivanova, N.N., Zamansky, Y.Y., Langinen, A.E., Sorokin, M.Y., 2006. Seismic profiling across the Mendeleev Ridge at 82°N: evidence of continental crust. *Geophysical Journal International* 165, 527–544. <http://dx.doi.org/10.1111/j.1365-246X.2006.02859.x>.
- Li, C., van der Hilst, R., Engdahl, E., Burdick, S., 2008. A new global model for P wave speed variations in Earth's mantle. *Geochemistry, Geophysics, Geosystems* 9, Q05018. <http://dx.doi.org/10.1029/2007GC001806>.
- Lithgow-Bertelloni, C., Richards, M.A., 1998. The dynamics of Cenozoic and Mesozoic plate motions. *Reviews of Geophysics* 36 (1), 27–78. <http://dx.doi.org/10.1029/97RG02282>.
- Maher Jr., H.D., 2001. Manifestations of the Cretaceous High Arctic large igneous province in Svalbard. *Journal of Geology* 109, 91–104. <http://dx.doi.org/10.1086/317960>.
- Matthews, K., Seton, M., Flament, N., Müller, R.D., 2012. Late Cretaceous to present-day opening of the southwest Pacific constrained by numerical models and seismic tomography. *Eastern Australasian Basins Symposium EABS IV: Exploration – Driving Future Energy Solutions*. Petroleum Exploration Society of Australia, pp. 105–119.
- McAdoo, D.C., Farrell, S.L., Laxon, S.W., Zwally, H.J., Yi, D., Ridout, A.L., 2008. Ocean gravity field derived from ICESat and ERS-2 altimetry: tectonic implications. *Journal of Geophysical Research* 113, B05408. <http://dx.doi.org/10.1029/2007JB005217>.
- Mihalynuk, M., Nelson, J., Diakow, L.J., 1994. Cache Creek terrane entrapment: oroclinal paradox within the Canadian Cordillera. *Tectonics* 13 (2), 575–595.
- Mihalynuk, M., Erdmer, P., Ghent, E.D., Cordey, F., Archibald, D.A., Friedman, R.M., Johannson, G.G., 2004. Coherent French Range blueschist: subduction to exhumation in <2.5 my.? *GSA Bulletin* 116 (7/8).
- Miller, E.L., Hudson, T.L., 1991. Mid-Cretaceous extensional fragmentation of a Jurassic–Early Cretaceous compressional orogen, Alaska. *Tectonics* 10 (4), 781–796.
- Miller, E.L., Verzhbitsky, V.E., 2009. Structural studies near Pevek, Russia: implications for formation of the East Siberian Shelf and Makarov Basin of the Arctic Ocean. *Stephan Mueller Special Publication Series* 4, 223–241.
- Miller, E.L., Toro, J., Gehrels, G.E., Amato, J.M., Prokopyev, A., Tuchkova, M.I., Akinin, V.V., Dumitru, T.A., Moore, T.E., Cecile, M.P., 2006. New insights into Arctic paleogeography and tectonics from U–Pb detrital zircon geochronology. *Tectonics* 25, 1–19. <http://dx.doi.org/10.1029/2005TC001830> (TC3013).
- Miller, E.L., Soloviev, A., Kuzmichev, A., Gehrels, G.E., Toro, J., Tuchkova, M., 2008. Jurassic and Cretaceous foreland basin deposits of the Russian Arctic: separated by birth of Makarov Basin? *Norwegian Journal of Geology* 88, 201–226.
- Miller, E.L., Kotkov, S.M., Strickland, A., Toro, J., Akinin, V.V., Dumitru, T.A., 2009. Geochronology and thermochronology of Cretaceous plutons and metamorphic country rocks, Anyui–Chukotka fold belt, North East Arctic Russia. *Stephan Mueller Special Publication Series* 4, 157–175.
- Monger, J.W.H., Berg, H.C., 1987. Lithotectonic Terrane Map of Western Canada and Southeastern Alaska: US Geological Survey Miscellaneous Field Studies Map MF-1874-B. 12.
- Monger, J.W.H., van der Heyden, P., Journeay, J.M., Evenchick, C.A., Mahoney, J.B., 1994. Jurassic–Cretaceous basins along the Canadian Coast belt: their bearing on pre-mid-Cretaceous sinistral displacements. *Geology* 22, 175–178.
- Montelli, R., Nolet, G., Dahlen, F.A., Masters, G., 2006. A catalogue of deep mantle plumes: new results from finite-frequency tomography. *Geochemistry, Geophysics, Geosystems* 7 (11), Q11007. <http://dx.doi.org/10.1029/2006GC001248>.
- Moore, T.E., Wallace, W.K., Bird, K.J., Karl, S.M., Mull, C.G., Dillon, J.T., 1994. Geology of northern Alaska. In: Plafker, G., Berg, H.C. (Eds.), *The Geology of Alaska. Geology of America vG-1*. Geological Society of America, Boulder, Colorado, pp. 535–554.
- Morgan, W.J., 1984. Hotspot tracks and the opening of the Atlantic and Indian Oceans. In: Emiliani, C. (Ed.), *The Oceanic Lithosphere. The Sea*, vol. 7. Wiley, New York, pp. 443–487.
- Mortensen, J.K., 1992. Pre-mid-Mesozoic tectonic evolution of the Yukon–Tanana terrane, Yukon and Alaska. *Tectonics* 11, 836–853.
- Müller, R.D., Royer, J.Y., Lawver, L.A., 1993. Revised plate motions from combined Atlantic and Indian Ocean hotspot tracks. *Geology* 21, 275–278.
- Nelson, J.L., Colpron, M., Piercey, S.J., Dusel-Bacon, C., Murphy, D.C., Roots, C.F., 2006. Paleozoic tectonic and metallogenic evolution of pericratonic terranes in Yukon, northern British Columbia and eastern Alaska. In: Colpron, M., Nelson, J.L. (Eds.), *Paleozoic Evolution of Metallogeny of Pericratonic Terranes at the Ancient Pacific Margin of North America. Canadian and Alaska Cordillera: Geological Association of Canada, Special Paper*, 45, pp. 323–360.
- Nokleberg, W.J., et al., 1994. Circum–North Pacific tectonostratigraphic terrane map. Open-File Report 94-714. U.S. Geological Survey (221 pp.).
- Nokleberg, W.J., Parfenov, L.M., Monger, J.W.H., Norton, I.O., Khanchuk, A.I., Stone, D.B., Scotese, C.R., Scholl, D.W., Fujita, K., 1998a. Phanerozoic tectonic evolution of the Circum–North Pacific. Open-File Report 98-754. U.S. Geological Survey (125 pp.).
- Nokleberg, et al., 1998b. Summary terrane, mineral deposit, and metallogenic belt maps of the Russian Far East, Alaska, and the Canadian Cordillera. Open-File Report 98-136. U.S. Geological Survey (Data downloaded from <http://pubs.usgs.gov/of/1998/of98-136/data>).
- Nokleberg, W.J., Parfenov, L.M., Monger, J.W.H., Norton, I.O., Khanchuk, A.I., Stone, D.B., Scotese, C.R., Scholl, D.W., Fujita, K., 2000. Phanerozoic tectonic evolution of the Circum–North Pacific. *Professional Paper* 1626. U.S. Geological Survey (122 pp.).
- O'Neill, C., Müller, R.D., Steinberger, B., 2005. On the uncertainties in hotspot reconstructions, and the significance of moving hotspot reference frames. *Geochemistry, Geophysics, Geosystems* 6. <http://dx.doi.org/10.1029/2004GC000784>.
- Ostenso, N.A., 1974. Arctic Ocean margins. In: Burk, C.A., Drake, C.L. (Eds.), *The Geology of Continental Margins*. Springer-Verlag, New York, pp. 753–763.
- Oxman, V.S., 2003. Tectonic evolution of the Mesozoic Verkhoyansk–Kolyma belt (NE Asia). *Tectonophysics* 365, 45–76.
- Parfenov, L.M., 1991. Tectonics of the Verkhoyansk–Kolyma Mesozoides in the context of plate tectonics. *Tectonophysics* 199, 319–342.
- Parfenov, L.M., 1997. Geological structure and geological history of Yakutia. In: Parfenov, L.M., Spektor, V.B. (Eds.), *Geological Monuments of the Sakha Republic (Yakutia) Novosibirsk, Russia*, pp. 60–77.
- Parfenov, L.M., Natapov, L.M., Sokolov, S.D., Tsukanov, N.V., 1993. Terrane analysis and accretion in North-East Asia. *The Island Arc* 2, 35–54.
- Parfenov, L.M., Prokopyev, A.V., Gaiduk, V.V., 1995. Cretaceous frontal thrusts of the Verkhoyansk fold belt, eastern Siberia. *Tectonics* 14 (2), 342–358.
- Pavlis, G.L., Sigloch, K., Burdick, S., Fouch, M.J., Vernon, F.L., 2012. Unravelling the geometry of the Farallon plate. Synthesis of three-dimensional from USArray. *Tectonophysics* 532, 82–102. <http://dx.doi.org/10.1016/j.tecto.2012.02.008>.
- Pease, V., 2011. Eurasian orogens and Arctic tectonics: an overview. In: Spencer, A.M., Embry, A.F., Gautier, D.L., Stoupakova, A.V., Sørensen, K. (Eds.), *Arctic Petroleum*

- Geology. Geological Society London, vol. 35, pp. 311–324. <http://dx.doi.org/10.1144/M35.20> (Chapter 20).
- Plafker, G., Berg, H.C., 1994. Overview of the geology and tectonic evolution of Alaska. *The Geology of North America Vol. G-1*. Geological Society of America Special Paper, 442, pp. 121–131.
- Plumley, P.W., Coe, R.S., Byrne, T., 1983. Paleomagnetism of the Paleocene Ghost Rocks Formation, Prince William terrane, Alaska. *Tectonics* 2, 295–314.
- Prokopyev, A.V., Oxman, V.S., 2009. Multi-phase tectonic structures in the collision zone of the Kolyma–Omolon microcontinent and the eastern margin of the North Asian craton, Northeastern Russia. *Stephan Mueller Special Publication Series* 4, 65–70.
- Prokopyev, A.V., Toro, J., Hourigan, J.K., Bakharev, A.G., Miller, E.L., 2009. Middle Paleozoic–Mesozoic boundary of the North Asian craton and the Okhotsk terrane: new geochemical and geochronological data and their geodynamic interpretation. *Stephan Mueller Special Publication Series* 4, 71–84.
- Redfield, T.F., Scholl, D.W., Fitzgerald, P.G., Beck Jr., M.E., 2007. Escape tectonics and the extrusion of Alaska: past, present and future. *Geology* 35 (11), 1039–1042. <http://dx.doi.org/10.1130/G23799A.1>.
- Ren, Y., Stutzmann, E., van der Hilst, R.D., Besse, J., 2007. Understanding seismic heterogeneities in the lower mantle beneath the Americas from seismic tomography and plate tectonic history. *Journal of Geophysical Research* 112. <http://dx.doi.org/10.1029/2005JB004154>.
- Ridgway, K., Flesche, L.M., 2012. Cenozoic tectonic processes along the southern Alaska convergent margin. *Geology* 35 (11), 1055–1056. <http://dx.doi.org/10.1130/focus112007.1>.
- Ritsema, J., Deuss, A., van Heijst, H.J., Woodhouse, J.H., 2010. S40RTS: a degree–40 shear-velocity model for the mantle from new Rayleigh wave dispersion, teleseismic traveltimes and normal-mode splitting function measurements. *Geophysical Journal International* 184, 1223–1236. <http://dx.doi.org/10.1111/j.1365-246X.2010.04884.x>.
- Rowley, D.B., Lottes, A.L., 1988. Plate-kinematic reconstructions of the North Atlantic and Arctic: Late Jurassic to Present. *Tectonophysics* 155, 73–120.
- Saltus, R.W., Miller, E.L., Gaina, C., Brown, P.J., 2011. Regional magnetic domains of the Circum-Arctic: a framework for geodynamic interpretation. In: Spencer, A.M., Embry, A.F., Gautier, D.L., Stoupakova, A.V., Sørensen, K. (Eds.), *Arctic Petroleum Geology*. Geological Society London, vol. 35, pp. 49–60. <http://dx.doi.org/10.1144/M35.4> (Chapter 4).
- Schellart, W.P., Stegman, D.R., Freeman, J., 2008. Global trench migration velocities and slab migration induced upper mantle volume fluxes: constraints to find an Earth reference frame based on minimizing viscous dissipation. *Earth-Science Reviews* 88. <http://dx.doi.org/10.1016/j.earscirev.2008.01.005>.
- Schellart, W.P., Kennett, B.L.N., Spakman, W., Amaru, M., 2009. Plate reconstructions and tomography reveal a fossil lower mantle slab below the Tasman Sea. *Earth and Planetary Science Letters* 278 (3–4), 143–151. <http://dx.doi.org/10.1016/j.epsl.2008.11.004>.
- Schiarizza, P., Massey, N., MacIntyre, D., 1998. *Geology of the Sitlika assemblage in the Talka Lake Area (93 N/3,4,5,12)*. Central British Columbia. Geological Fieldwork Paper, 1997. British Columbia Geological Survey Branch Contribution to the Nachako NATMAP Project, Paper 1998-1.
- Sengör, A.M.C., Natal'in, B.A., 1996. Palaeotectonics of Asia: fragments of a synthesis. In: Yin, A., Harrison, M. (Eds.), *The Tectonic Evolution of Asia*. Cambridge University Press, pp. 486–640.
- Seton, M., Müller, R.D., Zahirovic, S., Gaina, C., Torsvik, T.H., Shephard, G., Talsma, A., Gurnis, M., Turner, M., Maus, S., Chandler, M., 2012. Global continental and ocean basin reconstructions since 200 Ma. *Earth-Science Reviews* 113 (3–4), 212–270. <http://dx.doi.org/10.1016/j.earscirev.2012.03.002>.
- Shephard, G.E., Bunge, H.P., Schubert, B.S.A., Müller, R.D., Talsma, A.S., Moder, C., Landgrebe, T.C.W., 2012. Testing absolute plate reference frames and the implications for the generation of geodynamic mantle heterogeneity structure. *Earth and Planetary Science Letters* 317–318, 204–217.
- Sigloch, K., 2011. Mantle provinces under North America from multifrequency P wave tomography. *Geochimistry, Geophysics, Geosystems* 12 (2), Q02W08. <http://dx.doi.org/10.1029/2010GC003421>.
- Sigloch, K., Mihalynuk, M., 2013. Intra-oceanic subduction shaped the assembly of Cordilleran North America. *Nature* 496, 50–56. <http://dx.doi.org/10.1038/nature12019>.
- Sigloch, K., McQuarrie, N., Nolet, G., 2008. Two-stage subduction history under North America inferred from multiple-frequency tomography. *Nature Geoscience* 1, 458–462. <http://dx.doi.org/10.1038/ngeo231>.
- Simmons, N.A., Forte, A.M., Grand, S.P., 2007. Thermochemical structure and dynamics of the African superplume. *Geophysical Research Letters* 34, L02301. <http://dx.doi.org/10.1029/2006GL028009>.
- Simmons, N.A., Forte, A.M., Boschi, L., Grand, S.P., 2010. GyPSuM: a joint tomographic model of mantle density and seismic wave speeds. *Journal of Geophysical Research* 115, B12310. <http://dx.doi.org/10.1029/2010JB007631>.
- Sokolov, S.D., Bondarenko, G.Y., Morozov, O.L., Shekhovtsov, V.A., Glotov, S.P., Ganelin, A.V., Kravchenko-Berezhnoy, I.R., 2002. South Anyui Suture, northeast Arctic Russia: facts and problems. In: Miller, E.L., Grantz, A., Klemperer, S.L. (Eds.), *Tectonic Evolution of the Bering Shelf–Chukchi Sea–Arctic Margin and Adjacent Land Masses*. Special Papers, 360. Geological Society of America, Boulder, Colorado, pp. 209–224.
- Sokolov, S.D., Luchitskaya, M.V., Silantiev, S.A., Morozov, O.L., Ganelin, A.V., Bazylev, B.A., Osipenko, A.B., Palandzhan, A.A., Kravchenko-Berezhnoy, I.R., 2003. Ophiolites in accretionary complexes along the Early Cretaceous margin of NE Asia: age, composition and geodynamic diversity. In: Dilbk, Y., Robinson, P.T. (Eds.), *Ophiolites in Earth History*. Geological Society, London. Special Publications, 218, pp. 619–664.
- Sokolov, S.D., Bodarenko, G.Y., Khudoley, A.K., Morozov, O.L., Luchitskaya, M.V., Tuchkova, M.I., Layer, P.W., 2009. Tectonic reconstruction of Uda–Murgal arc and the Late Jurassic and Early Cretaceous convergent margin of Northeast Asia–Northwest Pacific. *Stephan Mueller Special Publication Series* 4, 273–288.
- Srivastava, S.P., Roest, W.R., 1989. Seafloor spreading history II–IV, in East Coast Basin Atlas Series: Labrador Sea, J.S. Bell (co-ordinator). Atlantic Geoscience Centre, Geologic Survey of Canada, Map sheets L17-2–L17-6.
- Stamatatos, J.A., Trop, J.M., Ridgway, K.D., 2001. Late Cretaceous paleogeography of Wrangellia: paleomagnetism of the MacCool Ridge Formation, southern Alaska, revisited. *Geology* 29 (10), 947–950.
- Steinberger, B., 2000a. Plumes in a convecting mantle: models and observations for individual hotspots. *Journal of Geophysical Research* 105, 11127–11152.
- Steinberger, B., 2000b. Slabs in the lower mantle—results of dynamic modelling compared with tomographic images and the geoid. *Physics of the Earth and Planetary Interiors* 118, 241–257.
- Steinberger, B., Torsvik, T., 2008. Absolute plate motions and true polar wander in the absence of hotspot tracks. *Nature* 452, 620–624. <http://dx.doi.org/10.1038/nature06842>.
- Steinberger, B., Torsvik, T.H., 2010. Toward an explanation for the present and past locations of the poles. *Geochemistry, Geophysics, Geosystems* Q06W06. <http://dx.doi.org/10.1029/2009GC002889>.
- Stone, D.B., Minyuk, P., Kolosev, E., 2003. New paleomagnetic paleolatitudes for the Omulevka terrane of northeast Russia: a comparison with the Omolon terrane and the eastern Siberian platform. *Tectonophysics* 377, 55–82.
- Stone, D.B., Layer, P.W., Raikovich, M.I., 2009. Age and paleomagnetism of the Okhotsk–Chukotka Volcanic Belt (OCVB) near Lake El'gygytyn, Chukotka, Russia. *Stephan Mueller Special Publication Series* 4, 243–260.
- Taylor, P.T., Kovacs, L.C., Vogt, P.R., Johnson, G.L., 1981. Detailed aeromagnetic investigation of the Arctic Basin, 2. *Journal of Geophysical Research* 86, 6323–6333. <http://dx.doi.org/10.1029/JB086iB07p06323>.
- Tegner, C., Storey, M., Holm, P.M., Thorarinnsson, S.B., Zhao, X., Lo, C.-H., Knudsen, M.F., 2011. Magmatism and Eureka deformation in the High Arctic large igneous province: ⁴⁰Ar–³⁹Ar age of Kap Washington Group volcanics, North Greenland. *Earth and Planetary Science Letters* 303, 203–214. <http://dx.doi.org/10.1016/j.epsl.2010.12.047>.
- Tempelmann-Kluit, D.J., 1979. Transported cataclite, ophiolite and granodiorite in Yukon: evidence of arc–continent collision. *Geological Survey of Canada Paper* 79–14, 27.
- Toro, J., Amato, J.M., Natal'in, B., 2003. Cretaceous deformation, Chegitun River area, Chukotka Peninsula, Russia: implications for the tectonic evolution of the Bering Strait region. *Tectonics* 22 (3), 19. <http://dx.doi.org/10.1029/2001TC001333>.
- Torsvik, T., Müller, R., van der Voo, R., Steinberger, B., Gaina, C., 2008. Global plate motion frames: toward a unified model. *Reviews of Geophysics* 46, 1–44. <http://dx.doi.org/10.1029/2007RG000227>.
- Trettin, H.P., 1991. The Proterozoic to Late Silurian record of Pearya, chapter 9. In: Trettin, H.P. (Ed.), *Geology of the Innuitian Orogen and Arctic Platform of Canada and Greenland*. *Geology of North America*, vol. E. Geological Society of America, Boulder, Colorado, pp. 241–259.
- Trop, J.M., Ridgway, K.D., 2007. Mesozoic and Cenozoic tectonic growth of southern Alaska: a sedimentary basin perspective. In: Ridgway, K.D., Trop, J.M., Gen, J.M.G., O'Neill, J.M. (Eds.), *Tectonic Growth of a Collisional Continental Margin: Crustal Evolution of Southern Alaska*. The Geological Society of America, Special Paper, 431, pp. 55–94. [http://dx.doi.org/10.1130/2007.2431\(04\)](http://dx.doi.org/10.1130/2007.2431(04)).
- Trop, J.M., Ridgway, K.D., Manuszak, J.D., Layer, P., 2002. Mesozoic sedimentary-basin development on the allochthonous Wrangellia composite terrane, Wrangell Mountains basin Alaska: a long-term record of terrane migration and arc construction. *GSA Bulletin* 114, 693–717.
- Van der Meer, D.G., Spakman, W., van Hinsbergen, D.J.J., Amaru, M.L., Torsvik, T.H., 2010. Towards absolute plate motions constrained by lower-mantle slab remnants. *Nature Geoscience* 3, 36–40. <http://dx.doi.org/10.1038/NGE0708>.
- Van der Meer, D.G., Torsvik, T.H., Spakman, W., van Hinsbergen, D.J.J., Amaru, M.L., 2012. Intra-Panthalassa Ocean and subduction zones revealed by fossil arcs and mantle structure. *Nature Geoscience* 5, 215–219. <http://dx.doi.org/10.1038/NGE01401>.
- Van der Voo, R., Spakman, W., Bijwaard, H., 1999. Tethyan subducted slabs under India. *Earth and Planetary Science Letters* 171 (1), 7–20.
- Vishnevskaya, V.S., Filatova, N.I., 2012. Allochthonous Mesozoic marine sequences of northeastern Asia and western North America: correlation of stratigraphic and geodynamic depositional settings. *Russian Journal of Pacific Geology* 6 (3), 189–208.
- Vogt, P.R., Taylor, P.T., Kovacs, L.C., Johnson, G.L., 1979. Detailed aeromagnetic investigation of the Arctic Basin. *Journal of Geophysical Research* 84, 1071–1089.
- Vogt, P.R., Taylor, P.T., Kovacs, L.C., Johnson, G.L., 1982. The Canada Basin: aeromagnetic constraints on structure and evolution. *Tectonophysics* 89, 295–336.
- Zhao, D., Pirajno, F., Dobretsov, N.L., Liu, L., 2010. Mantle structure and dynamics under East Russia and adjacent regions. *Russian Geology and Geophysics* 51, 925–938.
- Zonenshain, L.P., Kuzmin, M.I., Natapov, L.M., 1990. *Geology of the USSR: a plate tectonic synthesis*. In: Page, B.M. (Ed.), *Geodynamics Series*, vol. 21. American Geophysical Union, Washington, D.C.